



LUND UNIVERSITY

The uPA receptor in ovarian cancer. Regulation by EGF and the estrogen responsive membrane receptor GPR30. Soluble uPAR in diagnosis and prognosis.

Henic, Emir

2008

Document Version:

Publisher's PDF, also known as Version of record

[Link to publication](#)

Citation for published version (APA):

Henic, E. (2008). *The uPA receptor in ovarian cancer. Regulation by EGF and the estrogen responsive membrane receptor GPR30. Soluble uPAR in diagnosis and prognosis*. [Doctoral Thesis (compilation), Obstetrics and Gynaecology (Lund)]. Department of Obstetrics and Gynecology, Lund University.

Total number of authors:

1

General rights

Unless other specific re-use rights are stated the following general rights apply:

Copyright and moral rights for the publications made accessible in the public portal are retained by the authors and/or other copyright owners and it is a condition of accessing publications that users recognise and abide by the legal requirements associated with these rights.

- Users may download and print one copy of any publication from the public portal for the purpose of private study or research.
- You may not further distribute the material or use it for any profit-making activity or commercial gain
- You may freely distribute the URL identifying the publication in the public portal

Read more about Creative commons licenses: <https://creativecommons.org/licenses/>

Take down policy

If you believe that this document breaches copyright please contact us providing details, and we will remove access to the work immediately and investigate your claim.

LUND UNIVERSITY

PO Box 117
221 00 Lund
+46 46-222 00 00

The uPA receptor in ovarian cancer

**Regulation by EGF and the estrogen responsive membrane
receptor GPR30. Soluble uPAR in diagnosis and prognosis**

Emir Henic



Department of Obstetrics and Gynecology

Clinical Sciences, Lund

Lund University

Sweden

2008

© Emir Henic
Lund University, Faculty of Medicine Doctoral Dissertation Series 2008:103
ISSN 1652-8220
ISBN 978-91-86059-56-9
Printed by: Media-Tryck, Lund, Sweden 2008

To my family

CONTENTS

LIST OF PAPERS	6
ABBREVIATIONS	7
INTRODUCTION	9
Ovarian cancer	9
The urokinase plasminogen activator (uPA) system	11
<i>Cleavage and shedding of uPAR</i>	12
<i>The uPA system in cell migration</i>	13
<i>The uPA system in ovarian cancer</i>	14
The epidermal growth factor receptor (EGFR).....	15
Estrogen receptors (ER).....	17
G-protein coupled receptor 30 (GPR30).....	18
AIMS OF THE STUDY	20
MATERIAL AND METHODS.....	21
Peripheral blood plasma samples (IV).....	21
Tumor tissue samples (III).....	21
Ovarian cancer cell lines (I, II, III).....	22
Real-time PCR (I, II, III).....	22
Cell migration assay (I, II).....	24
Time-lapse video microscopy (I).....	25
Northern blotting for uPAR mRNA (I, II).....	25
Cellular binding of ¹²⁵ I-uPA (I, II).....	26
Cellular degradation of ¹²⁵ I-uPA:PAI-1 complex (I, II)	26
Western blotting for EGFR and uPAR (I)	26
Membrane protein extraction and Western blotting for GPR30 (III)	27
Biosynthetic labeling (I)	28
Immunoassays.....	29
Statistical methods	31
RESULTS AND COMMENTS.....	33
EGF stimulates cell migration and uPAR expression.....	33
The uPAR-EGFR relation.....	34
Estradiol (E2) attenuates the EGF effect	35
Identifying the E2 receptor	35
Expression and regulation of GPR30 in ovarian cancer cell lines.....	36
Expression of GPR30 in ovarian tumor tissue.....	36
Cleaved forms of uPAR as diagnostic markers	37
Cleaved forms of uPAR as prognostic markers.....	38
DISCUSSION.....	39
Mechanisms of EGF regulation of cell surface uPAR in ovarian cancer cells.....	39
uPAR-EGFR relation	40
Estradiol modulates the response to EGF on cell migration and uPAR expression	42
The estradiol effect involves GPR30	43
GPR30 expression in primary ovarian tumors and ovarian cancer cell lines	44
Diagnostic importance of cleaved forms of the uPA receptor.....	45
Prognostic importance of cleaved forms of the uPA receptor	48
SUMMARY.....	50
CONCLUSIONS.....	52
SAMMANFATTNING PÅ SVENSKA	53
ACKNOWLEDGEMENTS.....	55
REFERENCES	56

LIST OF PAPERS

- I Henic E, Sixt M, Hansson S, Høyer-Hansen G, Casslén B.
EGF-stimulated migration in ovarian cancer cells is associated with decreased internalization, increased surface expression, and increased shedding of the urokinase plasminogen activator receptor.
Gynecologic Oncology 101: 28 – 39, 2006
- II Henic E, Noskova V, Høyer-Hansen G, Hansson S, Casslén B.
Estradiol attenuates EGF-induced rapid uPAR mobilization and cell migration via the G-protein coupled receptor 30 (GPR30) in ovarian cancer cells.
International Journal of Gynecological Cancer, accepted January 25, 2008
- III Noskova V, Henic E, Kolkova Z, Ahmadi S, Åsander E, Brommesson S, Hansson S, Casslén B.
Expression and regulation of the estrogen responsive membrane receptor GPR30 in primary ovarian tumors and ovarian cancer cell lines.
Manuscript 2008
- IV Henic E, Borgfeldt C, Christensen I J, Casslén B, Høyer-Hansen G.
Cleaved forms of the uPA receptor in plasma have diagnostic potential and predict postoperative survival in patients with ovarian cancer.
Clinical Cancer Research 14(18): 5785-5793, 2008

The papers will be referred to in the text by their roman numerals.

ABBREVIATIONS

AUC	area under curve
BRCA	breast cancer related gene
CA125	cancer antigen 125
cAMP	cyclic adenosine monophosphate
cDNA	complementary deoxyribonucleic acid
E2	estradiol
ECM	extracellular matrix
EGF	epidermal growth factor
EGFR	epidermal growth factor receptor
ER	estrogen receptor
ERK	extracellular regulated kinase
FAK	focal adhesion kinase
FBS	fetal bovine serum
FIGO	International Federation of Gynecology and Obstetrics
GP(C)R	G protein-coupled receptor
GPI	glycosyl-phosphatidylinositol
GTP	guanidine triphosphate
HB-EGF	heparin-binding epidermal growth factor
HBSS	Hank's buffered salt solution
HER	human epidermal growth factor receptor
HMW	high molecular weight
HR	hazard ratio
HRT	hormone replacement therapy
¹²⁵ I	¹²⁵ iodine
MAPK	mitogen-activated protein kinase
mRNA	messenger ribonucleic acid
PAI	plasminogen activator inhibitor
PCR	polymerase chain reaction
PR	progesterone receptor
ROC	receiver operating characteristic
³⁵ S	³⁵ sulphur

SERM	selective estrogen receptor modulator
suPAR	soluble urokinase plasminogen activator receptor
TBS	TRIS buffered saline
TGF- α	transforming growth factor- α
TR-FIA	time-resolved fluorescence assay
uPA	urokinase plasminogen activator
uPAR	urokinase plasminogen activator receptor

INTRODUCTION

Ovarian cancer

Ovarian cancer is the leading cause of death from gynecological cancer in western countries. North European countries have the highest incidence, which however shows a steady decrease since 1975. Each year in Sweden, more than 700 women are diagnosed with ovarian cancer [1].

The etiology of epithelial ovarian cancer is not fully understood. Heredity plays a role and it is estimated that at least 10% of cases are associated with hereditary susceptibility [2]. This is mainly due to mutations in the tumor suppressor genes BRCA1 and BRCA2, and to a lesser degree in the mismatch repair (MMR) genes. The lifetime risk for Scandinavian women to develop ovarian cancer is estimated to 1.1%, but mutations in the BRCA1 and BRCA2 genes confer an increased lifetime risk up to 40% and 20%, respectively [3, 4]. Other factors that have been suggested to increase the risk of developing ovarian cancer are early menarche, late menopause, high gonadotropin levels, infertility, endometriosis, polycystic ovarian syndrome, and the use of ovulation stimulating drugs such as clomiphene [5-10].

According to the “incessant ovulation” hypothesis, each ovulation causes a trauma to the ovarian surface epithelium, and the subsequent repair induces cell proliferation. Any concomitant genetic instability can initiate carcinogenesis. Both epidermal growth factor (EGF) and estrogens are involved in growth of the ovarian epithelium and have potential roles in carcinogenesis.

The alternative “high gonadotrophin” hypothesis is based on the fact that most ovarian malignancies develop postmenopausally when levels of gonadotrophins are high.

Oral contraceptives are protective against ovarian cancer since they both reduce gonadotrophin levels and inhibit ovulations [11, 12]. Extensive use of oral contraceptives over the last four decades is the most probable explanation for the decreasing incidence of ovarian cancer. Childbearing, breastfeeding, hysterectomy, and tubal ligation have also been associated with decreased risk of ovarian cancer [13-15]. In contrast, women using HRT for more than five years have a slightly increased risk to develop ovarian cancer [16].

Epithelial ovarian cancer is a histopathologically heterogeneous disease, which includes various histological types of adenocarcinoma, i.e. serous, mucinous, endometrioid, and clear cells. Each histological type can present different levels of histological differentiation i.e. well, moderately, and poor. Tumors with different histopathological type and differentiation exhibit differences in clinical behavior, responsiveness to therapy, and prognosis. In addition to the truly malignant tumors, we identify possibly malignant, i.e. borderline tumors, which have malignant cells but no invasive behavior.

Ovarian cancer has a high mortality rate, since few symptoms in early stages often result in late diagnosis and subsequent poor prognosis. More than 70% of patients present with advanced disease (stage III and IV) and 5 year survival is about 30%, compared with more than 90% in stage I [17, 18]. No solid screening test for early detection of ovarian cancer is presently available. The best studied biomarker, CA125 level in peripheral blood, is unreliable due to low sensitivity in cases with early stage disease [19-24]. Transvaginal ultrasound has high sensitivity and acceptable specificity, but is too laborious to be employed for population screening.

Despite the fact that epithelial ovarian cancer includes tumors of different types and differentiation, treatment in advanced cases is uniform and includes debulking surgery followed by platinum based chemotherapy in combination with paclitaxel. Ovarian cancer is highly responsive to chemotherapy with response rates about 80%, but most tumors relapse [17, 25]. Attempts with various Selective Estrogen Receptor Modulators (SERM) as well as epidermal growth factor receptor-tyrosine kinase inhibitors gave only modest effects, but these drugs were usually given as second or third line treatments.

The urokinase plasminogen activator (uPA) system

The urokinase plasminogen activator (uPA) system plays a central role in cell adhesion, migration, invasion and tissue remodeling [26]. These processes are critical both during normal development and in growth and metastasis of malignant tumors. The uPA system consists of the serine protease uPA, its receptor (uPAR), and the specific inhibitors PAI-1 and PAI-2 (Fig. 1). Initially, uPA is produced as an inactive single-chain protein (pro-uPA). Activation of pro-uPA to uPA as well as the subsequent activation of plasminogen to plasmin by fully active uPA is focused on the cell surface by binding to uPAR. Plasmin is a potent serine protease, which promotes degradation of ECM proteins including vitronectin, fibrinogen, fibronectin, and furthermore the collagen structure of ECM through activation of matrix metalloproteinases. PAI-1 and PAI-2 are endogenous inhibitors of uPA and they regulate uPA-uPAR activity. PAI-1 is the major inhibitor of uPA in the extracellular space. Binding of PAI-1 to uPA in complex with uPAR leads to internalization of the whole uPAR:uPA:PAI-1 complex. The uPA:PAI-1 part of the complex is subsequently targeted for degradation in the lysosomes, while uPAR at least partly is recycled back to the cell surface [27].

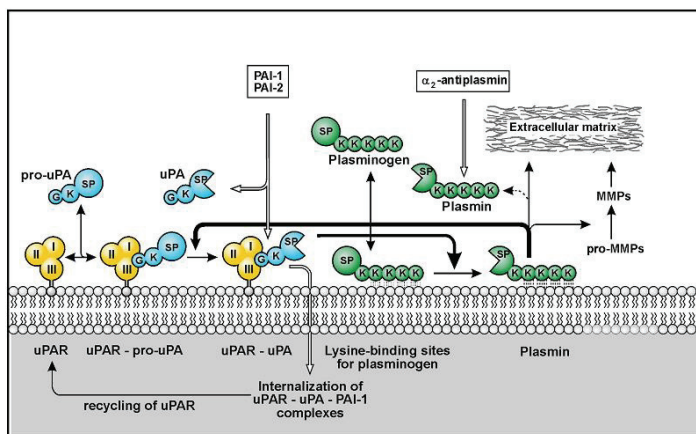


Figure 1. Schematic illustration of the plasminogen activation system (modified from Ploug 2003 [28]). G: growth factor domain, K: kringle domain, SP: protease domain.

The role of PAI-1 is controversial. On one hand, it inhibits uPA activity and cell invasion. On other hand, it positively influences and is even a prerequisite for cell invasion and angiogenesis [29]. High tumor tissue levels of PAI-1 are associated with poor prognosis in patients with breast cancer [30]. PAI-2 has lower uPA inhibitory capacity than PAI-1. It plays a role in controlling apoptosis and this function is independent of uPA inhibition [31].

The uPAR, which was identified in 1985 on U937 monocytes [32, 33], consists of three domains designated I, II, and III. The three domains are connected by two linker regions. The uPAR(III) attaches to the cell membrane by a glycosyl-phosphatidylinositol (GPI) anchor, which is added to the receptor protein during posttranslational processing. Intact uPAR(I-III) is required for efficient binding of ligands like uPA and vitronectin [34-36] Also, full-length uPAR is needed for lateral interactions on the cell membrane with e.g. integrin β subunits, which result in down-stream signaling via ERK1/2 [37].

Cleavage and shedding of uPAR

uPAR (I-III) can be cleaved in the linker region between domains I and II by uPA, liberating uPAR(I) and leaving the cleaved form, uPAR(II-III) on the cell surface [38, 39] (Fig. 2). *In vivo* uPA has been shown to be responsible for cleavage of uPAR [40, 41], but *in vitro* uPAR can also be cleaved in the linker region by other proteases like trypsin, chymotrypsin, elastase, metalloproteases, and cathepsin G [42]. Both full-length and cleaved uPAR can be shed from the cell surface and soluble forms of suPAR: suPAR(I-III), suPAR(II-III) and uPAR(I) have been detected in blood [43, 44] and in cystic fluid from patients with ovarian cancer [45]. Although the mechanism of suPAR shedding is not clarified, evidence has been provided that the glycolipid anchor can be cleaved by endogenous cellular GPI-specific phospholipase D (GPI-PLD) [46]. Whereas GPI-anchored uPAR(I-III) is readily cleaved by uPA, suPAR cannot be cleaved by uPA in the linker region between domains I and II [47]. The function of suPAR(I-III) is not fully elucidated but it has been shown to act as a scavenger receptor to free uPA, and reduces growth and metastasis of breast and ovarian cancer cells [48, 49]. In contrast, suPAR(I-III) can activate β 2 and β 1 integrins and induce ERK1/2 activation [50]. However, whereas no functional role

has been assigned to uPAR(II-III) its soluble counterpart has been shown to be a strong chemo-attractant important for the migration of various cell types [51, 52].

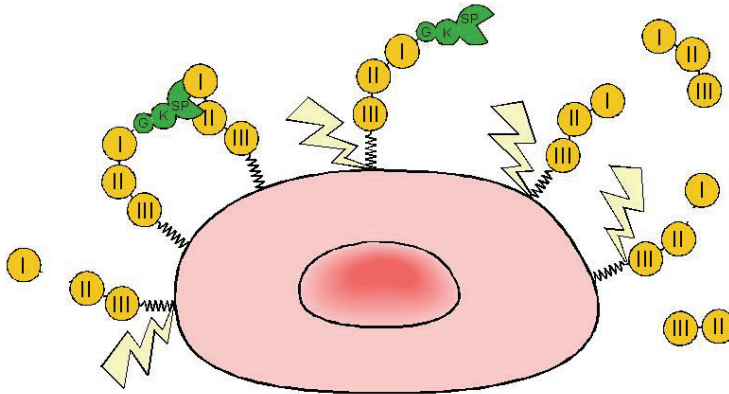


Figure 2. Schematic illustration of cleavage and shedding of uPAR. uPAR can be cleaved in the linker region between domains I and II by uPA and by other proteases. Shedding follows detachment of the GPI-anchor.

The uPA system in cell migration

Binding of uPA to uPAR activates uPAR and promotes interactions with other surface proteins. Eventually, this serves to focus proteolytic activity on the cell surface. Activated uPAR translocates on cell surface to focal contact domains and clusters in multiprotein aggregate [53]. This enables directional proteolysis and degradation of ECM to concentrate on the leading edge and facilitates cell migration. uPAR lacks transmembrane and intracellular domain and can not alone transduce intracellular signals. However, the uPA:uPAR complex interacts with a number of other cell membrane proteins, e.g β -subunits of integrin receptors and FPLR-1 (formyl peptide receptor-like receptor) that results in modulation of cell migration, which is independent of pericellular proteolysis [54, 55]. Through its lateral

interactions at focal adhesion sites, which have close connection to the cytoskeleton, uPAR initiates signaling that alter cell adhesion and migration [55]. Co-immunolocalization and co-immunoprecipitation of uPAR and several integrins has been reported [56-58]. Integrins form complexes with growth factor receptors and uPAR can regulate integrins function by association with these. Activation of ERK resulting in cell proliferation and migration in response to uPA is described as effect of interaction between uPAR, $\alpha_5\beta_1$ integrin, and EGFR [59].

The uPA system in ovarian cancer

The components of the uPA-system are up-regulated in a number of malignances and high concentrations correlate with poor prognosis [60]. We have previously shown that this is the case also in ovarian cancer [61, 62].

High levels of uPA, PAI-1, and PAI-2 in tumor tissue extracts from patients with ovarian cancer were associated with malignant progression and high levels of uPA and PAI-1 with short progression-free and overall survival [63]. Borgfeldt et al showed that increased expression of mRNA for uPA, uPAR and PAI-1 was associated with dedifferentiation of serous ovarian cancer from cystic to solid tumors [61]. Interestingly tumor tissue content of uPAR protein is lower in poorly differentiated than in borderline and well differentiated tumors [64]. A similar pattern was observed for suPAR in cystic fluid [45].

Increased peripheral blood levels of suPAR have been reported in patients with malignant tumors including ovarian, endometrial and cervical cancer [45, 65], non-small cell lung cancer [66], and colon cancer [67]. In addition high preoperative concentration of suPAR forms in blood from patients with breast and colorectal cancer correlates with poor prognosis [68, 69].

The level of suPAR in peripheral blood is higher in patients with ovarian cancer than in patients with benign ovarian tumors, and high level of suPAR was associated with poor prognosis [65, 70]. In contrast, other studies did not find any correlation between suPAR levels and survival in patients with ovarian cancer [71, 72].

The epidermal growth factor receptor (EGFR)

The epidermal growth factor receptor (EGFR/HER1, erbB1) belongs to a superfamily of cell membrane receptors with intrinsic tyrosine kinase activity [73]. This family also includes HER2/erbB2, HER3/erbB3, and HER4/erbB4 [74-76]. These receptors that have similar structure, consist of three domains, i.e. an extracellular ligand binding domain, a transmembrane hydrophobic domain, and an intracellular tyrosine kinase domain. The extracellular domains of all four receptors occur also in a detached soluble form.

Six ligands are known to bind to the EGFR, i.e. EGF, heparin-binding EGF (HB-EGF), transforming growth factor- α (TGF- α), amphiregulin, betacellulin, and epiregulin. EGF functions as an endocrine and/or paracrine agent, while HB-EGF and TGF- α are not secreted and serve as autocrine/juxtacrine signaling molecules. Ligand binding to the extracellular domain initiates conformational changes of the intracellular domain, which allows binding to another EGFR (homodimerization) or to another erbB family receptor (heterodimerisation). This results in autophosphorylation of specific tyrosine residues in the intracellular domain and subsequently in phosphorylation of adapter proteins as well as numerous intracellular signaling proteins. EGF binding to EGFR also induces internalization and subsequent lysosomal degradation of the ligand-receptor complex [77]. Signaling diversity is caused not only by the presence of different ligands, but also by the different properties of various receptor dimer combinations. The Ras/Raf/mitogen-activated protein kinase (MAPK) pathway regulates cell proliferation, whereas the phosphatidylinositol 3-kinase (PI3K)/Akt pathway regulates cell survival, apoptosis, migration, and invasion. The Src kinase pathways, which include focal adhesion kinase (FAK), regulates cell adhesion, migration, and proliferation. The signal transducers and activators of transcription (STAT) pathway is involved in cell survival and apoptosis. Activated EGFR interacts also with phospholipase C γ , which activates its downstream protein kinase C and calcium-mediated cascades.

Apart from the classical EGFR activation after ligand binding, EGFR tyrosine phosphorylation can be induced by transactivation via e.g. uPAR, growth hormone, estrogen but also by irradiation, reactive oxygen radicals and heavy metal ions [78-80].

The EGFR and its ligands play important roles in embryonic development and physiology. Mutations in the EGFR gene in genetically engineered mice lead to embryonic loss, perinatal death, or various organ failures. Imbalance in the EGFR/EGF system cause defects in epidermis, mammary gland, nervous system, pancreas, lung, intestine, and prostate [81, 82].

Furthermore, the EGFR system plays a role in neoplastic transformation. Several studies have confirmed that overexpressed EGFR, alone or coexpressed with HER2/erbB2, in the presence of ligands, can induce neoplastic transformation. The EGFR and its ligands are frequently overexpressed in malignant epithelial tumors of the breast, ovaries, bladder, head and neck, and lung, and this is associated with poor prognosis. In addition, mutations of the EGFR gene that result in constitutive activation of the receptor are also associated with more aggressive tumor phenotype. However, presence of EGFR mutations or gene amplification in non-small cell lung cancer is also associated with higher response rate to EGFR tyrosine kinase inhibitors and improved survival [83, 84].

EGFR in ovarian cancer

The EGFR and its ligands EGF, HB-EGF, and TGF- α are widely expressed in normal ovarian surface epithelium, but also by follicular cells, endothelial cells, and stromal fibroblasts. The system is involved in cell proliferation, regulation of cyclical ovarian functions, and in post-ovulatory tissue repair.

EGFR is over-expressed in the majority of ovarian carcinomas, and ovarian cancer cell lines secrete EGF [85-88]. Over-expression of the EGF system in primary ovarian carcinomas is associated with EGFR gene amplification whereas EGFR gene mutations are very rare [89-91]. High tumor tissue levels of EGFR protein has been associated with advanced stage and poorly differentiated histology [92-94]. Also, high tumor tissue content of EGFR has been directly associated with poor postoperative prognosis in long-term studies of patients with ovarian cancer [85, 92, 95, 96]. In contrast, other investigators did not find differences in EGFR staining intensity between benign and malignant ovarian tumors, or any association between EGFR expression and tumor histology, clinical stage, or overall survival [96-99].

Monoclonal antibodies to EGFR, which block ligand binding and receptor activation, as well as tyrosine kinase inhibitors, which prevent phosphorylation and

activation of downstream signaling, were tested in clinical studies, however with limited success [90, 100, 101]. In vitro studies with Iressa, a tyrosine kinase inhibitor, alone or in combination with cytotoxic drugs were promising, but phase II clinical trials showed that Iressa had minimal anti-tumor activity in a group of patients, whose tumors had not been screened for EGFR expression [90, 102].

Estrogen receptors (ER)

Estrogens are steroid hormones that initiate biologic and metabolic effects in target tissues. Besides important functions in the reproductive tract, estrogens reportedly protect the cardiovascular system and promote bone integrity [103]. The role of estrogens in carcinogenesis of the breast and the endometrium is well known, but its role in ovarian cancer is more controversial [104]. Several recent epidemiologic studies have identified an increased risk of ovarian cancer in women using HRT [105, 106]. Although such studies are not conclusive for the causative agent, other studies suggest that estrogens play a role in ovarian tumor growth. Estradiol stimulates proliferation and reduces also apoptosis in ovarian cancer cells, and these effects are mediated by ER α [107-110]. In support of these reports, Lindgren et al showed that regional distribution of high ER α expression in poorly differentiated epithelial tumors correlated with the distribution of lower apoptotic activity [111]. Furthermore, estrogens may influence responsiveness to chemotherapy in patients with ovarian cancer, since apoptosis that is induced by paclitaxel and cisplatin in ovarian cancer cells, is reduced by estrogens via phosphorylation of Akt [112, 113]. However, estrogens also induce expression of the progesterone receptor (PR) [114, 115], and PR status is a prognostic marker for progression-free survival in patients with ovarian cancer [111, 116, 117].

ERs are expressed in 40-60% of malignant ovarian tumors [118, 119]. Anti-estrogen therapy is however much less effective in patients with ovarian cancer than in those with breast cancer, and only about 15% of ER-positive ovarian tumors respond to this treatment [120].

The effects of estrogens are mediated through nuclear estrogen receptors ER α and ER β . These receptor proteins are encoded by two different genes, have different tissue distributions and different functions [121-123]. The receptors have high

structural homology in the DNA binding domain (97%), but differs more in the ligand binding domain (55% homology) [124]. ER β dominates in normal ovaries and benign tumors, whereas ER α predominates in ovarian cancer [125]. Thus, the ER α /ER β ratio increases with loss of histological differentiation. O'Donnell et al showed that ER α , but not ER β , mediates gene expression changes and growth response in PEO1 ovarian cancer cells [107].

The steps in the classical genomic pathway for estrogens include diffusion of the steroid through the cell and nuclear membranes, and binding to the nuclear estrogen receptors ER α and ER β , which subsequently dimerize and bind to estrogen response elements in estrogen-sensitive genes leading to gene transcription and eventually protein synthesis [126].

G-protein coupled receptor 30 (GPR30)

In addition to the classic genomic mechanism, estrogens elicit rapid cellular responses, which can be registered in seconds or minutes after cells have been exposed to estrogen. These responses are too rapid to be mediated by nuclear ER mechanisms. Such non-genomic estrogen responses are initiated at the cell membrane and involve rapid activation of second messengers, e.g. cAMP, calcium, and inositol phosphate [127-129].

A receptor that can potentially mediate these effects, is the G-protein coupled membrane receptor GPR30 [78]. GPR30 was cloned in 1996 by Owman et al and initially classified as an orphan receptor, since identity of the ligand was unknown [130].

G protein-coupled receptors (GPCRs) constitute the largest and most diverse superfamily of cell surface receptors in mammals. Characteristics of these receptors include their heptahelical-serpentine transmembrane structure and their signaling via a heterotrimeric G-protein complex consisting of G α , G β , and G γ . Ligand binding to GPCRs results in dissociation of the G α unit, which has GTPase activity, and subsequent activation of effector enzymes or ion channels [131] (Fig. 3).

GPR30 is expressed in ovarian, placental, hepatic, prostate, heart, breast cancer and lymphoid tissue [130, 132-134].

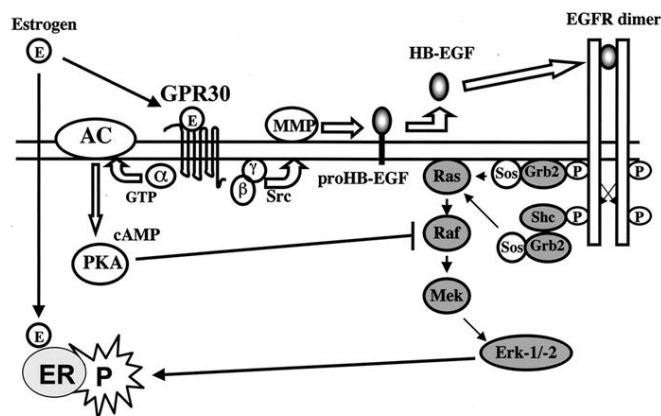


Figure 3. Proposed mechanism for estrogen action via GPR30, and subsequent regulation of EGFR signaling [135].

GPR30 binds estradiol with high affinity [136, 137], and has binding and signaling characteristics of a true membrane ER, i.e. saturability, displaceable binding, and a single binding site. Estrogen binding to GPR30 leads to activation of G proteins, with subsequent activation of the second messenger cAMP. GPR30 has also affinity for the ER α antagonists, ICI 182780 and tamoxifen [138]. However, binding of these molecules to GPR30 results in an agonistic rather than an antagonistic effect. Furthermore, evidence has been obtained for rapid trans-activation of EGFR after stimulation of GPR30 with estradiol [135](Fig. 3). It was recently reported that GPR30 mediates non-genomic signaling specifically through trans-activation of the EGFR in ovarian cancer cells [139].

Down-stream signaling from the EGFR includes activation of the MAP kinases ERK-1/2. However, ligand binding to GPR30 also results in increased cAMP activity, which via protein kinase A and suppression of Raf inhibits ERK-1/2 activity. In this way, activation of GPR30 and EGFR can balance ERK-1/2 activity by employing two pathways with opposite effects.

AIMS OF THE STUDY

- To study the role of EGF in cell migration and uPAR expression in ovarian cancer cell lines.
- To examine the influence of estradiol on cell migration and uPAR expression in ovarian cancer cell lines.
- To analyze GPR30 mRNA and protein expression in ovarian tumor tissue and ovarian cancer cell lines.
- To investigate the diagnostic and prognostic value of cleaved forms of the uPA receptor in plasma from patients with ovarian tumors.

MATERIAL AND METHODS

Peripheral blood plasma samples (IV)

Peripheral blood samples were obtained preoperatively in 335 patients admitted for primary surgery because of adnexal masses at the Department of Obstetrics and Gynecology in Lund 1993-2005. Blood was collected in citrate tubes, centrifuged, and the plasma stored at -20°C until analyzed. The standard surgical procedure in benign cases included resection of the cyst or unilateral oophorectomy, and in the malignant cases abdominal hysterectomy, bilateral salpingo-oophorectomy, and infracolic omentectomy. Cytological analyses of ascitic fluid, or when absent, of peritoneal washing were performed. All diagnoses were verified by histopathology of the tumors. Histopathological grade and stage of the disease (FIGO) were available in all malignant cases. Postoperative adjuvant treatment was given according to clinical standards in patients with invasive cancer. Patients with stage Ic or higher stage received platinum based chemotherapy, either alone or combined with paclitaxel or cyclophosphamide. Survival status of all patients, i.e. alive or dead including date of death was obtained on September 27, 2006 from the Swedish Population Register (Tumor registry center in Lund). For patients with benign cysts, the median age was 50 years (range 16.6-88), for borderline patients, the median age was 52.2 years (range 30.6-85.7) and for ovarian cancer patients, the median age was 62.6 (range 31-88). The median follow-up time for patients alive on September 27, 2006 was 64 months (range 20-154).

Tumor tissue samples (III)

Ovarian tumor tissue was obtained during operation at the Department of Obstetrics and Gynecology, Lund University Hospital, 2001-2007. As soon as the tumor was removed from the patient, tissue samples, 5x5x5 mm, were immediately frozen on dry ice, and subsequently stored at -80 °C until used. All tumors were classified by histo-pathological diagnosis.

Tissue collection was approved by the Regional Research Ethics Board at University Hospital in Lund, Sweden.

Ovarian cancer cell lines (I, II, III)

Seven different human ovarian cancer cell lines were used. All of them were derived from epithelial ovarian adenocarcinomas. Cells were cultured on uncoated plastic at 37°C in humidified atmosphere with 5% CO₂. Media were supplemented with fetal bovine serum (FBS), Penicillin (100 U/mL), Streptomycin (100 µg/mL), and Amphotericin B (0.25 µg/mL). All culture media and supplements were from Invitrogen, Gibco (Carlsbad, CA, USA).

The ES-2 cell line derives from a poorly differentiated clear cell carcinoma of the ovary. ES-2 cells were cultured in McCoy's 5A medium with 10% FBS.

The Hey-TG cell line is one of several aggressive cell lines derived from HEY cells, which originate from an intermediately differentiated serous adenocarcinoma of the ovary. Hey-TG cells were cultured in M199 medium with 10% FBS.

The OVCAR-3 cell line derives from ascitic fluid cells from a patient with poorly differentiated papillary ovarian adenocarcinoma. The cells are tumorigenic in mice. OVCAR-3 cells were cultured in M199 medium with insulin 0.01 mg/mL and 20% FBS.

The SKOV-3 cell line derives from a metastasis of an ovarian cancer with unknown histology. They form moderately differentiated tumors when injected subcutaneously in mice. SKOV-3 cells were cultured in M199 medium with 10% FBS.

The SKOV-3ip cell line is derived from SKOV-3 cells. They form intra-peritoneal metastases in mice. SKOV-3ip cells were cultured in M199 medium with 10% FBS.

The TOV112D cell line derives from an ovarian poorly differentiated endometrioid carcinoma. The cells were cultured in M199 medium with 10% FBS.

The TOV21G cell line derives from an ovarian poorly differentiated clear-cell carcinoma. The cells were cultured in M199 medium with 10% FBS.

Real-time PCR (I, II, III)

Extraction of total RNA

Total RNA was extracted from confluent cell cultures (I, II, and III) or frozen tissue samples (III). The concentration and purity of all the extracted RNA samples

was evaluated by spectrophotometry. The quality of each RNA sample was verified by 2% agarose gel electrophoresis with running buffer 1x MOPS at 70V for ~2 hours. If the total RNA had been successfully extracted, two bands could be detected under UV light, representing the 18S and 28S ribosome subunits. The samples with successfully extracted total RNA were further used in reverse transcription PCR.

Synthesis of cDNA

Synthesized of cDNA from the extracted RNA samples used Taqman Reverse Transcription Reagent (Applied Biosystems, Foster City, CA, USA, Part No. N808-0234). All the components come in ready to use state and include 10x Taqman RT buffer, 25 mmol/L MgCl₂, deoxy NTP mix, Random Hexamer, Rnase inhibitor and Multiscribe reverse transcriptase. The reactions were incubated at 25°C for 10 minutes, at 48°C for 30 minutes and then for 5 minutes of inactivation at 95°C. The final concentration of cDNA was 10 ng/μL.

Quantification of specific mRNA species

Real time PCR quantification of specific mRNA used the ABI Prism 7000 sequence detection system (Applied Biosystems, Foster City, CA, USA). The cDNA samples were run in duplicates with the final volume of 25 μL/well containing final concentrations: 1x Taqman Universal PCR Master Mix (Applied Biosystems, Foster City, CA, USA), 1x Assay Mix with pre-manufactured probes for studied genes (Applied Biosystems, Foster City, USA), and 2.2 μL of 10 ng/μL cDNA sample. The probes were labeled with fluorogenic dye FAM and ROX. The thermal cycling conditions were initiated by UNG activation at 50°C for 2 minutes, and an initial denaturation at 95°C for 10 minutes followed by 40 cycles at 95°C for 15 seconds and annealing at 60°C for 1 minute. In order to quantify the amplification products, a comparison with a calibration curve was made. This curve was obtained by 10-fold dilution of the template DNA (0.08-80 ng). Two negative controls were also included in each amplification. The expression of all other genes was divided by the value for the housekeeping gene beta-actin in order to standardize the results, which were finally expressed as relative values.

Cell migration assay (I, II)

Cell migration was assayed in 12-well tissue culture plate inserts having polyethylene terephthalate track-etched membranes (10.5 mm diameter) with 8 μm wide pores (Fig. 4). Cells were suspended in medium without FBS to a final concentration of 1.5×10^5 cells/mL. An aliquot of the cell suspension, 0.5 mL, was added to the upper compartment, and 1.5 mL serum-free medium to lower compartment. Chemo-attractants were added to the lower compartment, and the cells were incubated at 37°C. After 24 hours incubation, remaining cells on the upper surface of the membrane were removed with a cotton swab before the inserts were fixed with methanol for 5 minutes and stained with Giemsa (12.5 %) for 15 minutes. Cells, which had migrated to the lower surface of the membrane, were counted. Four fields were counted on each membrane, and the mean was used as one observation. At least six membranes were evaluated in each group.

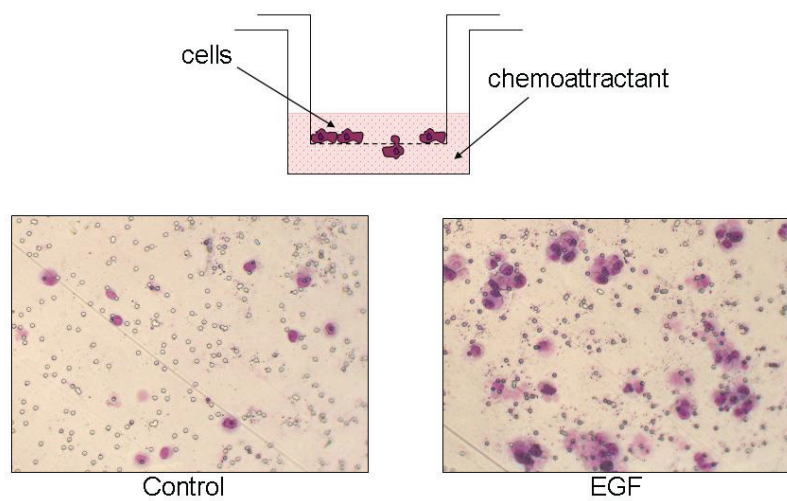


Figure 4. Cell migration assay in cell culture inserts. Cells were seeded on the insert membrane, which had 8 μm pores. Chemoattractants were added to the lower chamber. After 24 hours incubation, cells, which had migrated through the membrane, were counted on the bottom surface of the membrane.

Time-lapse video microscopy (I)

Cells were seeded on tissue culture dishes in low concentration ($4000/\text{cm}^2$) in order to visualize single cells (Fig. 5). One day after plating cells were given serum free medium for 3 hours before initiating the video microscope. The time-lapse video experiments were performed at 37°C and 5% CO_2 in a humidified and climatized chamber using a Zeiss Axiovert 200M microscope Goettingen, Germany.

Images were collected at 16 minutes intervals. EGF was added at time point 0 without interrupting the image collection. Pathways of cells were tracked using Improvion Velocity software 2.5 (London, UK) and median velocities were calculated for at least 36 cells per experiment.

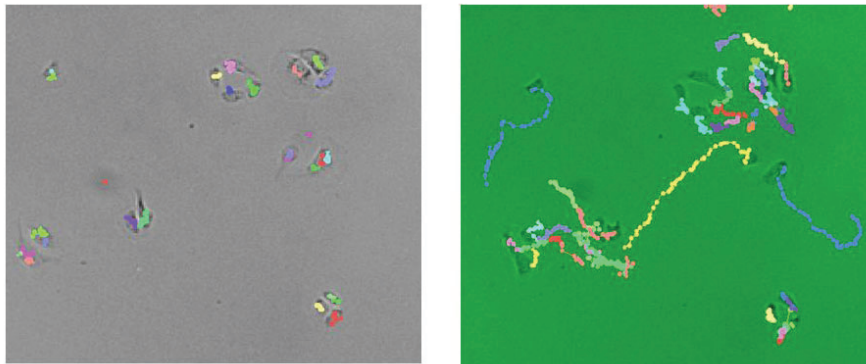


Figure 5. Time-lapse video microscopy. Individual cells are marked with different colors. Traces represent the migratory pathway of each cell during 24 hours following treatment with EGF.

Northern blotting for uPAR mRNA (I, II)

Total RNA was extracted from OVCAR-3 cells, size separated in agarose gels and transferred to GeneScreen Plus nitrocellulose filter [140]. The filters were hybridized with a cDNA probe for uPAR, which had been radiolabelled with ^{32}P -dCTP. In order to correct for unequal loading, the filters were subsequently hybridized with a probe for human β -actin, which had been identically labeled. After autoradiography, signal intensities were measured by computerized densitometric scanning (BioImage Products, Ann Arbor, MI, USA). Signal intensity of the uPAR probe was related to

intensity of the β -actin probe. The probe for uPAR, HUR06, was a 584-base pair BamHI fragment of the human uPAR gene subcloned into pBluescript KS [141].

Cellular binding of ^{125}I -uPA (I, II)

The HMW fraction of uPA was labeled with ^{125}I using the lactoperoxidase [142] or chloramine-T [143] procedures. Confluent cultures were incubated for 24 hours at 37°C in serum-free medium with stimulations as indicated. Following washing, cultures were incubated on ice for 2 hours with radio-labeled uPA in HBSS containing BSA 20 g/L. Cells were washed six times with ice-cold HBSS before being lysed with 1 mol/L NaOH. Radioactivity of the lysate was counted in a gamma counter. Specific binding was subsequently calculated by subtracting nonspecific binding, which was assayed in the presence of 100-fold molar excess of unlabeled uPA. The procedure described measures only free, i.e. non-occupied, receptor molecules. In order to assay the total number of receptor sites, endogenously bound uPA was removed by briefly (2-3 min) exposing the cells to acetate buffer 75 mmol/L, pH 3.0, containing CaCl_2 2.5 mmol/L, MgCl_2 0.5 mmol/L and NaCl 0.3 mol/L [144]. The number of occupied receptor sites was subsequently calculated as the difference between the numbers of total and free receptor sites.

Cellular degradation of ^{125}I -uPA:PAI-1 complex (I, II)

Cell cultures were incubated for 2 hours on ice with ^{125}I -uPA in complex with PAI-1, final concentration 1 nmol/L [144]. After washing 6 times with ice-cold HBSS, cultures were transferred to 37°C to allow internalization of the cell surface bound complex. After indicated time periods the media were collected, TCA added to a final concentration of 10%, and the mixture centrifuged at 3000 x g for 20 minutes. Radioactivity was measured in the supernatants. The cell pellets were lysed with NaOH for assay of protein content.

Western blotting for EGFR and uPAR (I)

EGFR. Cells to be analyzed for EGFR were extracted in lysis buffer and cell lysates were then centrifuged at 20,000 g for 10 minutes at 4 °C. Supernatants were

then assayed for protein concentrations and 20 µg was applied to each lane. Proteins were separated on NuPAGE 3-8% Tris-Acetate gel (Invitrogen, Carlsbad, California, USA). Proteins were blotted to PVDF membranes (BioRad, Hercules, California, USA). The primary antibodies were either a monoclonals directed to EGFR phosphorylated on tyrosine #1173(Santa Cruz Biotechnology), or to all forms of EGFR (Santa Cruz Biotechnology). For detection we used ECL Western blotting detection reagents and analysis system (Amersham Biosciences, Little Chalfont, UK).

uPAR. Confluent OVCAR-3 cells were grown with or without 10µg/L of EGF for 24 hours prior to harvesting. Cells to be analysed for uPAR were lysed, and the clarified lysates were subject to temperature-dependent phase separation [145]. Proteins were separated on 12% SDS-PAGE (Biorad) and electro blotted onto polyvinylidene difluoride membranes (Immobilon-P, Millipore, Bedford, MA, USA). Membranes were blocked using 2% skimmed milk powder in TBS, and subsequently probed with 5 µg/mL of monoclonal antibody R3 reacting with an epitope on domain I, and R2 reacting with an epitope on domain III. Both antibodies were kind gift from dr. Gunilla Høyer-Hanssen (Finsen lab., Copenhagen, Denmark). Peroxidase conjugated rabbit anti-mouse immunoglobulins (Dako, Glostrup, Denmark) diluted 1:2000 in TBS containing 2% skimmed milk powder were used for detection. The ECL detection system (Amersham) was used for visualization of the bands.

Membrane protein extraction and Western blotting for GPR30 (III)

Ovarian tumor tissue (65-75 mg) was disintegrated in homogenizing buffer at 4°C using QIAGEN TissueLyser (Retsch Technology GmbH, Haan, Germany). Tissue debris and nuclei were removed by spinning the lysates at 1000 g for 10 minutes at 4°C. Supernatants were filtered through one layer of gauze and subsequently centrifuged at 40 000 g for 45 minutes at 4°C, in order to obtain the membrane fraction. The pellet was washed, re-suspended in buffer, and sonicated for 5 seconds with the Ultrasonic processor UP50H (Hielscher Ultrasonics, GmbH, Teltow, Germany). The total protein concentration was determined by the BCATM protein assay kit (Pierce Biotechnology, Rockford, IL, USA #23227). Samples were stored at -20°C until used.

Each sample of membrane fraction (10-20 µg total protein) was mixed with LDS sample buffer (Invitrogen, Carlsbad, CA, USA #NP0007) and DTT 0.5 mol/L, and

incubated for 10 minutes at 70°C before they were subjected to SDS-PAGE on a 12% NuPage™ 12 lanes Bis-Tris gel (Invitrogen #NP0342BOX) using XCell Surelock™ MiniCell (Invitrogen #EI0002). Proteins were transferred to polyvinylidene difluoride membranes (Bio-Rad, Hercules, CA, USA #162-0184) by semi-dry electroblotting. Membranes were subsequently blocked with Non-Fat Dry Milk (Bio-Rad #170-6404) in TBS-Tween at 4°C overnight. Next day, the membranes were incubated for 1 hour with a rabbit antibody against human GPR30, LS-A4290 (Life Span Biosciences, Seattle, WA, USA) or PA1-24561 (Affinity Bioreagents, Golden, CO, USA) diluted 1:1000. After washing 1 x 15 minutes and then 3 x 5 minutes in TBS-Tween, the membranes were further incubated for 1 hour with a secondary antibody, i.e. goat antibody against rabbit IgG labeled with horseradish peroxidase (Santa Cruz Biotechnology Inc., CA, USA #sc-2030) diluted 1:10000. Membranes were again washed in TBS-Tween supplemented with sodium chloride 0.2 mol/L. Immune-complexes were detected by the ECL Plus Western Blotting Detection System (GE Healthcare, Amersham, Little Chalfont, UK #RPN2132) and membranes were exposed to Hyperfilm™ ECL (GE Healthcare #28906836) for 30 minutes.

Biosynthetic labeling (I)

Confluent OVCAR-3 cells in 6 well plates were grown for 12 hours in methionin-free DME medium, and subsequently in medium containing ³⁵S-methionin 10 mCi/L (Amersham) for 12 hours. After washing, the cells were incubated with EGF (10 µg/L), colchicine (1 mg/L) or vehicle for 24 hours, washed, extracted in lysis buffer containing EDTA 10 mmol/L, Triton X114 1%, aprotinin 2 mg/L, and PMSF 0.1 mol/L, and centrifuged at 20,000 g for 10 minutes at 4 °C. Each supernatant was pre-cleared with 10 µL Protein-A agarose for 30 minutes and centrifuged. uPAR was subsequently immuno-precipitated using a mixture of two monoclonal antibodies to uPAR, R3 and R4 (each 3 µg/well for supernatant, and 6 µg/well for cell lysates). This was followed by 20 µL Protein-A agarose centrifugation. Precipitates were washed three times with lysis buffer and subsequently counted in a liquid scintillator.

Immunoassays

ELISA for uPAR/suPAR (I, II)

The conditioned media were collected and cells were lysed with lysis buffer. The total amount of uPAR was assayed in cell lysates and suPAR was measured in conditioned media [146]. R2, which binds all forms of uPAR containing domain III, is used as catching antibody. The plates (96-well microtiter Maxisorp plate, Nunc) were coated over-night at 4°C with 3 µg/mL R2 diluted in 0.1 mol/L Na-carbonate buffer, pH 9.5. The plates were blocked by rinsing with Superblock solution (Pierce Chemical Company, Rockford, IL). The samples were diluted in 0.2 mol/L sodium phosphate buffer pH 7.2, containing 0.1 mol/L NaCl, 50,000 U heparin sodium salt (Sigma), 10 g/L BSA (Fraction V, Boeringer-Mannheim) and 1 g/L Tween 20. The plates were incubated for 2 hours at 30°C and subsequently washed 6 times with above-mentioned washing buffer. The detecting antibody, a polyclonal anti suPAR antibody, was added at 1 µg/mL and incubated over-night at 4°C. After washings a monoclonal anti-rabbit immunoglobulin antibody conjugated with alkaline phosphatase (Sigma), was added in 1:2000 dilution for 1-hour. After a final washing step, the substrate p-nitrophenyl phosphate (Sigma) was added, and the plates were read in a Ceres automatic plate reader (Bio-Tek Instruments) at absorbance 405 nm at room temperature. Six readings were obtained every 10 minutes for 1 hour and the slope of the color development curve is calculated by the KinetiCalc Software (Bio-Tek Instruments) using linear regression.

ELISA for uPA and PAI-1 (I)

The concentrations of uPA and PAI-1 in conditioned media were assayed using the commercial ELISA kits Tint Elise uPA™ and Immulyse PAI-1™ (Biopool, Umeå, Sweden).

Solid phase EIA for ERα (II)

ERα was assayed in cell lysates using a commercial enzyme immunoassay (EIA) kit ABBOTT ER-EIA Monoclonal (ABBOTT Laboratories, North Chicago, IL, USA). The assay used beads coated with a monoclonal anti-ERα. The secondary antibody was also a monoclonal anti-ERα conjugated with horseradish peroxidase. After washings, the beads were incubated with the substrate solution (hydrogen

peroxide and o-Phenylenediamine 2 HCl). The reaction was stopped with 1N sulphuric acid, and the color read at 492 nm. The assay was performed in an Oncology routine lab, and cellular content of ER α was related to the level, which is clinically relevant for breast tumor tissue.

TR-FIAs for uPAR fragments (IV)

Three uPAR immunoassays, TR-FIA 1, 2 and 3, have been designed for the specific measurement of uPAR(I-III), uPAR(I-III) + uPAR(II-III), and uPAR(I), respectively [44]. The detection limits were 0.3 pmol/L of suPAR(I-III) for TR-FIA 1 and 2 and 1.9 pmol/L of uPAR(I) for TR-FIA 3. The assays were previously validated for use in citrate plasma diluted 1:10 [44]. Since the amounts of uPAR(I) in citrate plasma diluted 1:10 is close to the limit of quantification we decided to only dilute our samples 1:5 in assay buffer (DELFI[®] assay buffer #1244-111). The assays were therefore validated for their use in citrate plasma diluted 1:5. The limit of quantification was determined by spiking suPAR depleted citrate plasma with purified suPAR and examining the coefficient of variation (CV). suPAR depletion of plasma diluted 1:5 was achieved as described previously [44]. The depleted plasma was spiked with a concentration range from 0.016 μ g/L to 10 μ g/L of purified standards (0.5–325 pmol/L suPAR(I-III), 1.5–961 pmol/L uPAR(I)). The limit of quantification was defined as the concentration at which CV exceeded 20%.

Intra-assay precision was determined by measuring the donor citrate plasma pool in TR-FIA 1 (n=26), TR-FIA 2 (n=28) and calculating the CVs. For TR-FIA 3 (n=27) we used donor citrate plasma pool spiked with 480 pmol/L of uPAR(I). The same samples were employed for determination of inter-assay precision (n=24).

The amount of suPAR(II-III) was obtained by subtracting the moles of suPAR(I-III) measured in TR-FIA 1 from those of suPAR(I-III) and suPAR(II-III) measured in TR-FIA 2.

Immunoassay for CA125 (IV)

Preoperative plasma samples were routinely assayed for CA125 using a commercial electro-chemo-luminescence immunoassay Elecsys CA125 kit[™] (Roche). The assay was performed according to the manufacturer's instructions.

Statistical methods

Data are presented as median and percentiles in box plots (I, II) or scatter plots (III). The Mann-Whitney test was used to evaluate the significance of differences between groups. Deviation of expression related to gradual histological de-differentiation was analyzed for statistical significance using test for trend (paper III). Comparing the number of samples with high versus low levels between groups used Fisher's exact test.

In paper IV, descriptive statistics for the plasma content of different suPAR forms and CA125 stratified by the histo-pathological group and stage are presented by box-whisker plots showing their medians, quartiles and extreme values. Tests for location comparing the histo-pathological groups was performed using the Kruskal-Wallis test and if significant, pair wise comparisons have been done using the Mann-Whitney U test. Tests for independence between the histo-pathological groups and uPAR(I) used the chi-square test. Trend tests for ordered groups employed linear regression with the dependent variable log transformed. Spearman's rank correlation was used as a measure of association between the studied biomarkers.

Analysis of discrimination between the benign, borderline and invasive tumor groups used a proportional odds model with biomarkers either log transformed or dichotomized. Backwards selection was used to identify the significant biomarkers (less than 5%). Results are presented by the respective odds ratios and 95% confidence intervals (CI). The receiver operating characteristic (ROC) curve and the area under curve (AUC) with 95% confidence intervals are presented for comparison of borderline and invasive tumors to benign tumors. The specificity for fixed sensitivities was calculated for the combination of suPAR(I-III)+suPAR(II-III) and CA125 as well as the false positive and false negative rates computed as posterior probabilities using Bayes' theorem. The Cox proportional hazards model was used for univariate and multivariate analysis. Point estimates are reported as hazard ratios (HR) with 95% CI. For graphical presentation of overall survival probabilities were estimated using the Kaplan-Meier method, dichotomizing biomarker levels by their respective medians. Multivariate analysis of the suPAR components using backwards selection was used to identify a model for use in a final model including CA125, grade, stage, age and residual tumor, all significant in univariate analysis.

All comparisons were two-sided, and a 5% level of significance was used. The statistical analyses were performed using SPSS™ (11.5.1) and SAS (v9.1, SAS Institute, Cary, N.C., USA).

RESULTS AND COMMENTS

EGF stimulates cell migration and uPAR expression

We found that EGF stimulated cell migration in all seven ovarian cancer cell lines we used in the study. Since the uPA-system plays a crucial role in the process of cell migration, we studied the effects of EGF on the u-PA system in three of these cell lines: OVCAR-3, SKOV-3, and SKOV3-IP. Stimulation with EGF resulted in increased content of uPAR, uPA and PAI-1 in all three cell lines. Further on, using OVCAR-3 cells as a representative cell line, we explored possible mechanisms whereby EGFR activation regulates the expression of uPAR.

OVCAR-3 cells express both EGFR and uPAR. EGF stimulation of cell cultures resulted in fast increase of uPAR mRNA after 2 hours, and uPA mRNA and PAI-1 mRNA after 1 hour, suggesting a direct effect of EGFR signaling on transcription of these genes. The level of mRNA stayed increased for 12 hours. Extractable cell-associated uPAR as well as shed soluble uPAR (suPAR) in the conditioned medium was increased. Western blot demonstrated that only full-length uPAR, consisting of three domains, was present. Binding experiments with radio-labeled uPA and OVCAR-3 cells demonstrated that only the endogenously occupied fraction of uPAR was increased after stimulation with EGF.

Increased concentration of receptor molecules on the cell surface can result from increased production, but also from decreased shedding from the cell surface or decreased internalization and intracellular degradation. As mentioned above, we found EGF stimulation to result in an increase of uPAR mRNA, suggesting an increased production. Also as mentioned, we found increased rather than decreased accumulation of shed suPAR in the medium, thus eliminating decreased shedding as a possible mechanism.

Next, we wanted to examine whether EGF may increase the amount of cell surface uPAR by inhibiting the internalization and degradation processes. This seemed like a real possibility, since we found that colchicine, which blocks the internalization mechanism through disruption of the cytoskeleton, increased uPAR on the cell surface. By measuring accumulation of free ^{125}I in the medium after binding of ^{125}I -uPA:PAI-1 complex to the cells it was possible to compare degradation of the

complex in EGF-treated and non-treated cells. We found that EGF inhibited the internalization and degradation process. Since the complex is bound to uPAR during internalization, our results suggest that internalization of uPAR is also decreased. Decreased internalization is thus a second mechanism whereby EGF increases expression of uPAR. Furthermore, since treatment with colchicine results in accumulation of uPAR both in the cells and in the medium in the absence of cell migration, we conclude that shedding is independent of cell migration and rather secondary to accumulation of uPAR at the cell surface.

Finally, monitoring the response to EGF over 24 hours by quantifying uPAR protein in cell lysates with ELISA and cell migration with time-lapse video microscopy, demonstrated that cell migration as well as uPAR protein had two maxima. The first increase of uPAR came within minutes after EGF stimulation and lasted for two hours. This very early increase of uPAR protein is likely to result from mobilization of uPAR from detergent-resistant domains, like lipid rafts [147]. The second increase, which was detected between 8 and 12 hours after EGF stimulation, fits time-wise with translation of increased uPAR mRNA. Decreased internalization and degradation of uPAR may add to both peaks. Cell migration mimicked the pattern of uPAR expression. The first increase started after 1 hour and lasted 6 hours, and the second increase started 10 hours after stimulation with EGF.

The uPAR-EGFR relation

Both EGF and uPA stimulate cell migration. According to previous reports, the EGFR serves as a transducer of the signal from activated uPAR [59, 148]. We showed that migration in response to uPA was reduced by Iressa, an inhibitor of intrinsic EGFR tyrosine kinase. Furthermore, a monoclonal antibody to uPAR, R3, which inhibits binding of the ligands uPA and vitronectin, abrogated EGF stimulated cell migration. There was no additive effect when R3 and Iressa were combined. These data suggest that activations of EGFR and uPAR are steps in the same chain of events and engaged in the same multi-protein signaling complex.

Tyrosine #1173 in the EGFR molecule is reportedly phosphorylated after ligand activation of both EGFR and $\alpha\beta 3$ integrin receptor [149]. Since activated uPAR can interact with the $\beta 3$ integrin subunit [55], we used an antibody directed to phosphorylated tyrosine #1173 to explore the relation between stimulation of EGFR

and uPAR in our system. Stimulation of OVCAR-3 cells with EGF resulted in fast phosphorylation of tyrosine residue #1173 of EGFR and subsequent down-regulation of EGFR within 6 hours. In contrast, neither phosphorylation of tyrosine residue #1173 nor down-regulation of EGFR was seen after stimulation with uPA.

Estradiol (E2) attenuates the EGF effect

Estradiol alone had no effect on cell migration in any of the seven ovarian cancer cell lines. In contrast, E2 reduced EGF-induced cell migration in all of them. The amount of cell membrane bound uPAR mimicked the pattern of cell migration, after EGF and E2 treatment. Assay of cell surface bound ¹²⁵I-uPA in OVCAR-3 cells showed that E2 reduced only the endogenously occupied fraction of uPAR, i.e. the fraction that was increased by EGF. Neither EGF nor E2 affected non-occupied uPAR.

We investigated which of the EGF mechanisms that is modulated by E2. The EGF-induced increase of uPAR mRNA was not reduced by E2. Also, E2 did not modify EGF-reduced internalization and degradation of the ¹²⁵I-uPA:PAI-1 complex. The EGF-induced increase of shed uPAR was also not modified by E2. Thus, E2 affects neither EGF-induced increase of uPAR mRNA nor EGF-induced decrease of internalization and degradation. However, E2 did reduce EGF-induced rapid increase of uPAR, which probably reflects inhibition of mobilization of uPAR from detergent resistant lipid rafts.

Identifying the E2 receptor

Next question was which estrogen receptor that mediates this effect, since OVCAR-3 cells express only insignificant amounts of ER α mRNA and protein. They do however express ER β mRNA as well as GPR30 mRNA.

We used ligands, which are antagonists for nuclear ER, but agonists for the recently identified estrogen receptor GPR30, i.e. ICI 182780 and tamoxifen. We also employed a specifically constructed GPR30 agonist G1, which does not bind to nuclear ER. All these compounds mimicked the effect of E2 on uPAR expression and cell migration. Also, when given together ICI 182780 did not inhibit the effect of E2, which would have been the case if this effect was mediated by a nuclear ER. These

data taken together suggest that the effect of E2 is not mediated via any known nuclear ER, but via the membrane estrogen receptor GPR30.

Expression and regulation of GPR30 in ovarian cancer cell lines

All seven ovarian cancer cell lines expressed GPR30 mRNA. Highest expression was found in TOV-112D and TOV-21G cells.

Expression of ER α mRNA was highest in Hey-TG and SKOV3-ip cells. The message was barely detectable in OVCAR-3, and not detectable in TOV-112D and TOV-21G.

The pattern of ER β mRNA expression had similarities to that of GPR30 mRNA. The highest expression was found in TOV-112D followed by TOV-21G.

The highest expression of EGF mRNA was seen in Hey-TG cells, followed by ES-2 cells. TOV-21G had low and TOV-112D had no expression of EGF mRNA.

Expression of HB-EGF mRNA was detected in all cell lines. It was highest in ES-2 cells and lowest in TOV-112D cells.

EGFR mRNA was detected in all seven cell lines. Expression was low in TOV-112D and in TOV-21G, but on a similar level in the other five cell lines.

The level of HER2 mRNA was high in Hey-TG cells and low in TOV-112D and TOV-21G cells. ES-2 cells expressed the message in very low quantities.

We analyzed GPR30 mRNA expression in the cell lines after treatment with E2 or/and EGF for 6 hours. Either E2 or EGF regulated expression of GPR30 in all seven cell lines. We identified three patterns of regulation, i.e. up-regulation by estradiol in ES-2 cells, up-regulation by EGF in TOV-21G cells, and down-regulation by EGF in the other five cell lines.

Expression of GPR30 in ovarian tumor tissue

All samples of ovarian tumor tissue expressed GPR30 mRNA. The level of expression was not different between histological types of tumors, but it varied with histological differentiation. The expression was higher in benign tumors than in poorly differentiated malignant tumors. However, there was a peak of expression in the well differentiated tumor group, which gives this group significantly higher levels than the benign and poorly differentiated tumor groups. No other parameter had a similar peak in the well differentiated tumor group. When analyzing six samples with

markedly elevated GPR30 mRNA levels we found that they were not different with respect to histological type. They tended to have higher levels of ER α (p=0.06), but not of ER β or any member of the EGF system. There was also a weak positive correlation between GPR30 and ER α when the poorly differentiated group was excluded. This may indicate either that expression of GPR30 is upregulated by ER α , or that both receptors are co-regulated by yet another mechanism. A significant but incomplete association between GPR30 and ER α has also been described in breast carcinomas [150].

ER α mRNA was higher in truly malignant tumors than in benign and borderline tumors whereas the opposite was true for ER β . Thus EGF influences GPR30 expression, we analysed expression of mRNA of components of EGF system. The expression of EGF mRNA and HER2 mRNA tend to increase with loss of histologic differentiation, whereas EGFR had opposite trend.

Western blots demonstrated GPR30 protein in both benign ovarian tumors and malignant tumors of different histological differentiation. The bands were stronger in malignant than in benign tumors. Also, all seven ovarian cancer cell lines had GPR30 protein.

Cleaved forms of uPAR as diagnostic markers

The different forms of suPAR were measured in preoperative plasma samples obtained from 335 patients with ovarian tumors using three different time-resolved fluorescence immuno-assays (TR-FIA). TR-FIA 1 measures only intact suPAR, i.e. suPAR(I-III). TR-FIA 2 measures suPAR(I-III) together with the cleaved form suPAR(II-III). TR-FIA 3 measures only the cleaved uPAR(I). Tumors were classified as benign (n=211), borderline = possibly malignant (n=30), and well (n=19), moderately (n=15), and poorly (n=60) differentiated malignant.

There were no differences in levels of any suPAR form between patients with different variants of benign ovarian cysts. In contrast, CA125 levels were significant higher in patients with endometriosis compared to other ovarian benign cysts (p<0.001).

We found the plasma level of each suPAR form to be higher in patients with borderline and invasive tumors than in those with benign tumors. Furthermore, the level of both suPAR(II-III) and suPAR(I-III)+suPAR(II-III) was higher in patients

with malignant tumors as compared to those with borderline tumors ($p < 0.009$; $p = 0.03$). These results suggest that proteolytic cleavage as well as shedding of uPAR is increased already in borderline tumors but most pronounced in malignant tumors. In contrast, we did not find any difference in the levels of suPAR(I-III)+suPAR(II-III), suPAR(I-III), suPAR(II-III) or uPAR(I) between histologic grades or clinical stages within the malignant group. The fact that suPAR was independent of clinical stage indicates that it does not reflect tumor extension, involvement of peritoneal surfaces, formation of ascitic fluid, or metastases.

All suPAR forms, as well as CA125, discriminated between benign, borderline, and malignant tumors in univariate analysis ($P < 0.0001$). We showed that the plasma content of suPAR(I-III)+suPAR(II-III) has diagnostic potential in patients with ovarian cancer. The product of suPAR(I-III)+suPAR(II-III) and CA125 detects early stage tumors better than each marker separately. The ROC curve for the product of suPAR(I-III)+suPAR(II-III) and CA125 yields AUC 0.94 (95% CI, 0.90-0.98) when comparing benign and invasive tumors, and AUC 0.78 (95% CI, 0.67-0.89) when comparing benign and borderline tumors. This is higher than any other proposed biomarker.

Cleaved forms of uPAR as prognostic markers

We have analyzed overall survival in 94 patients with invasive malignant ovarian tumors. Median follow-up time was 64 months. We found that elevated levels of all suPAR forms were associated with poor prognosis in univariate Cox regression analyses and Kaplan-Meier curves.

Furthermore, in multivariate analyses, which included the preoperatively available covariates uPAR(I), CA125 and age, high levels of uPAR(I) came out as an independent predictor of poor prognosis (HR=1.84, 95% CI: 1.15-2.95, $P = 0.011$).

DISCUSSION

Mechanisms of EGF regulation of cell surface uPAR in ovarian cancer cells

EGF stimulates cell migration in ovarian cancer cells and upregulates components of uPA system: uPAR, uPA, and PAI-1. Upregulation of uPAR, uPA, and PAI-1 mRNA was significant already after 1 to 2 hours suggesting direct effect of EGFR signaling on transcription of these genes. This is in contrast to previous report in squamous carcinoma cells, which suggested that up-regulation of uPA and uPAR genes was secondary to induction of c-fos and c-jun, which constitutes activator protein-1 (AP-1), a transcription factor [151].

Expression of uPAR on the cell surface reflects the balance between production on one hand, and shedding from the cell surface and internalization with subsequent intracellular degradation on the other hand. We analysed in which way EGF influenced these processes in OVCAR-3 cells.

EGF stimulation increased uPAR mRNA significantly after 2 hours and significant increase of cell-associated protein uPAR was seen, as expected, after 8 hours. Western blot experiments showed that only intact 3-domain uPAR was present, despite the presence of uPA. This is interesting, since uPAR can be cleaved in the linker region between domains I and II by uPA, but also by other proteases like trypsin, chymotrypsin, elastase, metalloproteases, and cathepsin G [42]. Possible explanations include that the uPA concentration was not high enough, that other uPAR interactions prevented cleavage, or that the crucial enzyme is different from uPA, or that the cleaving enzyme is not produced by cancer cells but stromal cells.

Cell surface uPAR can be eliminated either via shedding to the extra-cellular fluid or via internalization and subsequent degradation together with the uPA:PAI-1 complex. Decreased shedding as a cause for increased cell surface uPAR after stimulation with EGF was excluded, since we found increased suPAR in conditioned media in EGF treated cultures. The mechanism of suPAR shedding is not clarified. In order to clarify if shedding is consequence of cell migration or just secondary to the accumulation of uPAR at the cell surface, we treated cells with colchicine and EGF. Colchicine deranges cytoskeleton and inhibits both cell migration and endocytosis. Decreased internalization results in accumulation of uPAR at cell surface, but also, as we found, extensive shedding. In contrast, EGF stimulation, which also results in

accumulation of uPAR on the cell surface and increased shedding of uPAR, was accompanied by increased cell migration. We concluded that shedding was secondary to accumulation of uPAR at the cell surface and independent of cell migration.

The second mechanism whereby EGF increases expression of uPAR is decreased internalization, which we found significant 8 hours after treatment with EGF. Internalization of the uPAR:uPA:PAI-1 complex is mediated by endocytosis receptors like LRP or VLDLR, which target the complex for degradation in the lysosomes. Even though some of internalized uPAR is reportedly recycled back to the cell surface, receptor binding of the uPA:PAI-1 complex results in significant down-regulation of uPAR [27, 152]. A mechanism that can possibly explain our observation that internalization and degradation of uPAR in complex with ¹²⁵I-uPA:PAI-1 decrease after treatment with EGF, is down-regulation of involved endocytosis receptors, as previously reported [153].

Finally we found a mechanism, which was unexpected. EGF stimulation was followed by an immediate increase of cell surface uPAR, and this was accompanied by transient increase of cell migration. This can neither be explained by increased production nor by decreased internalization/degradation of uPAR. The response within minutes suggests translocation of uPAR molecules from cryptic detergent resistant domains to the cell surface where uPAR is detergent extractable. Our finding is comparable with that of Plesner et al, who showed a rapid increase of uPAR in neutrophils after treatment with cytokines or phorbol esters [154]. Thus uPAR occurs in different compartments with different detergent solubility. The instant increase in detergent soluble uPAR in response to EGF is likely to represent recruitment of uPAR from detergent-resistant domains, like lipid rafts [147].

uPAR-EGFR relation

Both uPAR and EGFR are over-expressed in ovarian cancer and both play important roles in migration, invasion and proliferation of tumor cells. The interaction between these two membrane receptors is not fully clarified. OVCAR-3 cells express both uPAR and EGFR and both are involved in the migratory response to uPA and EGF. We found that inhibition of EGFR activation by Iressa inhibited migration in response to uPA. This is in agreement with a previous report that EGFR is a transducer of the uPAR initiated signal [59, 148]. Activated uPAR binds the β -

subunits of several integrins, and promotes integrin association with and transactivation of EGFR. Such activation of EGFR is ligand independent. Recently, Lee et al also showed that Iressa suppresses proliferation and invasion of human oral squamous carcinoma cells via a uPAR dependent mechanism [155].

Furthermore, we found the migratory response to EGF to be blocked by the anti-uPAR antibody R3, which prevents binding of uPA to uPAR. This observation suggests that uPAR and EGFR activations are steps in the same chain of events, and are engaged in the same multi-protein signaling complex. The fact that blocking both receptors is not more efficient than blocking each of them separately gives further support to this statement. Activated uPAR as well as activated EGFR can potentially associate with several integrin receptors in multiprotein signaling receptor complexes, which influence cell functions like adhesion, migration, and proliferation, and result in a malignant phenotype [57, 58, 149, 156]. Actually, uPAR and EGFR coimmunoprecipitate and $\beta 1$ integrin has been co-localized on the cell surface with both uPAR and EGFR [59, 79, 157].

Ligand binding as well as binding of integrin receptors to EGFR results in autophosphorylation of specific tyrosine residues within intracellular domain of EGFR. Subsequently the ligand-receptor complex is internalized for lysosomal degradation [77]. Our Western blotting experiments confirmed phosphorylation of the specific tyrosine residue #1173 after stimulation with EGF. Down-regulation of activated EGFR was also seen after 6 hours. In contrast, neither phosphorylation of tyrosine #1173, nor down-regulation of EGFR was seen after stimulation with uPA. This was in contrast to what might have been expected, since activation of uPAR results in association of integrin receptors with EGFR and its activation [59, 149]. Phosphorylation of EGFR probably occurred in our experiments in response to uPA stimulation since Iressa inhibited the migratory response to uPA, but apparently it did not involve tyrosine #1173. In this context it may be more surprising that the EGFR was not down-regulated following uPA stimulation. This may suggest that EGFR was not trans-activated in our experimental design and that Iressa blocks tyrosine phosphorylation in some other crucial signaling molecule.

Estradiol modulates the response to EGF on cell migration and uPAR expression

Estrogens reportedly stimulate proliferation in ovarian cancer cells, and this effect is mediated via ER α and involves stimulation of growth regulating genes [110, 158]. In contrast to estrogens role in cell proliferation, their role in cell migration and invasion has remained unclear. However, recently Park et al showed that E2 promotes cell migration in ER α positive BG-1 ovarian cancer cells through down-regulation of E-cadherin, which was secondary to up-regulation of the transcription suppressors Snail and Slug [159]. In contrast to this stimulatory effect of ER α , over-expression of ER β had inhibitory effect on cell motility.

Our results show that E2 had no effect by itself on migration in any of seven ovarian cancer cell lines we examined. However, we did not have the opportunity to study BG-1 cells. Expression of ER α mRNA in our cell lines was in general low, and also those cell lines with highest expression of ER α mRNA, Hey-TG and SKOV-3ip, had ER α protein levels below the cut-off level used for ER α positivity in malignant breast tumors. From this point of view, our result is in agreement with Parks finding.

Thus, E2 attenuates the invasive phenotype, which results from EGF stimulation by reducing EGF stimulated cell migration as well as cell surface uPAR. Only the endogenously occupied pool of uPAR was affected. This ligated pool of uPAR is concentrated at focal adhesion sites in the leading edge of migrating cells [53]. We found that EGF up-regulates cell surface uPAR via three distinct mechanisms, but E2 modulates neither EGF increased expression of uPAR mRNA, nor decreased internalization and degradation of PAR. However, E2 inhibited the rapid mobilization of uPAR from detergent resistant domains, which occurs within few minutes of EGF stimulation. This seems to be a generalized effect, since migration was inhibited to varying extent in all of seven cell lines. The mechanism whereby uPAR is re-located from detergent insoluble domains, presumably lipid rafts, to the detergent soluble pool is poorly understood. Lipid rafts are cholesterol and sphingolipid rich morphologically distinct membrane domains. Several membrane receptors including EGFR and uPAR associate with membrane rafts. The lipophilic character of the GPI anchor attracts uPAR to lipid rafts. Interestingly, only occupied uPAR accumulates within this domain [147]. Lipid rafts serve as platforms to concentrate receptors and assemble the signal transduction machinery, but also to recruit endocytosis proteins [160].

The estradiol effect involves GPR30

Generally, effects of E2 can be mediated either by nuclear ERs, i.e. ER α and ER β , which in their ligated state bind to response elements in estrogen sensitive genes, or by a membrane ER like the recently identified G-protein coupled receptor GPR30 [136, 137, 161]. We found that OVCAR-3 cells express GPR30 and ER β , whereas the level of both ER α protein and ER α mRNA was negligible. The fact that both ICI 182780 and tamoxifen showed agonistic properties with E2 in modulating the response to EGF suggest that this effect is not mediated via nuclear ER, but via GPR30, since these ligands are agonists to GPR30 [135]. Furthermore, our finding that a specifically designed GPR30 agonist G1, inhibited EGF stimulated cell migration, strongly supports our conclusion. Also, the observation that ICI 182780, which is a pure inhibitor of E2 binding to nuclear ER, did not antagonize the effect of E2 further supports the conclusion.

The interaction between GPR30 and EGFR is complex. Filardo et al showed that E2 and anti-estrogens trans-activate EGFR via GPR30 [78, 136]. Actually, two distinct G protein signaling pathways seem to have opposing signaling effects on the EGFR to MAPK axis [135]. One pathway, including G β and G γ , activates Src and metalloproteinase dependent release of HB-EGF, which acts as a ligand to the EGFR with subsequent activation of the MAPK pathway. The other pathway involves G-protein α activation of adenylyl cyclase and cAMP, which inhibits Raf activation [135]. Activation of GPR30 results in activation of second messengers, which may influence mobilization of uPAR from lipid rafts. Furthermore, E2 is potent activator of sphingosine kinase-1, which may potentially influence sphingolipids as well as proteins bound to them in the lipid rafts [162].

The data we have presented, together with the fact that all seven analyzed cell lines express GPR30, support the suggestion that EGF induced cell migration is inhibited by E2 via GPR30, and that this effect is a common feature in variety of ovarian cancer cells.

GPR30 expression in malignant ovarian tumors opens new perspectives and should be explored for prognostic relevance. More importantly, specifically designed agonist molecules may be employed for targeted tumor therapy.

GPR30 expression in primary ovarian tumors and ovarian cancer cell lines

Expression of GPR30 protein was previously reported in primary breast and endometrial cancer as well as in variety of cell lines originating in hormone producing or dependant tumors, like breast cancer [163] [78] [136] [137], endometrial cancer [137] [164], choriocarcinoma [137], 2005), and thyroid cancer [165]. Furthermore, Wang et al showed that GPR30 is expressed in hamster ovarian tissue, and that expression is regulated by gonadotropins [134].

We found that primary ovarian tumors as well as ovarian cancer cell lines, express both GPR30 mRNA and protein (III). GPR30 mRNA expression was lower in poorly differentiated malignant tumors than in benign tumors. However, in addition to this decline, which seemed to accompany loss of histological differentiation, there was a peak in well differentiated malignant tumors. This pattern, which is unlike the other genes we examined in this set of tumors, suggests one mechanism which up-regulates GPR30 gene expression in well differentiated tumors, but also another mechanism which down-regulates gene expression in poorly differentiated tumors.

Correlation between GPR30 mRNA and GPR30 protein expression is however poor, since our Western blot results indicate that poorly differentiated tumors contain considerably more GPR30 protein than benign tumors. Well differentiated tumors express at least as much GPR30 protein as poorly differentiated tumors. Thus, our GPR30 protein data suggest a different expression pattern between benign and malignant tumors than that suggested by our GPR30 mRNA results. Possible explanations include more efficient translation of the mRNA or reduced turnover of the protein in malignant samples. Alternatively, since the probe used for real-time PCR is rather short and covers only one exon-intron border, the low levels of GPR30 mRNA detected in poorly differentiated tumors do not exclude that other molecular forms of the message is present. In fact, we have actually observed different molecular forms of GPR30 protein in Western blots of ovarian tumor tissue.

Immuno-histochemistry performed in a large number of malignant breast tumors found that over-expression of GPR30 protein was associated with poor prognostic parameters, like large tumor size, distant metastases, and over-expression of HER2 [150]. Interestingly, a subsequent study of GPR30 mRNA in breast carcinomas failed to identify similar correlations [166]. The discrepancy between GPR30 mRNA and

protein in breast cancer seems to parallel what we report for ovarian cancer in this paper.

We found that expression of the GPR30 gene was downregulated by EGF in five out of seven ovarian cancer cell lines. Since GPR30 gene expression was significantly down-regulated in poorly differentiated ovarian tumors, where expression of EGF and HER2 was up-regulated, it is possible that the EGF system actually is involved in down-regulation of the GPR30 gene in poorly differentiated malignant tumors, although we found no statistical correlation between mRNA for GPR30 and members of the EGF system in this set of ovarian tumors.

Expression of the two nuclear estrogen receptors ER α and ER β mRNA had opposite patterns in the tumors, i.e. ER α mRNA was increased whereas ER β mRNA was decreased in malignant as compared to benign tumors. This result is in accordance with previous studies of ER α and ER β in ovarian tumors in ovarian cancer [125, 167]. Thus, mRNA data as well as protein data suggest that over-expression of ER α as well as loss of ER β expression parallels malignant transformation in ovarian tumors. Differential expression of ER α and ER β in malignant tumors compared to benign tumors and normal tissue have previously been reported also in other estrogen dependent tumors such as breast and prostate cancer [168-170]. The relation of ER α and ER β respectively to malignant progression is furthermore highlighted by the following observations. Experiments using over-expression as well as knockdown of ER α and ER β demonstrate that estradiol up-regulates via ER α but down-regulates via ER β molecular markers for an invasive pro-metastatic phenotype in ovarian cancer cells [159]. High ER α expression in poorly differentiated ovarian tumors co-localize histologically with high proliferation index and low apoptotic activity [111]. Finally, Skliris et al found that high ER β expression was an independent predictor for disease-free survival as well as overall survival in multivariate analysis of patients with malignant ovarian tumors [168].

Diagnostic importance of cleaved forms of the uPA receptor

Ovarian cancer in stage I, when the disease is confined to the ovaries, has excellent curability as compared to the poor outcome in later stages. Thus, detection of ovarian cancer in early stages would be a most significant step to improve survival. However,

despite extensive efforts in biomarker discovery, current screening tests are still inadequate, mainly because of poor sensitivity in cases with early stage ovarian cancer, but also lack of specificity for some screening markers. The most useful tumor marker, CA125, is elevated in more than 90% of patients with advanced ovarian cancer, but only in 50% of patients with early-stage disease [23]. Combination of CA125 and trans-vaginal ultrasound improved sensitivity, but did not reach the specificity needed for a screening test, since it resulted in too many false positive tests leading to unnecessary surgery. Because of the relatively low incidence, an effective screening test requires almost 100% specificity, which will result in a low rate of false positive findings [171]. In order to reach this specificity, it is necessary to combine several biomarkers.

In the case of cervical cancer, effective screening for the pre-invasive stage radically reduced the mortality rate. In contrast, ovarian cancer has no corresponding pre-invasive stage, and may actually spread to extra-ovarian sites early in its development.

We found that concentrations of individual suPAR forms are different in peripheral blood plasma from patients with malignant as compared to benign ovarian tumors. However, we also found a clear distinction between benign and borderline tumors for all suPAR forms. Our previous study, where all forms of suPAR were measured collectively in an ELISA, did however not show a difference between benign and borderline tumors [45]. Our present results indicate that both shedding and cleavage of uPAR is increased in borderline tumors, although more pronounced in invasive tumors, and this is an important diagnostic aspect.

The level of suPAR in plasma seems not to be dependent on tumor burden, since there was no relationship between plasma suPAR levels and FIGO stage. Although stage does not necessarily reflect tumor burden or invasiveness, it reflects tumor extension, involvement of peritoneal surfaces, formation of ascitic fluid and metastases. In contrast to our present findings, two previous studies found a correlation between clinical stage and suPAR concentration in plasma. Riisbro et al. reported that the level of suPAR increased gradually from clinical stage I to stage IV [65], whereas Sier et al. found the highest levels of suPAR in clinical stage II [70]. In both studies suPAR was assayed with ELISAs, which measured a sum of suPAR forms. Furthermore, the number of patients included in these studies was considerably less than in our study.

We have previously reported that the content of uPAR mRNA in ovarian tumor tissue increased gradually with loss of histological differentiation [61]. In contrast, tumor tissue content of uPAR protein is actually highest in borderline and well differentiated malignant tumors, and is substantially reduced in poorly differentiated tumors [64]. This situation was also found in the cystic fluid of ovarian tumors [45]. These findings were interpreted to indicate an increased turnover of uPAR protein in the tumor tissue, when it is internalized together with an increasing load of uPA:PAI-1 complex. This may explain why concentrations of the suPAR forms in plasma do not increase with loss of histological differentiation.

In contrast to suPAR, plasma CA125 increased with loss of histological differentiation. This observation suggests that suPAR and CA125 are not involved in related pathophysiological processes. This is furthermore supported by the fact that plasma levels of individual suPAR forms did not differ between patients with endometriosis and those with other benign cysts, whereas CA125 was significantly increased in patients with endometriosis compared to other benign cysts.

Of all suPAR forms measured suPAR(I-III)+suPAR(II-III) discriminated best between benign, borderline and truly malignant tumors, and we used this parameter in the final algorithm in combination with CA125. A linear combination of suPAR(I-III)+suPAR(II-III) and CA125 discriminated clearly between malignant and benign tumors as well as between borderline and benign. Analysis of the ROC curve showed that this combination discriminates between invasive and benign tumors with an AUC of 0.94 (95% CI, 0.90-0.98), which is higher than most other proposed plasma markers. Similar result is found when restricting the analysis to early-stage invasive tumors.

Sensitivities and specificities of the product of suPAR(I-III)+suPAR(II-III) and CA125 in discriminating borderline from benign and invasive ovarian cancer from benign cases are far from those needed for use of this algorithm in screening, but they are better than those for each marker separately, and can constitute a platform for combinations with new markers.

The proposed suPAR/CA125 marker may also offer an approach to avoid risky surgery in patients with ovarian cysts and serious co-morbidity. The marker may also, in conjunction with trans-vaginal ultrasonography, help to select those patients with ovarian cysts, who should be referred to centers with oncology expertise for optimal primary surgery.

Prognostic importance of cleaved forms of the uPA receptor

The standard treatment of ovarian cancer, which includes primary surgery followed by chemotherapy, is stressful for the patient, associated with high postoperative morbidity, and with side effects of the chemotherapy. In addition, chemotherapy seems to improve the short-term survival more than the long-term survival. Development of prognostic factors, which are available pre-operatively, may serve to individualize treatment and also to provide valuable information for patients. Elevated levels of suPAR in plasma have been reported in patients with various malignant tumors and significant correlation between increased suPAR levels and shorter survival was demonstrated in breast and colorectal cancer [68, 69, 172].

In our survival analyses using the Kaplan-Meier method, we found that patients with suPAR values above median had significantly shorter survival than patients with levels below median. This feature was in common for all individual suPAR forms. It is in agreement with results from previous studies [65, 70]. However, these studies assayed only total suPAR with ELISA, less patients was included, and follow up time was much shorter than in our study. In contrast other studies did not find any correlation between suPAR levels and survival, neither in patients with stage III ovarian cancer, nor in patients with recurrent ovarian cancer [71, 72].

We found that uPAR(I) was an independent marker of poor prognosis in multivariate analyses, which included the preoperatively available risk factors CA125, age, and uPAR(I), and 85% of patients with uPAR(I) levels above detection limit that we used to dichotomize uPAR(I), died within 5 years. The level of uPAR(I) is the measure of uPA activity, since uPA cleaves uPAR on cell surface in linker region between domains I and II, liberating uPAR(I) [42]. A previous study found that high levels of uPA in tumor tissue extracts from patients with ovarian cancer were associated with short progression-free and overall survival [63]. In contrast, plasma levels of the other cleavage product suPAR(II-III) are dependent both on uPA-mediated cleavage of uPAR(I-III) at the cell surface and on shedding of uPAR(II-III) from cell surface.

The median follow-up time for patients in this study was 64 months, which together with the uniform treatment regimes increases credibility of results. The overall survival was chosen as endpoint since death among patients with ovarian

cancer is most often related to progression of malignant disease. Future studies with more patients are needed to confirm our results since the number of events (49) limited the power of our study in multivariate analyses.

In conclusion, our study indicates that individual suPAR forms, in particular uPAR(I), measured preoperatively in patients with ovarian cancer, may identify a subgroup of patients with poor prognosis. Clinically, prognostic markers that are available preoperatively can be used to guide the effort of surgery, e.g. more radical surgery in patients with high levels of uPAR(I), or alternatively limited palliative therapy in elderly patients with significant co-morbidity and high uPAR(I).

Such individualized treatment may actually improve survival as well as quality of life in this group of patients.

SUMMARY

Ovarian cancer has still the worst prognosis of all gynecological cancer. The lack of effective screening method frequently results in diagnosis in advanced stage of the disease, and thus, despite improved chemotherapy and operative techniques, long-term survival has not improved.

Hormones and growth factors play important roles in both carcinogenesis and tumor growth. Unfortunately, attempts with hormonal therapy and therapy with growth factor inhibitors gave only modest effect. Ovarian cancer is a heterogeneous disease, and the molecular basis of this heterogeneity is only partly understood. Improved understanding of ovarian tumor biology can help to find new makers for early diagnosis, and to design patient-tailored therapy.

Cell migration is the first step of the invasive process, which in turn is part of the malignant phenotype, and the uPA receptor (uPAR) plays a central role in cell migration. We studied the role of EGF and estrogen on cell migration and uPAR expression in ovarian cancer cell lines. We also analyzed the diagnostic and prognostic value of cleaved forms of the uPAR in plasma from patients with ovarian tumors.

We found that EGF stimulates cell migration through up-regulation of cell surface uPAR in ovarian cancer cells. Up-regulation of uPAR occurs via three distinct mechanisms: mobilization of uPAR from detergent resistant domains, which occurs within minutes of EGF stimulation, increased expression of uPAR mRNA, and decreased internalization and degradation of uPAR. Furthermore, EGF stimulated shedding of uPAR from the cell surface, and this was secondary to accumulation of uPAR on cell surface but independent of cell migration. Furthermore, we found that an anti-uPAR antibody, R3, which inhibits binding of uPA to uPAR, as well as Iressa that inhibits phosphorylation of EGFR, inhibited migration in response to each uPA and EGF, suggesting that uPAR and EGF receptor engage in the same multi-protein signaling complex on the cell membrane.

Estradiol attenuates EGF-induced rapid uPAR mobilization and thus also cell migration, but it influences neither the level of uPAR mRNA, nor internalization and degradation of uPAR protein. In further experiments with OVCAR-3 cells, we showed that this effect of E2 was mimicked by tamoxifen and ICI 182780, two

antagonists to nuclear ER, and G-1, a specific agonist to the membrane receptor GPR30. These results strongly suggest that the response to estradiol involved GPR30, but not ER α or ER β . For this reason we found it of interest to study expression of GPR30 in ovarian tumors and in ovarian cancer cell lines. Seven ovarian cancer cell lines and all ovarian tumor tissue samples expressed GPR30 mRNA. Expression was lower in poorly differentiated malignant tumors than in benign tumors. However, the expression of GPR30 mRNA and GPR30 protein did not correlate, since in the tissue samples we examined with Western blot, poorly differentiated tumors contained considerably more GPR30 protein than benign tumors.

Using time-resolved fluorescence immune assays, we measured the levels of intact and cleaved forms of suPAR (suPAR I-III, II-III, and I) in preoperative plasma samples from 335 patients with ovarian tumors. We found that all suPAR forms discriminated between benign, borderline, and invasive tumors. In particular, the combination of suPAR(I-III + II-III) and CA125 gave better discrimination between benign and invasive tumors (AUC 0.94) than either marker alone. Moreover, a high preoperative level of uPAR(I) was an independent predictor of poor prognosis. Thus, suPAR forms can both contribute to early diagnosis and serve as prognostic markers in patients with ovarian cancer.

CONCLUSIONS

- EGF increases cell surface uPAR via three distinct mechanisms: rapid mobilization of uPAR from detergent resistant domains, increased expression of uPAR mRNA, and decreased internalization and degradation of uPAR.
- Both the anti-uPAR antibody R3, which inhibits uPA binding to uPAR, and EGFR phosphorylation inhibitor Iressa, inhibits cell migration in response to uPA as well as to EGF, suggesting that uPAR and EGFR are engaged in the same multi-protein complex on the cell membrane.
- Shedding of suPAR is secondary to accumulation of cell surface uPAR and independent of cell migration.
- Estradiol attenuates EGF-induced rapid uPAR mobilization from detergent resistant domains and subsequent migration in ovarian cancer cells.
- This effect of estradiol is not mediated via classical nuclear ERs but via the membrane receptor GPR30.
- Both ovarian cancer cell lines and ovarian tumors express GPR30 mRNA and protein.
- Correlation between GPR30 mRNA and GPR30 protein in ovarian tumors is poor.
- All suPAR forms shows increasing concentrations between benign, borderline and invasive ovarian tumors.
- The combination of plasma suPAR(I-III) + suPAR(II-III) and CA125 discriminates between benign and malignant tumors with high accuracy (AUC 0.94).
- High plasma concentrations of all suPAR forms correlates with poor prognosis in univariate analyses of patients with ovarian cancer.
- High plasma concentration of uPAR(I) is an independent preoperative marker of poor prognosis in multivariate analysis of patients with ovarian cancer.

SAMMANFATTNING PÅ SVENSKA

(Summary in swedish)

Ovarialcancer har sämst prognos av alla gynekologiska maligniteter. Någon effektiv screeningsmetod finns fortfarande inte, vilket gör att majoriteten av patienter upptäcks i sena stadier av sjukdomen. Trots förbättrad kemoterapi och operativ teknik, har långtidsöverlevnaden inte visat avgörande förbättring.

Hormoner och tillväxtfaktorer är viktiga för såväl tumörutveckling som tumörtillväxt. Hormonterapi, som är väletablerad i behandlingen av bröstcancer, liksom inhibitorer av receptorer för tillväxtfaktorer har gett mkt blygsam effekt i behandlingen av ovarialcancer. Ovarialcancer är en heterogen sjukdom, och den molekylära bakgrunden till denna heterogenitet är bara delvis klarlagd. Förbättrad kunskap om ovarialcancersbiologi kan bidra till upptäckt av nya markörer för tidig diagnostik och planering av mer individualiserad och skräddarsydd behandling.

Cellmigration är ett första steg i invasionsprocessen, vilket är en viktig egenskap för maligna tumörer. Urokinas plasminogen aktivator receptorn (uPAR) har en centrall roll i migrationprocessen.

Vi har analyserat hur EGF och estrogen påverkar cellmigration och uttryck av uPAR i ovarialcancer cellinjer. Vi har också analyserat det diagnostiska och prognostiska värdet av kluvna former av uPAR i plasma från patienter med ovariala tumörer.

Vi fann att EGF stimulerar cellmigration genom uppreglering av uPAR på cellytan i ovarialcancer celler. Denna uppreglering sker genom tre skilda mekanismer: mobilisering av uPAR från detergent olösliga domäner i cellmembran, vilket inträffar inom bara några minuter efter stimulering med EGF, ökat uttryck av mRNA för uPAR och minskad internalisering och degradering av uPAR. Vidare stimulerar EGF ”shedding” av uPAR från cellytan som en följd av ökad ackumulering av uPAR på cellytan, men som är oberoende av cellmigration. Vi fann också att en anti-uPAR antikropp R3, som inhiberar bindning av uPA till uPAR, liksom Iressa, som inhiberar fosforylering av EGFR, inhiberar migration stimulerad av både uPA och EGF. Detta indikerar att uPAR och EGFR ingår i samma mutiproteinkomplex på cellytan.

Vi kunde visa att estradiol minskar EGF-inducerad snabb mobilisering av uPAR och på så sätt också cellmigration, men påverkar inte, varken nivå av uPAR mRNA eller internalisering och degradering av uPAR protein. I fortsatta experiment med OVCAR-3 celler visade vi att både tamoxifen och ICI 182780, antagonister till nukleär estrogen receptor, och G-1, en specifik agonist till membranreceptor GPR30, hade liknande effekt som estradiol. Dessa resultat talar starkt att GPR30, och inte ER α eller ER β , medierar svaret på estradiol.

Av den avledningen analyserade vi uttrycket av GPR30 i såväl ovarialtumörvävnad som i sju ovarialcancer cellinjer. Samtliga cellinjer och tumörvävnader uttryckte GPR30 mRNA. Lågt differentierade tumörer hade lägre uttryck än benigna tumörer. Emellertid fann vi en dålig korrelation mellan GPR30 mRNA och GPR30 protein, d.v.s. lågt differentierade tumörer hade betydligt mer GPR30 protein än benigna tumörer i Western blot analysen.

Slutligen, vi har kvantiterat såväl fullängds som kluvna former av löslig uPAR (suPAR I-III, II-III, och I) i preoperativ plasma från 335 patienter med ovarialtumörer. Vi fann att koncentrationen av alla former suPAR skiljer mellan benigna, borderline och invasiva tumörer. Speciellt kombination av suPAR(I-III + II-III) och CA125 ger god diskriminering mellan benigna och invasiva tumörer (AUC 0.94), och kombinationen av markörerna är bättre än var markör för sig. Vidare var hög preoperativ nivå av uPAR(I) en oberoende predictor för dålig prognos. Lösliga kluvna former av uPAR kan således vara användbara i tidig diagnostik av ovarialcancer, och även användas som prognostiska markörer.

ACKNOWLEDGEMENTS

I wish to express my greatest gratitude to all people that have supported and encouraged me through the time I worked on my thesis.

In particular I am grateful to:

Bertil Casslén, associate professor, my supervisor, for introducing me in scientific work, for support, knowledge, and patience. Thank you for your friendship and nice company on our travels.

Gunilla Høyer-Hansen, research leader, Ph.D., co-author, for fruitful collaboration and enthusiasm.

Christer Borgfeldt, co-author, colleague, for support, encouragement, valuable discussions and help with statistics.

Stefan Hansson, associate professor, co-supervisor, for constructive scientific suggestions and friendship.

Vera Noskova, co-author, for help with RT-PCR and kindness.

Karel Maršál, professor, for interest in my project, for useful comments and friendly support.

Irene Larsson, laboratory technician, for skillful technician assistance and always being nice and friendly.

Britt-Marie Agmell, secretary, always helpful, for excellent secretarial assistance.

Bengt Lindahl, associate professor, colleague, for support and encouragement.

Tove Sandberg and Barbro Gustavsson, for introducing me in laboratory work.

Zuzana Kolkova, colleague, for help with Western blot.

Minola, Eleonor, Sara A, Sara B, Magnus, Bodil, friends from the lab, for pleasant time together and interesting discussions during coffee breaks.

My colleagues and staff of Department of Obstetrics and Gynecology, University hospital Lund, for support and help with collecting research material.

Demila and Munib, my parents, for endless love and support from the first day.

Lejla, my wife, for all love, enormous patience, understanding, and for our sons Elvir and Edvin.

REFERENCES

1. Socialstyrelsen, *Cancer incidence in Sweden 2006*. 2007: p. 19.
2. Whittemore, A.S., *Characteristics relating to ovarian cancer risk: implications for prevention and detection*. Gynecol Oncol, 1994. 55(3 Pt 2): p. S15-9.
3. Wingo, P.A., T. Tong, and S. Bolden, *Cancer statistics, 1995*. CA Cancer J Clin, 1995. 45(1): p. 8-30.
4. King, M.C., J.H. Marks, and J.B. Mandell, *Breast and ovarian cancer risks due to inherited mutations in BRCA1 and BRCA2*. Science, 2003. 302(5645): p. 643-6.
5. Riman, T., S. Nilsson, and I.R. Persson, *Review of epidemiological evidence for reproductive and hormonal factors in relation to the risk of epithelial ovarian malignancies*. Acta Obstet Gynecol Scand, 2004. 83(9): p. 783-95.
6. Choi, J.H., et al., *Gonadotropins and ovarian cancer*. Endocr Rev, 2007. 28(4): p. 440-61.
7. Brinton, L., *Long-term effects of ovulation-stimulating drugs on cancer risk*. Reprod Biomed Online, 2007. 15(1): p. 38-44.
8. Bristow, R.E. and B.Y. Karlan, *The risk of ovarian cancer after treatment for infertility*. Curr Opin Obstet Gynecol, 1996. 8(1): p. 32-7.
9. Elmasry, K. and S.A. Gayther, *Ovarian cancer aetiology: facts and fiction*. J Fam Plann Reprod Health Care, 2006. 32(2): p. 82-6.
10. Franceschi, S., et al., *Pooled analysis of 3 European case-control studies of ovarian cancer: II. Age at menarche and at menopause*. Int J Cancer, 1991. 49(1): p. 57-60.
11. Narod, S.A., et al., *Oral contraceptives and the risk of hereditary ovarian cancer*. Hereditary Ovarian Cancer Clinical Study Group. N Engl J Med, 1998. 339(7): p. 424-8.
12. Whittemore, A.S., et al., *Oral contraceptive use and ovarian cancer risk among carriers of BRCA1 or BRCA2 mutations*. Br J Cancer, 2004. 91(11): p. 1911-5.
13. Hankinson, S.E., et al., *A prospective study of reproductive factors and risk of epithelial ovarian cancer*. Cancer, 1995. 76(2): p. 284-90.
14. Green, A., et al., *Tubal sterilisation, hysterectomy and decreased risk of ovarian cancer*. Survey of Women's Health Study Group. Int J Cancer, 1997. 71(6): p. 948-51.
15. Siskind, V., et al., *Breastfeeding, menopause, and epithelial ovarian cancer*. Epidemiology, 1997. 8(2): p. 188-91.
16. Narod, S.A., *Ovarian cancer and HRT in the Million Women Study*. Lancet, 2007. 369(9574): p. 1667-8.
17. Jemal, A., et al., *Cancer statistics, 2008*. CA Cancer J Clin, 2008. 58(2): p. 71-96.
18. Edwards, B.K., et al., *Annual report to the nation on the status of cancer, 1975-2002, featuring population-based trends in cancer treatment*. J Natl Cancer Inst, 2005. 97(19): p. 1407-27.
19. Hakama, M., et al., *CA 125 as a screening test for ovarian cancer*. J Med Screen, 1996. 3(1): p. 40-2.

20. Jacobs, I.J., et al., *Risk of diagnosis of ovarian cancer after raised serum CA 125 concentration: a prospective cohort study.* *Bmj*, 1996. 313(7069): p. 1355-8.
21. Rosenthal, A.N. and I.J. Jacobs, *The role of CA 125 in screening for ovarian cancer.* *Int J Biol Markers*, 1998. 13(4): p. 216-20.
22. Taylor, K.J. and P.E. Schwartz, *Screening for early ovarian cancer.* *Radiology*, 1994. 192(1): p. 1-10.
23. Tingulstad, S., et al., *Evaluation of a risk of malignancy index based on serum CA125, ultrasound findings and menopausal status in the pre-operative diagnosis of pelvic masses.* *Br J Obstet Gynaecol*, 1996. 103(8): p. 826-31.
24. Woolas, R.P., et al., *Elevation of multiple serum markers in patients with stage I ovarian cancer.* *J Natl Cancer Inst*, 1993. 85(21): p. 1748-51.
25. Cannistra, S.A., *Cancer of the ovary.* *N Engl J Med*, 2004. 351(24): p. 2519-29.
26. Andreassen, P.A., et al., *The urokinase-type plasminogen activator system in cancer metastasis: a review.* *Int J Cancer*, 1997. 72(1): p. 1-22.
27. Nykjaer, A., et al., *Recycling of the urokinase receptor upon internalization of the uPA:serpin complexes.* *Embo J*, 1997. 16(10): p. 2610-20.
28. Ploug, M., *Structure-function relationships in the interaction between the urokinase-type plasminogen activator and its receptor.* *Curr Pharm Des*, 2003. 9(19): p. 1499-528.
29. Bajou, K., et al., *Host-derived plasminogen activator inhibitor-1 (PAI-1) concentration is critical for in vivo tumoral angiogenesis and growth.* *Oncogene*, 2004. 23(41): p. 6986-90.
30. Leissner, P., et al., *Prognostic significance of urokinase plasminogen activator and plasminogen activator inhibitor-1 mRNA expression in lymph node- and hormone receptor-positive breast cancer.* *BMC Cancer*, 2006. 6: p. 216.
31. Dickinson, J.L., et al., *Plasminogen activator inhibitor type 2 inhibits tumor necrosis factor alpha-induced apoptosis. Evidence for an alternate biological function.* *J Biol Chem*, 1995. 270(46): p. 27894-904.
32. Stoppelli, M.P., et al., *Differentiation-enhanced binding of the amino-terminal fragment of human urokinase plasminogen activator to a specific receptor on U937 monocytes.* *Proc Natl Acad Sci U S A*, 1985. 82(15): p. 4939-43.
33. Vassalli, J.D., D. Baccino, and D. Belin, *A cellular binding site for the Mr 55,000 form of the human plasminogen activator, urokinase.* *J Cell Biol*, 1985. 100(1): p. 86-92.
34. Behrendt, N., E. Ronne, and K. Dano, *Domain interplay in the urokinase receptor. Requirement for the third domain in high affinity ligand binding and demonstration of ligand contact sites in distinct receptor domains.* *J Biol Chem*, 1996. 271(37): p. 22885-94.
35. Hoyer-Hansen, G., et al., *The intact urokinase receptor is required for efficient vitronectin binding: receptor cleavage prevents ligand interaction.* *FEBS Lett*, 1997. 420(1): p. 79-85.
36. Sidenius, N. and F. Blasi, *Domain 1 of the urokinase receptor (uPAR) is required for uPAR-mediated cell binding to vitronectin.* *FEBS Lett*, 2000. 470(1): p. 40-6.
37. Montuori, N., et al., *The cleavage of the urokinase receptor regulates its multiple functions.* *J Biol Chem*, 2002. 277(49): p. 46932-9.
38. Hoyer-Hansen, G., et al., *Cell-surface acceleration of urokinase-catalyzed receptor cleavage.* *Eur J Biochem*, 1997. 243(1-2): p. 21-6.

39. Hoyer-Hansen, G., et al., *Urokinase plasminogen activator cleaves its cell surface receptor releasing the ligand-binding domain*. J Biol Chem, 1992. 267(25): p. 18224-9.
40. Bolon, I., et al., *Plasminogen mediates the pathological effects of urokinase-type plasminogen activator overexpression*. Am J Pathol, 2004. 164(6): p. 2299-304.
41. Zhou, H.M., et al., *Urokinase-type plasminogen activator and its receptor synergize to promote pathogenic proteolysis*. Embo J, 2000. 19(17): p. 4817-26.
42. Hoyer-Hansen, G. and I.K. Lund, *Urokinase receptor variants in tissue and body fluids*. Adv Clin Chem, 2007. 44: p. 65-102.
43. Mustjoki, S., et al., *Soluble urokinase receptor levels correlate with number of circulating tumor cells in acute myeloid leukemia and decrease rapidly during chemotherapy*. Cancer Res, 2000. 60(24): p. 7126-32.
44. Piironen, T., et al., *Specific immunoassays for detection of intact and cleaved forms of the urokinase receptor*. Clin Chem, 2004. 50(11): p. 2059-68.
45. Wahlberg, K., G. Hoyer-Hansen, and B. Casslen, *Soluble receptor for urokinase plasminogen activator in both full-length and a cleaved form is present in high concentration in cystic fluid from ovarian cancer*. Cancer Res, 1998. 58(15): p. 3294-8.
46. Wilhelm, O.G., et al., *Cellular glycosylphosphatidylinositol-specific phospholipase D regulates urokinase receptor shedding and cell surface expression*. J Cell Physiol, 1999. 180(2): p. 225-35.
47. Hoyer-Hansen, G., et al., *Urokinase-catalysed cleavage of the urokinase receptor requires an intact glycolipid anchor*. Biochem J, 2001. 358(Pt 3): p. 673-9.
48. Kruger, A., et al., *Reduction of breast carcinoma tumor growth and lung colonization by overexpression of the soluble urokinase-type plasminogen activator receptor (CD87)*. Cancer Gene Ther, 2000. 7(2): p. 292-9.
49. Lutz, V., et al., *High level synthesis of recombinant soluble urokinase receptor (CD87) by ovarian cancer cells reduces intraperitoneal tumor growth and spread in nude mice*. Biol Chem, 2001. 382(5): p. 789-98.
50. Aguirre Ghiso, J.A., K. Kovalski, and L. Ossowski, *Tumor dormancy induced by downregulation of urokinase receptor in human carcinoma involves integrin and MAPK signaling*. J Cell Biol, 1999. 147(1): p. 89-104.
51. Resnati, M., et al., *Proteolytic cleavage of the urokinase receptor substitutes for the agonist-induced chemotactic effect*. Embo J, 1996. 15(7): p. 1572-82.
52. Selleri, C., et al., *Involvement of the urokinase-type plasminogen activator receptor in hematopoietic stem cell mobilization*. Blood, 2005. 105(5): p. 2198-205.
53. Pollanen, J., et al., *Ultrastructural localization of plasma membrane-associated urokinase-type plasminogen activator at focal contacts*. J Cell Biol, 1988. 106(1): p. 87-95.
54. Blasi, F. and P. Carmeliet, *uPAR: a versatile signalling orchestrator*. Nat Rev Mol Cell Biol, 2002. 3(12): p. 932-43.
55. Ossowski, L. and J.A. Aguirre-Ghiso, *Urokinase receptor and integrin partnership: coordination of signaling for cell adhesion, migration and growth*. Curr Opin Cell Biol, 2000. 12(5): p. 613-20.
56. Chapman, H.A., et al., *Role of urokinase receptor and caveolin in regulation of integrin signaling*. Thromb Haemost, 1999. 82(2): p. 291-7.

57. Simon, D.I., et al., *Identification of a urokinase receptor-integrin interaction site. Promiscuous regulator of integrin function.* J Biol Chem, 2000. 275(14): p. 10228-34.
58. Wei, Y., et al., *Regulation of integrin function by the urokinase receptor.* Science, 1996. 273(5281): p. 1551-5.
59. Liu, D., et al., *EGFR is a transducer of the urokinase receptor initiated signal that is required for in vivo growth of a human carcinoma.* Cancer Cell, 2002. 1(5): p. 445-57.
60. Andreasen, P.A., R. Egelund, and H.H. Petersen, *The plasminogen activation system in tumor growth, invasion, and metastasis.* Cell Mol Life Sci, 2000. 57(1): p. 25-40.
61. Borgfeldt, C., et al., *Dedifferentiation of serous ovarian cancer from cystic to solid tumors is associated with increased expression of mRNA for urokinase plasminogen activator (uPA), its receptor (uPAR) and its inhibitor (PAI-1).* Int J Cancer, 2001. 92(4): p. 497-502.
62. Casslen, B., et al., *Plasminogen activators and plasminogen activator inhibitors in blood and tumour fluids of patients with ovarian cancer.* Eur J Cancer, 1994. 30A(9): p. 1302-9.
63. Konecny, G., et al., *Association of urokinase-type plasminogen activator and its inhibitor with disease progression and prognosis in ovarian cancer.* Clin Cancer Res, 2001. 7(6): p. 1743-9.
64. Borgfeldt, C., et al., *High tumor tissue concentration of urokinase plasminogen activator receptor is associated with good prognosis in patients with ovarian cancer.* Int J Cancer, 2003. 107(4): p. 658-65.
65. Riisbro, R., et al., *Soluble urokinase plasminogen activator receptor in preoperatively obtained plasma from patients with gynecological cancer or benign gynecological diseases.* Gynecol Oncol, 2001. 82(3): p. 523-31.
66. Pappot, H., et al., *Elevated plasma levels of urokinase plasminogen activator receptor in non-small cell lung cancer patients.* Eur J Cancer, 1997. 33(6): p. 867-72.
67. Stephens, R.W., et al., *ELISA determination of soluble urokinase receptor in blood from healthy donors and cancer patients.* Clin Chem, 1997. 43(10): p. 1868-76.
68. Riisbro, R., et al., *Prognostic significance of soluble urokinase plasminogen activator receptor in serum and cytosol of tumor tissue from patients with primary breast cancer.* Clin Cancer Res, 2002. 8(5): p. 1132-41.
69. Stephens, R.W., et al., *Plasma urokinase receptor levels in patients with colorectal cancer: relationship to prognosis.* J Natl Cancer Inst, 1999. 91(10): p. 869-74.
70. Sier, C.F., et al., *The level of urokinase-type plasminogen activator receptor is increased in serum of ovarian cancer patients.* Cancer Res, 1998. 58(9): p. 1843-9.
71. Begum, F.D., et al., *The prognostic value of plasma soluble urokinase plasminogen activator receptor (suPAR) levels in stage III ovarian cancer patients.* Anticancer Res, 2004. 24(3b): p. 1981-5.
72. Begum, F.D., et al., *Prognostic value of plasma soluble urokinase plasminogen activator receptor (suPAR) in Danish patients with recurrent epithelial ovarian cancer (REOC).* Apmis, 2006. 114(10): p. 675-81.

73. Ullrich, A., et al., *Human epidermal growth factor receptor cDNA sequence and aberrant expression of the amplified gene in A431 epidermoid carcinoma cells*. *Nature*, 1984. 309(5967): p. 418-25.
74. Coussens, L., et al., *Tyrosine kinase receptor with extensive homology to EGF receptor shares chromosomal location with neu oncogene*. *Science*, 1985. 230(4730): p. 1132-9.
75. Kraus, M.H., et al., *Isolation and characterization of ERBB3, a third member of the ERBB/epidermal growth factor receptor family: evidence for overexpression in a subset of human mammary tumors*. *Proc Natl Acad Sci U S A*, 1989. 86(23): p. 9193-7.
76. Plowman, G.D., et al., *Ligand-specific activation of HER4/p180erbB4, a fourth member of the epidermal growth factor receptor family*. *Proc Natl Acad Sci U S A*, 1993. 90(5): p. 1746-50.
77. Sorkin, A. and C.M. Waters, *Endocytosis of growth factor receptors*. *Bioessays*, 1993. 15(6): p. 375-82.
78. Filardo, E.J., et al., *Estrogen-induced activation of Erk-1 and Erk-2 requires the G protein-coupled receptor homolog, GPR30, and occurs via trans-activation of the epidermal growth factor receptor through release of HB-EGF*. *Mol Endocrinol*, 2000. 14(10): p. 1649-60.
79. Guerrero, J., et al., *EGF receptor transactivation by urokinase receptor stimulus through a mechanism involving Src and matrix metalloproteinases*. *Exp Cell Res*, 2004. 292(1): p. 201-8.
80. Yamauchi, T., et al., *Tyrosine phosphorylation of the EGF receptor by the kinase Jak2 is induced by growth hormone*. *Nature*, 1997. 390(6655): p. 91-6.
81. Sibilian, M. and E.F. Wagner, *Strain-dependent epithelial defects in mice lacking the EGF receptor*. *Science*, 1995. 269(5221): p. 234-8.
82. Miettinen, P.J., et al., *Epithelial immaturity and multiorgan failure in mice lacking epidermal growth factor receptor*. *Nature*, 1995. 376(6538): p. 337-41.
83. Normanno, N., et al., *Epidermal growth factor receptor (EGFR) signaling in cancer*. *Gene*, 2006. 366(1): p. 2-16.
84. Cappuzzo, F., et al., *Increased HER2 gene copy number is associated with response to gefitinib therapy in epidermal growth factor receptor-positive non-small-cell lung cancer patients*. *J Clin Oncol*, 2005. 23(22): p. 5007-18.
85. Berchuck, A., et al., *Epidermal growth factor receptor expression in normal ovarian epithelium and ovarian cancer. I. Correlation of receptor expression with prognostic factors in patients with ovarian cancer*. *Am J Obstet Gynecol*, 1991. 164(2): p. 669-74.
86. Kohler, M., et al., *Epidermal growth factor receptor and transforming growth factor alpha expression in human ovarian carcinomas*. *Eur J Cancer*, 1992. 28A(8-9): p. 1432-7.
87. Maihle, N.J., et al., *EGF/ErbB receptor family in ovarian cancer*. *Cancer Treat Res*, 2002. 107: p. 247-258.
88. Vermeij, J., et al., *Genomic activation of the EGFR and HER2-neu genes in a significant proportion of invasive epithelial ovarian cancers*. *BMC Cancer*, 2008. 8: p. 3.
89. Lacroix, L., et al., *Response of ovarian carcinomas to gefitinib-carboplatin-paclitaxel combination is not associated with EGFR kinase domain somatic mutations*. *Int J Cancer*, 2006. 118(4): p. 1068-9.

90. Schilder, R.J., et al., *Phase II study of gefitinib in patients with relapsed or persistent ovarian or primary peritoneal carcinoma and evaluation of epidermal growth factor receptor mutations and immunohistochemical expression: a Gynecologic Oncology Group Study*. Clin Cancer Res, 2005. 11(15): p. 5539-48.
91. Stadlmann, S., et al., *Epithelial growth factor receptor status in primary and recurrent ovarian cancer*. Mod Pathol, 2006. 19(4): p. 607-10.
92. Lassus, H., et al., *Gene amplification, mutation, and protein expression of EGFR and mutations of ERBB2 in serous ovarian carcinoma*. J Mol Med, 2006. 84(8): p. 671-81.
93. Suo, Z., et al., *Papillary serous carcinoma of the ovary: an ultrastructural and immunohistochemical study*. Ultrastruct Pathol, 2004. 28(3): p. 141-7.
94. Volm, M., et al., *Microvessel density, expression of proto-oncogenes, resistance-related proteins and incidence of metastases in primary ovarian carcinomas*. Clin Exp Metastasis, 1996. 14(3): p. 209-14.
95. Fischer-Colbrie, J., et al., *EGFR and steroid receptors in ovarian carcinoma: comparison with prognostic parameters and outcome of patients*. Anticancer Res, 1997. 17(1B): p. 613-9.
96. Psyrri, A., et al., *Effect of epidermal growth factor receptor expression level on survival in patients with epithelial ovarian cancer*. Clin Cancer Res, 2005. 11(24 Pt 1): p. 8637-43.
97. Castellvi, J., et al., *Phosphorylated 4E binding protein 1: a hallmark of cell signaling that correlates with survival in ovarian cancer*. Cancer, 2006. 107(8): p. 1801-11.
98. Elie, C., et al., *Lack of relationship between EGFR-1 immunohistochemical expression and prognosis in a multicentre clinical trial of 93 patients with advanced primary ovarian epithelial cancer (GINECO group)*. Br J Cancer, 2004. 91(3): p. 470-5.
99. Nielsen, J.S., et al., *Prognostic significance of p53, Her-2, and EGFR overexpression in borderline and epithelial ovarian cancer*. Int J Gynecol Cancer, 2004. 14(6): p. 1086-96.
100. Konner, J., et al., *A phase II study of cetuximab/paclitaxel/carboplatin for the initial treatment of advanced-stage ovarian, primary peritoneal, or fallopian tube cancer*. Gynecol Oncol, 2008. 110(2): p. 140-5.
101. Secord, A.A., et al., *Phase II trial of cetuximab and carboplatin in relapsed platinum-sensitive ovarian cancer and evaluation of epidermal growth factor receptor expression: a Gynecologic Oncology Group study*. Gynecol Oncol, 2008. 108(3): p. 493-9.
102. Ciardiello, F., et al., *Antitumor effect and potentiation of cytotoxic drugs activity in human cancer cells by ZD-1839 (Iressa), an epidermal growth factor receptor-selective tyrosine kinase inhibitor*. Clin Cancer Res, 2000. 6(5): p. 2053-63.
103. Simpson, E.R., et al., *Estrogen--the good, the bad, and the unexpected*. Endocr Rev, 2005. 26(3): p. 322-30.
104. Persson, I., *Estrogens in the causation of breast, endometrial and ovarian cancers - evidence and hypotheses from epidemiological findings*. J Steroid Biochem Mol Biol, 2000. 74(5): p. 357-64.
105. Lacey, J.V., Jr., et al., *Menopausal hormone replacement therapy and risk of ovarian cancer*. Jama, 2002. 288(3): p. 334-41.

106. Riman, T., et al., *Hormone replacement therapy and the risk of invasive epithelial ovarian cancer in Swedish women*. J Natl Cancer Inst, 2002. 94(7): p. 497-504.
107. O'Donnell, A.J., et al., *Estrogen receptor-alpha mediates gene expression changes and growth response in ovarian cancer cells exposed to estrogen*. Endocr Relat Cancer, 2005. 12(4): p. 851-66.
108. Langdon, S.P., et al., *The regulation of growth and protein expression by estrogen in vitro: a study of 8 human ovarian carcinoma cell lines*. J Steroid Biochem Mol Biol, 1994. 50(3-4): p. 131-5.
109. Rahman, K.M. and F.H. Sarkar, *Steroid hormone mimics: molecular mechanisms of cell growth and apoptosis in normal and malignant mammary epithelial cells*. J Steroid Biochem Mol Biol, 2002. 80(2): p. 191-201.
110. Choi, K.C., et al., *Estradiol up-regulates antiapoptotic Bcl-2 messenger ribonucleic acid and protein in tumorigenic ovarian surface epithelium cells*. Endocrinology, 2001. 142(6): p. 2351-60.
111. Lindgren, P., et al., *Steroid receptors and hormones in relation to cell proliferation and apoptosis in poorly differentiated epithelial ovarian tumors*. Int J Oncol, 2001. 19(1): p. 31-8.
112. Yuan, Z.Q., et al., *AKT2 inhibition of cisplatin-induced JNK/p38 and Bax activation by phosphorylation of ASK1: implication of AKT2 in chemoresistance*. J Biol Chem, 2003. 278(26): p. 23432-40.
113. Mabuchi, S., et al., *Estrogen inhibits paclitaxel-induced apoptosis via the phosphorylation of apoptosis signal-regulating kinase 1 in human ovarian cancer cell lines*. Endocrinology, 2004. 145(1): p. 49-58.
114. Langdon, S.P., et al., *Functionality of the progesterone receptor in ovarian cancer and its regulation by estrogen*. Clin Cancer Res, 1998. 4(9): p. 2245-51.
115. Akahira, J., et al., *Differential expression of progesterone receptor isoforms A and B in the normal ovary, and in benign, borderline, and malignant ovarian tumors*. Jpn J Cancer Res, 2002. 93(7): p. 807-15.
116. Hempling, R.E., et al., *Progesterone receptor status is a significant prognostic variable of progression-free survival in advanced epithelial ovarian cancer*. Am J Clin Oncol, 1998. 21(5): p. 447-51.
117. Munstedt, K., et al., *Steroid hormone receptors and long term survival in invasive ovarian cancer*. Cancer, 2000. 89(8): p. 1783-91.
118. Kommoss, F., et al., *Steroid receptors in ovarian carcinoma: immunohistochemical determination may lead to new aspects*. Gynecol Oncol, 1992. 47(3): p. 317-22.
119. Rao, B.R. and B.J. Slotman, *Endocrine factors in common epithelial ovarian cancer*. Endocr Rev, 1991. 12(1): p. 14-26.
120. Hatch, K.D., et al., *Responsiveness of patients with advanced ovarian carcinoma to tamoxifen. A Gynecologic Oncology Group study of second-line therapy in 105 patients*. Cancer, 1991. 68(2): p. 269-71.
121. Enmark, E., et al., *Human estrogen receptor beta-gene structure, chromosomal localization, and expression pattern*. J Clin Endocrinol Metab, 1997. 82(12): p. 4258-65.
122. Hall, J.M., J.F. Couse, and K.S. Korach, *The multifaceted mechanisms of estradiol and estrogen receptor signaling*. J Biol Chem, 2001. 276(40): p. 36869-72.

123. Menance, L.P., et al., *Localization of the estrogen receptor locus (ESR) to chromosome 6q25.1 by FISH and a simple post-FISH banding technique.* Genomics, 1993. 17(1): p. 263-5.
124. Enmark, E. and J.A. Gustafsson, *Oestrogen receptors - an overview.* J Intern Med, 1999. 246(2): p. 133-8.
125. Brandenberger, A.W., M.K. Tee, and R.B. Jaffe, *Estrogen receptor alpha (ER-alpha) and beta (ER-beta) mRNAs in normal ovary, ovarian serous cystadenocarcinoma and ovarian cancer cell lines: down-regulation of ER-beta in neoplastic tissues.* J Clin Endocrinol Metab, 1998. 83(3): p. 1025-8.
126. Nilsson, S., et al., *Mechanisms of estrogen action.* Physiol Rev, 2001. 81(4): p. 1535-65.
127. Le Mellay, V., B. Grosse, and M. Lieberherr, *Phospholipase C beta and membrane action of calcitriol and estradiol.* J Biol Chem, 1997. 272(18): p. 11902-7.
128. Morley, P., et al., *A new, nongenomic estrogen action: the rapid release of intracellular calcium.* Endocrinology, 1992. 131(3): p. 1305-12.
129. Pietras, R.J. and C.M. Szego, *Specific binding sites for oestrogen at the outer surfaces of isolated endometrial cells.* Nature, 1977. 265(5589): p. 69-72.
130. Owman, C., et al., *Cloning of human cDNA encoding a novel heptahelical receptor expressed in Burkitt's lymphoma and widely distributed in brain and peripheral tissues.* Biochem Biophys Res Commun, 1996. 228(2): p. 285-92.
131. Dorsam, R.T. and J.S. Gutkind, *G-protein-coupled receptors and cancer.* Nat Rev Cancer, 2007. 7(2): p. 79-94.
132. Carmeci, C., et al., *Identification of a gene (GPR30) with homology to the G-protein-coupled receptor superfamily associated with estrogen receptor expression in breast cancer.* Genomics, 1997. 45(3): p. 607-17.
133. O'Dowd, B.F., et al., *Discovery of three novel G-protein-coupled receptor genes.* Genomics, 1998. 47(2): p. 310-3.
134. Wang, C., E.R. Prossnitz, and S.K. Roy, *Expression of G protein-coupled receptor 30 in the hamster ovary: differential regulation by gonadotropins and steroid hormones.* Endocrinology, 2007. 148(10): p. 4853-64.
135. Filardo, E.J., *Epidermal growth factor receptor (EGFR) transactivation by estrogen via the G-protein-coupled receptor, GPR30: a novel signaling pathway with potential significance for breast cancer.* J Steroid Biochem Mol Biol, 2002. 80(2): p. 231-8.
136. Thomas, P., et al., *Identity of an estrogen membrane receptor coupled to a G protein in human breast cancer cells.* Endocrinology, 2005. 146(2): p. 624-32.
137. Revankar, C.M., et al., *A transmembrane intracellular estrogen receptor mediates rapid cell signaling.* Science, 2005. 307(5715): p. 1625-30.
138. Filardo, E.J. and P. Thomas, *GPR30: a seven-transmembrane-spanning estrogen receptor that triggers EGF release.* Trends Endocrinol Metab, 2005. 16(8): p. 362-7.
139. Albanito, L., et al., *G protein-coupled receptor 30 (GPR30) mediates gene expression changes and growth response to 17beta-estradiol and selective GPR30 ligand G-1 in ovarian cancer cells.* Cancer Res, 2007. 67(4): p. 1859-66.
140. Thomas, P.S., *Hybridization of denatured RNA and small DNA fragments transferred to nitrocellulose.* Proc Natl Acad Sci U S A, 1980. 77(9): p. 5201-5.

141. Roldan, A.L., et al., *Cloning and expression of the receptor for human urokinase plasminogen activator, a central molecule in cell surface, plasmin dependent proteolysis*. *Embo J*, 1990. 9(2): p. 467-74.
142. Thorell, J.I. and B.G. Johansson, *Enzymatic iodination of polypeptides with ¹²⁵I to high specific activity*. *Biochim Biophys Acta*, 1971. 251(3): p. 363-9.
143. Hunter, W.M. and F.C. Greenwood, *Preparation of iodine-131 labelled human growth hormone of high specific activity*. *Nature*, 1962. 194: p. 495-6.
144. Casslen, B., et al., *Progesterone stimulates degradation of urokinase plasminogen activator (u-PA) in endometrial stromal cells by increasing its inhibitor and surface expression of the u-PA receptor*. *J Clin Endocrinol Metab*, 1995. 80(9): p. 2776-84.
145. Behrendt, N., et al., *The human receptor for urokinase plasminogen activator. NH2-terminal amino acid sequence and glycosylation variants*. *J Biol Chem*, 1990. 265(11): p. 6453-60.
146. Riisbro, R., Piironen, T., Br nner, N., Larsen, B., Nielsen, H.J., Stephens, R.W., H yer-Hansen, B., *Measurement of soluble urokinase plasminogen activator receptor in serum*. *J Clin Ligand Assay*, 2002. 25: p. 53-56.
147. Cunningham, O., et al., *Dimerization controls the lipid raft partitioning of uPAR/CD87 and regulates its biological functions*. *Embo J*, 2003. 22(22): p. 5994-6003.
148. Jo, M., et al., *Epidermal growth factor receptor-dependent and -independent cell-signaling pathways originating from the urokinase receptor*. *J Biol Chem*, 2003. 278: p. 1642-1646.
149. Moro, L., et al., *Integrin-induced epidermal growth factor (EGF) receptor activation requires c-Src and p130Cas and leads to phosphorylation of specific EGF receptor tyrosines*. *J Biol Chem*, 2002. 277: p. 9405-9415.
150. Filardo, E.J., et al., *Distribution of GPR30, a seven membrane-spanning estrogen receptor, in primary breast cancer and its association with clinicopathologic determinants of tumor progression*. *Clin Cancer Res*, 2006. 12(21): p. 6359-66.
151. Siratsuchi, T., H. Ishibashi, and K. Shirasuna, *Inhibition of epidermal growth factor-induced invasion by dexamethasone and AP-1 decoy in human squamous cell carcinoma cell lines*. *Cell Physiol*, 2002. 193: p. 340-348.
152. Olson, D., et al., *Internalization of the urokinase-plasminogen activator inhibitor type-1 complex is mediated by the urokinase receptor*. *J Biol Chem*, 1992. 267(13): p. 9129-33.
153. Conese, M. and F. Blasi, *Urokinase/urokinase receptor system: internalization/degradation of urokinase-serpin complexes: mechanism and regulation*. *Biol Chem Hoppe Seyler*, 1995. 376(3): p. 143-55.
154. Plesner, T., et al., *The receptor for urokinase-type plasminogen activator and urokinase is translocated from two distinct intracellular compartments to the plasma membrane on stimulation of human neutrophils*. *Blood*, 1994. 83(3): p. 808-15.
155. Lee, E.J., et al., *The epidermal growth factor receptor tyrosine kinase inhibitor ZD1839 (Iressa) suppresses proliferation and invasion of human oral squamous carcinoma cells via p53 independent and MMP, uPAR dependent mechanism*. *Ann N Y Acad Sci*, 2007. 1095: p. 113-28.
156. Wei, Y., et al., *A role for caveolin and the urokinase receptor in integrin-mediated adhesion and signaling*. *J Cell Biol*, 1999. 144(6): p. 1285-94.

157. Aguirre-Ghiso, J.A., et al., *Urokinase receptor and fibronectin regulate the ERK(MAPK) to p38(MAPK) activity ratios that determine carcinoma cell proliferation or dormancy in vivo*. *Mol Biol Cell*, 2001. 12(4): p. 863-79.
158. Song, R.X., et al., *Effect of long-term estrogen deprivation on apoptotic responses of breast cancer cells to 17beta-estradiol*. *J Natl Cancer Inst*, 2001. 93(22): p. 1714-23.
159. Park, S.H., et al., *Estrogen regulates Snail and Slug in the down-regulation of E-cadherin and induces metastatic potential of ovarian cancer cells through estrogen receptor alpha*. *Mol Endocrinol*, 2008. 22(9): p. 2085-98.
160. Puri, C., et al., *Relationships between EGFR signaling-competent and endocytosis-competent membrane microdomains*. *Mol Biol Cell*, 2005. 16(6): p. 2704-18.
161. Filardo, E.J., et al., *Estrogen action via the G protein-coupled receptor, GPR30: stimulation of adenylyl cyclase and cAMP-mediated attenuation of the epidermal growth factor receptor-to-MAPK signaling axis*. *Mol Endocrinol*, 2002. 16(1): p. 70-84.
162. Sukocheva, O.A., et al., *Sphingosine kinase transmits estrogen signaling in human breast cancer cells*. *Mol Endocrinol*, 2003. 17(10): p. 2002-12.
163. Carmeci, C., et al., *Analysis of estrogen receptor messenger RNA in breast carcinomas from archival specimens is predictive of tumor biology*. *Am J Pathol*, 1997. 150(5): p. 1563-70.
164. Vivacqua, A., et al., *The G protein-coupled receptor GPR30 mediates the proliferative effects induced by 17beta-estradiol and hydroxytamoxifen in endometrial cancer cells*. *Mol Endocrinol*, 2006. 20(3): p. 631-46.
165. Vivacqua, A., et al., *17beta-estradiol, genistein, and 4-hydroxytamoxifen induce the proliferation of thyroid cancer cells through the g protein-coupled receptor GPR30*. *Mol Pharmacol*, 2006. 70(4): p. 1414-23.
166. Kuo, W.H., et al., *The interactions between GPR30 and the major biomarkers in infiltrating ductal carcinoma of the breast in an Asian population*. *Taiwan J Obstet Gynecol*, 2007. 46(2): p. 135-45.
167. Chan, K.K., et al., *Estrogen receptor subtypes in ovarian cancer: a clinical correlation*. *Obstet Gynecol*, 2008. 111(1): p. 144-51.
168. Skliris, G.P., et al., *Reduced expression of oestrogen receptor beta in invasive breast cancer and its re-expression using DNA methyl transferase inhibitors in a cell line model*. *J Pathol*, 2003. 201(2): p. 213-20.
169. Iwao, K., et al., *Quantitative analysis of estrogen receptor-beta mRNA and its variants in human breast cancers*. *Int J Cancer*, 2000. 88(5): p. 733-6.
170. Horvath, L.G., et al., *Frequent loss of estrogen receptor-beta expression in prostate cancer*. *Cancer Res*, 2001. 61(14): p. 5331-5.
171. Rosenthal, A. and I. Jacobs, *Ovarian cancer screening*. *Semin Oncol*, 1998. 25(3): p. 315-25.
172. Fernebro, E., et al., *Prognostic importance of the soluble plasminogen activator receptor, suPAR, in plasma from rectal cancer patients*. *Eur J Cancer*, 2001. 37(4): p. 486-91.

I



EGF-stimulated migration in ovarian cancer cells is associated with decreased internalization, increased surface expression, and increased shedding of the urokinase plasminogen activator receptor

Emir Henic^{a,*}, Michael Sixt^b, Stefan Hansson^a, Gunilla Høyer-Hansen^c, Bertil Casslén^a

^a Department of Obstetrics & Gynecology, University Hospital, SE-221 85 Lund, Sweden

^b Department of Pathology, University Hospital, SE-221 85 Lund, Sweden

^c Finsen Laboratory, Rigshospitalet, DK-2100 Copenhagen Ø, Denmark

Received 13 June 2005

Available online 2 November 2005

Abstract

Objectives. The EGFR is expressed in malignant ovarian tumor tissue, and tissue content of EGFR has been directly associated with poor prognosis in patients with ovarian cancer. The uPA system plays a role in pericellular proteolysis, cell migration, invasion, and is over-expressed in ovarian cancer. This study explored the effects of EGF on uPAR expression in the ovarian cancer cell line OVCAR-3.

Methods. We used OVCAR-3 cells and the following methods: cell migration assay, time-lapse video microscopy, real-time PCR, assays for cellular binding of ¹²⁵I-uPA and cellular degradation of ¹²⁵I-uPA:PAI-1 complex, biosynthetic labeling using ³⁵S-methionin, Western blot, Northern blot, and ELISAs for uPA, PAI-1, and uPAR.

Results. EGF up-regulates both protein and mRNA not only for uPAR, but also for the ligand uPA and its inhibitor PAI-1. Cell surface uPAR, in control as well as EGF-stimulated cells, is present only in the intact, not the cleaved, form. Ligand binding experiments showed an increase of endogenously occupied uPAR, whereas non-occupied receptor sites were not increased. In addition, EGF treatment resulted in decreased degradation of radiolabeled uPA:PAI-1 complex. This suggests decreased internalization of uPAR, since the complex is internalized together with uPAR. Like EGF, colchicine, which inhibits endocytosis, increased cell surface expression of uPAR. In addition, we found an immediate increase of uPAR after exposing the cells to EGF and this was accompanied by a transient increase of cell migration. The increase of cell surface uPAR in response to EGF is accompanied by increased release of the soluble form of uPAR (suPAR) to the medium as well as by increased cell migration. Both uPAR and suPAR increased in cells treated with the endocytosis inhibitor colchicine even though cell migration was inhibited, suggesting that the mechanism of uPAR shedding is not related to cell migration.

Conclusion. Increased cell surface uPAR in response to EGF stimulation results from mobilization of uPAR from detergent-resistant domains, increased expression of uPAR mRNA, and decreased internalization and degradation of uPAR. Both the anti-uPAR antibody R3, which inhibits binding of uPA, and the EGFR phosphorylation inhibitor Iressa inhibited cell migration in response to uPA as well as to EGF, suggesting that EGFR and uPAR are engaged in the same multiprotein assembly on the cell surface.

© 2005 Elsevier Inc. All rights reserved.

Introduction

The epidermal growth factor receptor (EGFR) is the archetypal member of a super-family of cell membrane receptors with intrinsic tyrosine kinase activity. Ligands include EGF, transforming growth factor- α (TGF- α), and heparin-binding EGF (HB-EGF), and their binding to the

extracellular domain initiates receptor dimerization, resulting in auto-phosphorylation on tyrosine residues within the cytoplasmic domain, and subsequently phosphorylation of adapter proteins and signaling molecules [1,2]. Biological responses to EGFR signaling involve such diverse cellular functions as proliferation, differentiation, motility, and metabolism.

The urokinase plasminogen activator (uPA) and its receptor (uPAR) play a role in pericellular proteolysis, cell migration, and invasion [3]. Activation of pro-uPA, and further activation of plasminogen by fully active uPA, is focused on the cell membrane by binding to uPAR. uPAR is a glycosyl phospho-

* Corresponding author.

E-mail address: emir.henic@med.lu.se (E. Henic).

tidyl inositol (GPI) anchored cell membrane protein, consisting of three domains. In addition to binding to uPAR, uPA cleaves uPAR in the linker region between domains I and II [4]. Ligand activation of uPAR initiates cell migration in several cell types [5,6]. Ligation modifies conformation of uPAR, which results in high affinity for the β -subunits of several integrin receptors [7]. In fact, activated or cleaved uPAR acts as an integrin ligand [8,9]. Subsequent assembly of multimolecular complexes at focal adhesions modifies cell attachment and stimulates cell migration [10]. Thus, binding of uPA to uPAR sets the stage for both pericellular proteolysis and cell migration, two cellular functions, which together constitute the basis for the invasive phenotype of tumor cells.

The EGFR is expressed in malignant ovarian tumor tissue [11], and tissue content of EGFR has been directly associated with poor postoperative prognosis in long-term studies of patients with ovarian cancer [12]. Also, expression of EGFR correlated with poor response to chemotherapy in short-term observation studies [13]. Similarly, the uPA system is over-expressed in conditions involving tissue remodeling, and tumor tissue content of uPA, uPAR, and plasminogen activator inhibitor-1 (PAI-1) is increased in a variety of human malignancies [14]. Ovarian cancer is no exception, and in particular poorly differentiated tumors and metastases have very high expression of all three mRNA species [15–17]. Furthermore, peripheral blood concentrations and tumor tissue levels of some components of the PA-system correlate with postoperative prognosis [18–20].

Some recent reports have suggested that the EGFR is a transducer of the signal from ligand activated uPAR, leading to cell migration [21–23]. Also, activated EGFR mediates up-regulation of the uPA-system via the MEK-ERK pathway [24]. Both EGFR and uPAR are elevated in ovarian cancer and our preliminary results indicated that EGF increases expression of uPA, PAI-1 and uPAR as well as cell migration in OVCAR-3, SKOV-3, and SKOV3-IP cells. We explored possible mechanisms whereby EGFR activation regulates the expression of uPAR, using OVCAR-3, as a representative cell line. OVCAR-3 is derived from a malignant ovarian adenocarcinoma.

Material and methods

Materials

Epidermal growth factor (EGF) and colchicine were obtained from SIGMA (St Louis, MO, USA). The EGFR specific tyrosine kinase inhibitor Iressa (ZD1839) was kindly provided by AstraZeneca (Macclesfield, Cheshire, UK). Polycarbonate membrane inserts with a pore size of 8 μ m and plastic ware were obtained from Becton Dickinson (Franklin Lakes, NJ, USA). RNeasy Total RNA preparation kit was from QIAGEN (Hilden, Germany). PAI-1 was kindly provided by Dr. Peter Andreassen (Aarhus, Denmark).

Cell culture

Human ovarian adenocarcinoma OVCAR-3 cells were cultured in M199 supplemented with FBS 20%, insulin 10 mg/L, glutamine 2 mmol/L, penicillin 100,000 IU/L, streptomycin 100 mg/L, and fungizone 0.25 mg/L, and incubated in humidified air with 5% CO₂ at 37°C. SKOV-3 and SKOV3-IP

cells were cultured in same conditions supplemented with 15%, respectively 10% FBS. Experiments were performed in serum-free medium.

Cell migration assay

Cell migration was assayed in 12-well tissue culture plate inserts having polyethylene terephthalate track-etched membranes (10.5 mm diameter) with 8 μ m wide pores. Cells were suspended in medium without FBS to a final concentration of 1.5×10^7 cells/mL. An aliquot of the cell suspension, 0.5 mL, was added to the upper compartment, and 1.5 mL serum-free medium to lower compartment. Chemoattractants were added to the lower compartment, and the cells were incubated at 37°C. After 24 h incubation, remaining cells on the upper surface of the membrane were removed with a cotton swab before the inserts were fixed with methanol for 5 min and stained with Giemsa (12.5%) for 15 min. Cells, which had migrated to the lower surface of the membrane, were counted. Four fields were counted on each membrane, and the mean was used as one observation. At least six membranes were evaluated in each group.

Time-lapse video microscopy

Cells were seeded on tissue culture dishes in low concentration (4000/cm²) in order to visualize single cells. One day after plating cells were given serum-free medium for 3 h before initiating the video microscope. The time-lapse video experiments were performed at 37°C and 5% CO₂ in a humidified and climatized chamber using a Zeiss Axiovert 200 M microscope Goettingen, Germany.

Images were collected at 16 min intervals. EGF was added at time point 0 without interrupting the image collection. Pathways of cells were tracked using Improvise Velocity software 2.5 (London, UK) and median velocities were calculated for at least 36 cells per experiment.

Real-time PCR

Confluent cultures in serum-free medium were stimulated with EGF, 10 ng/mL, or vehicle for 1, 2, 3, 4, 8, 12, and 24 h. Conditioned media were removed, cells were lysed, and total RNA extracted with Trizol Reagent™ (Life Technologies, Sweden). Lysates were stored at –80°C until further use. The quality of RNA samples was checked by electrophoresis through a 1.5% agarose/2% formalin denaturing gel using 1 × MOPS buffer (Intergen company). RNA loader (GenHunter, Nashville, TN, USA) was used to verify the 18S and 28S RNA bands under UV light. Samples with visible 18S/28S bands were included for further analysis.

RNA was reverse transcribed according to protocols from Applied Biosystems in 50 μ L reaction mixture containing 0.5 μ L total RNA, and a final concentration of 1 × TaqMan RT buffer, 5.5 mM MgCl₂, 500 μ M dNTPs, 2.5 μ M random hexamers, 0.4 U/ μ L RNase inhibitor, and 1.25 U/ μ L MultiScribe Reverse Transcriptase. The reactions were incubated at 25°C for 10 min, at 48°C for 30 min, and then 5 min of inactivation at 95°C. The samples were stored at –20°C until further use.

Gene transcripts were quantified using real-time PCR on ABI PRISM™ 7000 sequence detection system (Applied Biosystems). Primers and probes were ordered from Assays on Demand™ (Applied Biosystems): PAI-1 (SERPINE1): accession # NM_000602, assay on demand # Hs00167155_m1; uPA (PLAU): accession # NM_002658, assay on demand # Hs00170182_m1; uPAR (PLAUR): accession # NM_002659, assay on demand # Hs00182181_m1. Each primer pair was located on different exons of the investigated gene in order to avoid genomic DNA contamination. Oligonucleotide probes labeled with fluorogenic dye, 6 carboxyfluorescein (Fam) were used.

PCR reactions were carried out in a 25 μ L final volume containing final concentrations: 1 × Universal PCR Master Mix (Applied Biosystems), 0.5 μ M TaqMan probe, 0.9 μ M of forward and reverse primers, respectively, and 1 μ L of 10 ng/ μ L of DNA aliquot. For transcripts analyses with pre-manufactured probes, the reactions were carried out in 25 μ L final volume containing final concentrations: 1 × Universal PCR Master Mix (Applied Biosystems), 1 × Assaymix (Applied Biosystems), 0.25 μ M probe, 0.9 μ M of forward and reverse primers, respectively, and 1 μ L of 10 ng/ μ L of DNA aliquot. The

thermal cycling conditions were initiated by Uracil-DNA *N*-glucosylase (UNG) activation at 50°C for 2 min and initial denaturation at 95°C for 10 min, then 40 cycles at 95°C for 15 s, annealing at 60°C for 1 min. Two negative controls, without template, were included in every amplification reaction. RNA samples were tested for genomic DNA contamination prior to further investigation. For each reaction, duplicate assay was carried out. Transcript of β -actin, as a house-keeping gene, was quantified as endogenous RNA of reference to normalize each sample. Quantification was achieved through a calibration curve obtained by serial 10-fold dilutions of the template DNA (0.08–80 ng). Results are expressed as relative values.

Cellular binding of ^{125}I -uPA

This assay was performed as previously described [25]. The HMW fraction of uPA was labeled with ^{125}I using the lactoperoxidase [26] or chloramine-T [27] procedures. Confluent cultures were incubated for 24 h at 37°C in serum-free medium with stimulations as indicated. Following washing, cultures were incubated on ice for 2 h with radiolabeled uPA in HBSS containing BSA 20 g/L. Cells were washed six times with ice-cold HBSS before being lysed with 1 mol/L NaOH. Radioactivity of the lysate was counted in a gamma counter. Specific binding was subsequently calculated by subtracting non-specific binding, which was assayed in the presence of 100-fold molar excess of unlabeled uPA. The procedure described measures only free, i.e. non-occupied, receptor molecules. In order to assay the total number of receptor sites, endogenously bound uPA was removed by briefly (2–3 min) exposing the cells to acetate buffer 75 mmol/L, pH 3.0, containing CaCl_2 2.5 mmol/L, MgCl_2 0.5 mmol/L, and NaCl 0.3 mol/L [25]. The number of occupied receptor sites was subsequently calculated as the difference between the numbers of total and free receptor sites.

Cellular degradation of ^{125}I -uPA:PAI-1 complex

Cell cultures were incubated for 2 h on ice with ^{125}I -uPA in complex with PAI-1, final concentration 1 nmol/L [25]. After washing 6 times with ice-cold HBSS, cultures were transferred to 37°C to allow internalization of the cell surface bound complex. After indicated time periods, the media were collected, TCA added to a final concentration of 10%, and the mixture centrifuged at $3000 \times g$ for 20 min. Radioactivity was measured in the supernatants. The cell pellets were lysed with NaOH for assay of protein content.

Northern blotting for uPAR mRNA

After size-separation of total RNA, it was transferred from agarose gels to GeneScreen Plus nitrocellulose filters [28]. Probes, radiolabeled with ^{32}P -dCTP, were hybridized to the filters. Autoradiography was performed for 1–12 h, and signal intensities were measured by computerized densometric scanning (BioImage Products, Ann Arbor, MI). To correct for unequal loading, filters were hybridized to a human β -actin cDNA probe in addition to the probe for uPAR. The signal intensity of uPAR was subsequently related to intensity of the β -actin cDNA probe.

The probe for uPAR, HUR06, was a 584-base pair *Bam*HI fragment of the human uPAR gene subcloned into pBluescript KS [29].

Western blotting for EGFR and uPAR

EGFR

Cells to be analyzed for EGFR were extracted in lysis buffer (NP40 1%, HEPES 50 mmol/L, NaCl 150 mmol/L, ZnCl_2 50 $\mu\text{mol/L}$, NaF 50 $\mu\text{mol/L}$, EDTA 2 mmol/L, Na_3VO_4 0.5 mmol/L, PMSF 0.1 mmol/L, aprotinin 2 mg/L, leupeptin 2 mg/L). Cell lysates were then centrifuged at $20,000 \times g$ for 10 min at 4°C. Supernatants were then assayed for protein concentrations and 20 μg was applied to each lane. Proteins were separated on NuPAGE 3–8% Tris-Acetate gel (Invitrogen, Carlsbad, California, USA). Proteins were blotted to PVDF membranes (BioRad, Hercules, California, USA). The primary antibodies were either monoclonals directed to EGFR phosphorylated on tyrosine #1173 (Santa Cruz Biotechnology), or to all forms of EGFR (Santa Cruz Biotechnology). For detection, we used ECL Western blotting detection reagents and analysis system (Amersham Biosciences, Little Chalfont, UK).

uPAR

Confluent OVCAR-3 cells were grown with or without 10 $\mu\text{g/L}$ of EGF for 24 h prior to harvesting. Cells to be analyzed for uPAR were lysed using 2 mL/ 10^8 cells of lysis-buffer containing 0.1 mol/L Tris-HCl, pH 8.1, 1% Triton X-114, 10 mmol EDTA, 10 mg/L trasyolol, and 1 mmol/L PMSF, and the clarified lysates were subject to temperature-dependent phase separation [30]. Proteins were separated on 12% SDS-PAGE (BioRad) and electro-blotted onto polyvinylidene difluoride membranes (Immobilon-P, Millipore, Bedford, MA, USA). Membranes were blocked using 2% skimmed milk powder in TBS, and subsequently probed with 5 $\mu\text{g/mL}$ of monoclonal antibody R3 reacting with an epitope on domain I, and R2 reacting with an epitope on domain III. Both antibodies were kind gifts from dr. Gunilla Hoyer-Hanssen (Finsen lab., Copenhagen, Denmark). Peroxidase conjugated rabbit anti-mouse immunoglobulins (Dako, Glostrup, Denmark), diluted 1:2000 in TBS containing 2% skimmed milk powder were used for detection. The ECL detection system (Amersham) was used for visualization of the bands.

Biosynthetic labeling

Confluent OVCAR-3 cells in 6 well plates were grown for 12 h in methionin-free DME medium, and subsequently in medium containing ^{35}S -methionin 10 mCi/L (Amersham) for 12 h. After washing, the cells were incubated with EGF (10 $\mu\text{g/L}$), colchicine (1 mg/L) or vehicle for 24 h, washed, extracted in lysis buffer containing EDTA 10 mmol/L, Triton X 114 1%, aprotinin 2 mg/L, and PMSF 0.1 mol/L, and centrifuged at $20,000 \times g$ for 10 min at 4°C. Each supernatant was pre-cleared with 10 μL Protein-A agarose for 30 min and centrifuged. uPAR was subsequently immunoprecipitated using a mixture of two monoclonal antibodies to uPAR, R3, and R4 (each 3 $\mu\text{g/well}$ for supernatant, and 6 $\mu\text{g/well}$ for cell lysates). This was followed by 20 μL Protein-A agarose centrifugation. Precipitates were washed three times with lysis buffer and subsequently counted in a liquid scintillator.

ELISAs for uPAR

Confluent cultures in serum-free medium were stimulated with EGF, 10 ng/mL, or vehicle. After collection of conditioned media, cells were lysed with lysis buffer (Tris-HCl 100 mmol/L, EDTA 10 mmol/L (pH 8.1), Triton X-114 1%, phenylmethylsulfonyl fluoride 100 mmol/L, aprotinin 10 mg/L) at 4°C for 10–30 min.

The total amount of uPAR and suPAR was assayed in cell lysates and conditioned media. The ELISA used to quantitate the total amount of suPAR [31] has R2 as catching antibody, which binds all forms of uPAR containing domain III. The plates (96-well microtiter Maxisorp plate, Nunc) were coated overnight at 4°C with 3 $\mu\text{g/mL}$ R2 diluted in 0.1 mol/L Na-carbonate buffer, pH 9.5. The plates were blocked by rinsing with Superblock solution (Pierce Chemical Company, Rockford, IL) diluted 1:2 with PBS, followed by 3 washes with PBS containing 1 g/L Tween 20. The samples were diluted in 0.2 mol/L sodium phosphate buffer pH 7.2, containing 0.1 mol/L NaCl, 50,000 U heparin sodium salt (Sigma), 10 g/L BSA (Fraction V, Boehringer-Mannheim), and 1 g/L Tween 20. The plates were incubated for 2 h at 30°C and subsequently washed 6 times with the abovementioned washing buffer. The detecting polyclonal anti suPAR antibody was added at 1 $\mu\text{g/mL}$ and incubated overnight at 4°C. After another 6 washings, a monoclonal anti-rabbit immunoglobulin antibody conjugated with alkaline phosphatase (Sigma) was added in 1:2000 dilution for 1 h. After a final washing step the substrate *p*-nitrophenyl phosphate (Sigma) was added, and the plates were read in a Ceres automatic plate reader (Bio-Tek Instruments) at absorbance 405 nm at room temperature. Six readings were obtained every 10 min for 1 h and the slope of the color development curve is calculated by the KinetiCalc Software (Bio-Tek Instruments) using linear regression.

The concentrations of uPA and PAI-1 in conditioned media were assayed using the commercial ELISA kits Tint Elise uPATM and Immulyse PAI-1TM (Biopool, Umeå, Sweden).

Statistical methods

Results are given as median and percentiles, and Mann-Whitney test for non-paired comparison was used for testing of differences between groups.

Results

We observed EGF effects on cell migration and expression of the uPA-system in three ovarian cancer cell lines (Fig. 1). EGF-stimulated migration in OVCAR-3, SKOV-3, and SKOV3-IP cells. Also, EGF increased cell-associated uPAR in OVCAR-3 and SKOV3-IP, and tended to increase in SKOV-3 cells. The release of uPA in conditioned media after stimulation with EGF was increased in all cell lines, and PAI-1 was increased in OVCAR-3 and SKOV3-IP. OVCAR-3 was chosen as a representative cell line and was subsequently used in the experiments.

Using Western blotting, we found that EGFR is present in lysates of OVCAR-3 cells (Fig. 2). One to six hours after stimulation with EGF, the EGFR was visibly down-regulated. In contrast, uPA stimulation did not result in detectable down-regulation of EGFR. Also, stimulation with EGF resulted in activation of tyrosine residue #1173 of the EGFR, whereas, stimulation with uPA did not result in detectable phosphory-

lation. We chose an antibody directed to tyrosine #1173, since this site is reportedly phosphorylated after ligand activation of both the $\alpha v \beta 3$ integrin receptor and the EGFR [32].

Using ELISAs, we measured uPAR and sheddable soluble uPAR (suPAR) after stimulation of OVCAR-3 cells with EGF for 24 h. EGF increased the content of uPAR in cell lysates as well as sheddable soluble uPAR (suPAR) in the conditioned media (Fig. 3). Western blotting of the OVCAR-3 cell lysates confirmed that uPAR is increased after EGF stimulation (Fig. 4a). Furthermore, only one form of uPAR is present on the blot and this has the same mobility when probed with either uPAR domain I or uPAR domain III specific antibodies. The observation indicates that uPAR is only present in the intact form in OVCAR-3 cells under these conditions. Using radioligand binding, we assayed the endogenously occupied and the non-occupied fractions of uPAR separately, and found that the increase of cell-associated uPAR after treatment with EGF was entirely accounted for by an increase of occupied receptor sites (Fig. 5). In contrast, EGF did not increase the number of non-

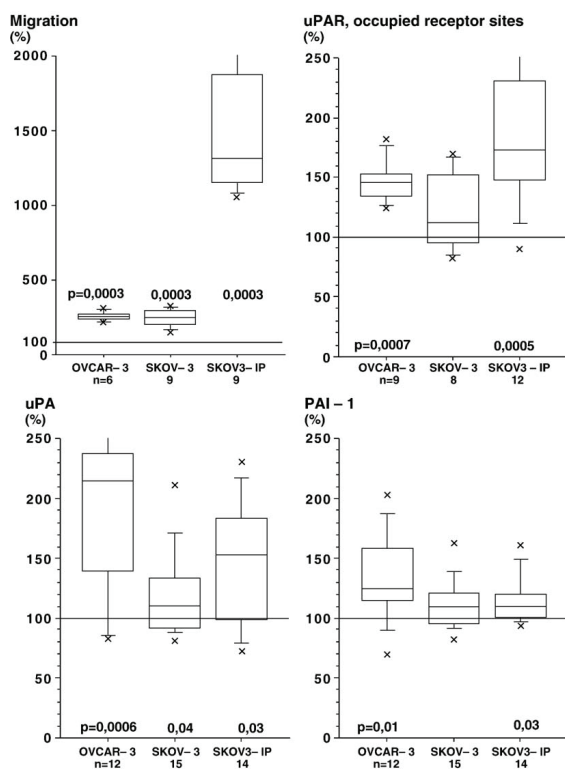


Fig. 1. The response to EGF 10 ng/mL was studied in three ovarian cancer cell lines, OVCAR-3, SKOV-3, SKOV3-IP, with respect to cell migration, content of endogenously occupied uPAR, and release of uPA and PAI-1. Levels in EGF-stimulated cells are expressed as percent of levels in non-stimulated cells. Number of experiments in each group is given in the graphs. Significance levels given in the figure refer to the comparisons between EGF-stimulated and non-stimulated cells.

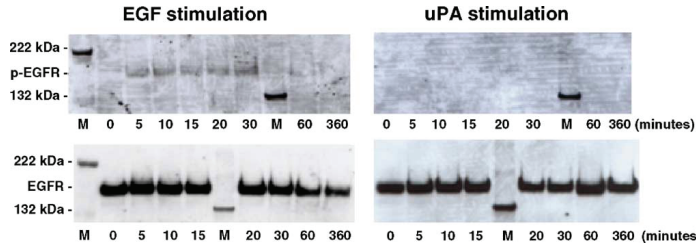


Fig. 2. Western blot of OVCAR-3 cell extracts after stimulation with either EGF (left panels) or uPA (right panels) for 6 h. The primary antibody was detecting either EGFR phosphorylated on tyrosine #1173 (upper panels) or all forms of EGFR (lower panels). Phosphorylation of the EGFR was detected after 5 min and was maximal after 30 min in cells stimulated with EGF. The receptor was down-regulated after 6 h. Significant phosphorylation on tyrosine #1173 and subsequent down-regulation of EGFR was not detected after stimulation with uPA.

occupied receptor sites. It is interesting that even though expression of uPA is up-regulated and more uPAR molecules are endogenously occupied in EGF-stimulated cells, we were not able to detect the cleaved form of uPAR.

Next, we evaluated potential mechanisms responsible for the increase of uPAR in EGF-stimulated cells. RNA extracts analyzed with Northern blotting showed that OVCAR-3 cells stimulated with EGF had increased level of uPAR mRNA (Fig. 4b). Northern blots also showed corresponding increase of uPA and PAI-1 mRNAs (not in figure). Even though the increase of uPAR mRNA by itself may account for the subsequent increase of cell-associated uPAR and suPAR, we also explored other possible mechanisms. Fig. 3 shows that the increase of cell-associated uPAR is accompanied by increased suPAR in the

conditioned media, thus eliminating reduced shedding as a cause of the increase of cell-associated uPAR.

Next we asked whether decreased internalization and degradation might contribute to the increase of cell surface uPAR. We compared uPAR and suPAR in OVCAR-3 cultures treated with EGF and/or colchicine. In addition to disrupting the cytoskeleton, and thus preventing cell migration, colchicine

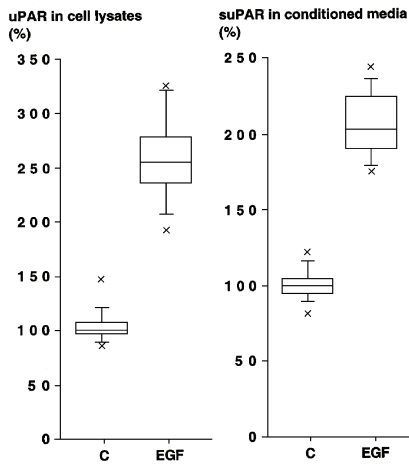


Fig. 3. OVCAR-3 cell cultures ($n = 12$) were stimulated with EGF 10 ng/mL (EGF) or vehicle (C) for 24 h. Cell lysates were assayed for uPAR, and conditioned media were assayed for suPAR using ELISA. EGF treatment increased uPAR in cell lysates ($P < 0.0001$), and suPAR in conditioned media ($P < 0.0001$). Median concentrations in the control groups were 3.2 ng uPAR/mg cellular protein in cell lysates, and 0.6 ng suPAR/mg cellular protein in conditioned media.

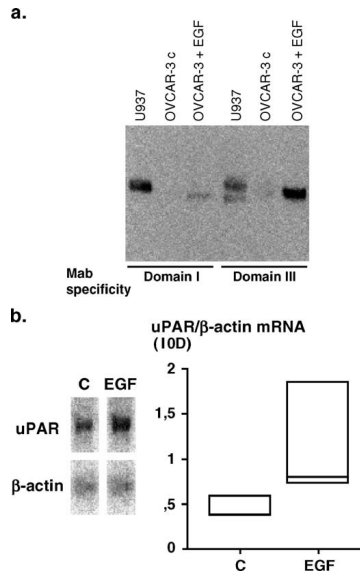


Fig. 4. (a) Detection of cell-surface GPI-anchored uPAR on OVCAR-3 cells. Triton X-114 detergent phase extracts of 1.25×10^6 OVCAR-3 cells, stimulated with EGF 10 ng/mL (OVCAR-3 + EGF) or vehicle (OVCAR-3C) for 24 h, as well as 7.5×10^5 human monocyte-like U937 cells (U937) were analyzed by SDS-PAGE and Western blot, using 5 μ g/mL of either the domain I specific R3 or the domain III specific R4 as primary antibody. (b) Northern blot of uPAR mRNA in OVCAR-3 cells stimulated for 24 h with EGF 10 ng/mL (EGF) or vehicle (C). The graph shows the integrated optical density (IOD) of uPAR mRNA corrected for β -actin mRNA ($n = 4$). Stimulation with EGF increased uPAR mRNA ($P = 0.03$).

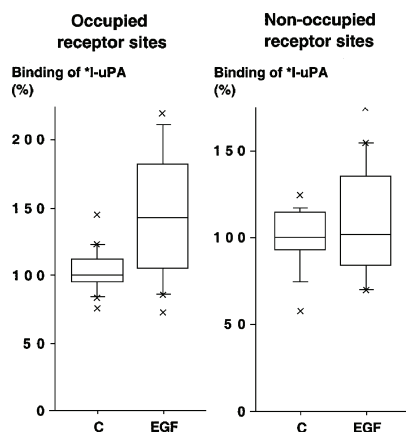


Fig. 5. Cell surface binding sites for ^{125}I -uPA were evaluated after stimulation of OVCAR-3 cells with EGF for 24 h ($n = 18$). The number of occupied receptor sites was calculated as the difference between the numbers of total and non-occupied receptor sites. The number of occupied receptor sites was increased in EGF treated cultures ($P = 0.002$). EGF did not affect the number of non-occupied receptor sites. The median binding level in control wells was 92 fmol/mg cellular protein for occupied and 38 fmol/mg cellular protein for non-occupied receptor sites.

also inhibits cellular endocytosis [25]. Treatment with either colchicine or EGF resulted in accumulation of uPAR on the cell surface (Fig. 6a). Furthermore, in contrast to our findings in the absence of colchicine, treatment with EGF in the presence of colchicine did not significantly increase cell surface uPAR.

This absence of an additive effect suggests that activated EGFR, like colchicine, acts to inhibit the internalization process. Because of difficulties to study internalization of endogenous cell surface uPAR, we studied degradation of the ^{125}I -uPA:PAI-1 complex, which is internalized together with uPAR [33]. Degradation of the complex was significantly reduced in cultures treated with EGF (Fig. 7), thus lending further support to the conclusion that EGF signaling acts to reduce internalization and degradation of uPAR.

The response to EGF stimulation was monitored over a 24 h period by quantifying uPAR, uPA, and PAI-1 mRNAs with real-time PCR, uPAR protein in cell lysates, suPAR in conditioned media, and cell migration using two-dimensional time-lapse video microscopy. The amount of uPAR mRNA increased after 2 h and stayed high for 12 h (Fig. 8). Both uPA and PAI-1 mRNA were significantly increased already after 1 h (data not shown). Cell related uPAR protein had two maxima during the 24 h period. The first increment appeared within minutes after contact with EGF and lasted for 2 h. Thus, cells, which had been briefly (<5 min) exposed to EGF prior to lysis, had about 40% increase of extractable uPAR. It is likely that this early increase represents recruitment of a pool of uPAR, which becomes extractable as a result of EGF stimulation. At 4 and 6 h, the uPAR level was not different between EGF-stimulated and control wells, but at 8 and 12 h, it was again increased in EGF-stimulated cells. The second increase is likely to result from translation of increased uPAR mRNA, as well as decreased internalization of uPAR protein. Accumulation of suPAR in the conditioned media was significantly increased in EGF-stimulated cultures at 12 and 24 h. Cell migration showed two maxima after stimulation with EGF. The first increase lasted between 1 and 7 h after start of stimulation,

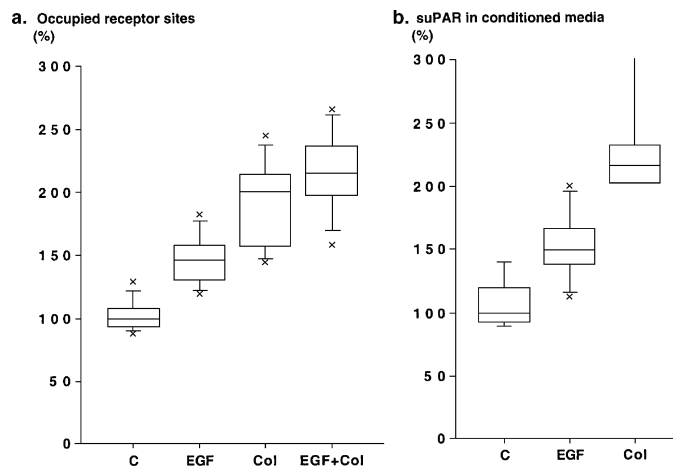


Fig. 6. (a) Binding of ^{125}I -uPA to confluent OVCAR-3 cell cultures after treatment with vehicle, EGF 10 ng/mL, colchicine 1 $\mu\text{g}/\text{mL}$, or their combination for 24 h ($n = 9$). The number of occupied uPAR sites (calculated as in Fig. 5) was increased by EGF ($P = 0.0007$), colchicine ($P = 0.0005$), and EGF + colchicine ($P = 0.0003$). Presence of colchicine eliminated the effect of EGF ($P = 0.1$). (b) suPAR in conditioned medium, measured in ELISA, was increased by both EGF ($P = 0.03$) and colchicine ($P = 0.004$).

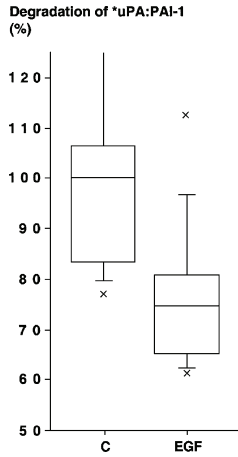


Fig. 7. Radiolabeled ¹²⁵I-uPA:PAI-1 complex 1 nmol/L was allowed to bind to confluent OVCAR-3 cultures (n = 12) at 0°C for 2 h. Subsequent internalization and degradation of the complex at 37°C was measured as TCA soluble radioactivity in the medium after 8 h. Cells had been pre-treated for 24 h with either vehicle (C) or EGF 10 ng/mL. EGF reduced degradation of the ¹²⁵I-uPA:PAI-1 complex (P = 0.003).

and the second increase started at 10 h. Although somewhat delayed, this pattern mimicked that of cell surface uPAR.

We also attempted to address the mechanism of cellular shedding of uPAR, i.e. whether suPAR is secondary either to the accumulation of uPAR on the cell surface, or to the cell migration. For this purpose, we compared the effects of EGF and colchicine. Both EGF and colchicine increase cell surface uPAR as well as suPAR in the conditioned medium (Fig. 6). However, while EGF stimulates, colchicine inhibits cell migration (Fig. 9). Taken together, these experiments suggest that shedding of suPAR is secondary to accumulation of cell surface uPAR and independent of cell migration. However, in another set of experiments with metabolic labeling, we found that cell-associated uPAR was increased by both EGF and colchicine, whereas conditioned medium content of suPAR was increased by EGF only, not by colchicine (Fig. 10). The observation suggests that the mechanism of shedding within this subset of newly synthesized uPAR molecules is different from that we found for the entire population of uPAR (Fig. 6b).

The uPAR–EGFR relation is far from being fully understood. We explored this interaction, and stimulated OVCAR-3 cells with either buffer, uPA, or EGF in the presence or absence of an EGFR specific tyrosine kinase inhibitor Iressa, a monoclonal anti-uPAR antibody R3, which is a competitive inhibitor for binding of uPA and vitronectin to uPAR, a monoclonal anti-uPAR antibody R4, which does not interact with uPAR ligand binding [34,35], and a monoclonal antibody to an irrelevant antigen trinitrophenol (TNP) [36]. The results show that both R3 and Iressa efficiently inhibited the chemotactic response to EGF as well as to uPA whereas R4 and anti-TNP had no effect (Fig. 11). Furthermore, the

combination of R3 and Iressa was not more effective than each compound separately. The result suggests that neither uPAR nor EGFR is up-stream to the other, but rather that both receptors are engaged at the same level and that both need to be functional for cell migration to occur.

Discussion

We found that EGF stimulates cell migration and up-regulates uPAR, uPA, and PAI-1 in ovarian cancer cells. Transcriptional regulation of these components by growth factors and cytokines has been described in many cell systems [37,38]. EGF mediated induction of uPA, PAI-1, and uPAR

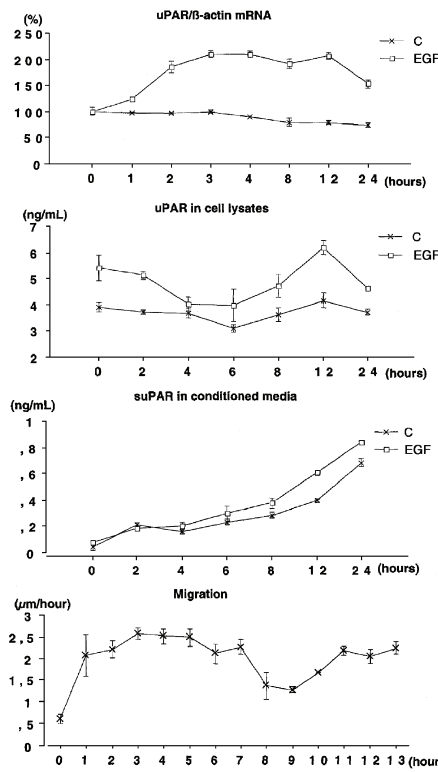


Fig. 8. The effect of EGF on uPAR mRNA and protein in OVCAR-3 cells (n = 6) was studied over 24 h. Cell migration was evaluated with two-dimensional time-lapse video microscopy for 13 h. EGF-stimulated cultures at 0 h were briefly (<5 min) exposed to EGF before being washed and lysed. uPAR mRNA was significantly increased in EGF-stimulated cultures from 2 h on. uPAR in cell lysates was significantly increased by EGF at 0 and 2 h, was not different from control at 4 and 6 h, and was then again increased at 8 and 12 h. suPAR was elevated in conditioned media of EGF treated cultures at 12 and 24 h. EGF-stimulated cell migration in a biphasic manner, i.e. from 1–7 h and from 11 h on.

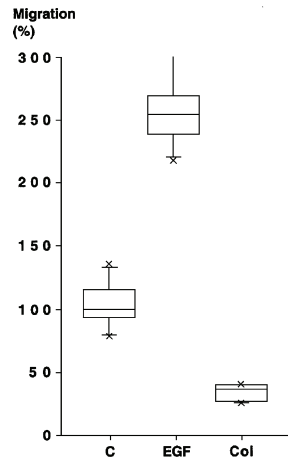


Fig. 9. OVCAR-3 cell migration ($n = 18$) was assayed during 24 h stimulation with EGF 10 ng/mL or colchicine 1 μ g/mL. EGF treatment stimulated ($P < 0.0001$) whereas colchicine inhibited ($P = 0.003$) migration.

mRNA was remarkably fast with a significant increase after 1 and 2 h, respectively. This strongly suggests a direct effect of EGFR signaling on transcription of these genes. This is in contrast to a previous report in a squamous carcinoma cell line, which suggested that up-regulation of the uPA and uPAR genes is secondary to induction of the activator protein-1 constituents cFos and cJun [39]. Induction of uPAR mRNA

starting at 2 h fits well with the increase of cell-associated uPAR starting at 8 h.

Even though we found that production of uPAR was increased, we explored the possibility that in addition elimination of uPAR was decreased. Cell surface uPAR can be eliminated either via shedding to the conditioned medium, or via internalization together with the uPA:PAI-1 complex. We excluded decreased shedding as a possibility through our finding of increased suPAR in conditioned medium of EGF treated cultures. Next, we focused on cellular endocytosis of uPAR.

Cell surface uPAR accompanies the uPA:PAI-1 complex during internalization via scavenger receptors, like the α_2 -macroglobulin receptor/low density lipoprotein receptor related protein (LRP) and the very low density lipoprotein receptor (VLDLR) [33,40,41]. Even though some of internalized uPAR molecules may be recycled back to the cell surface, receptor binding of the uPA:PAI-1 complex results in significant down-regulation of cell surface uPAR [42]. Ligand activated uPAR, which is not targeted for internalization, translocates on the cell surface to focal contact domains [10], and clusters in multiprotein aggregates of migrating cells [7,9,43–45]. Thus, our finding of increased numbers of occupied receptor molecules is likely to represent accumulation of tightly engaged uPAR in such multiprotein aggregates. Such uPAR molecules are not available for internalization and degradation. However, unavailability of the occupied fraction of uPAR cannot by itself account for reduced internalization of ligated uPAR in EGF-stimulated cells, since experimentally added radiolabeled uPA:PAI-1 complex is likely to bind to uPAR molecules from the non-occupied pool, which are subsequently free to undergo

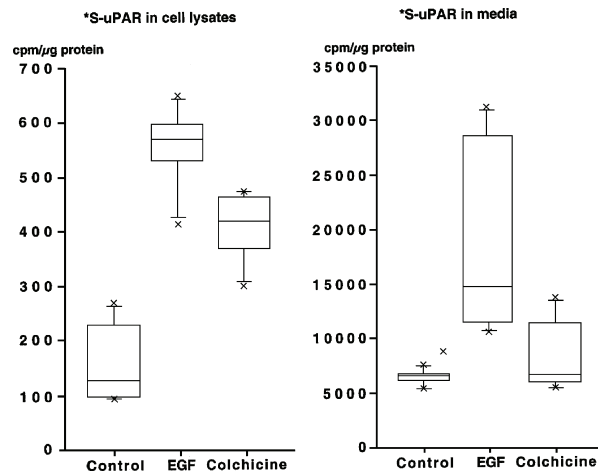


Fig. 10. OVCAR-3 cells ($P = 6$) were labeled with 35 S-methionin for 12 h and subsequently stimulated with either EGF or colchicine for 24 h. uPAR in cell lysates and suPAR in conditioned media were immunoprecipitated using a mixture of two monoclonal antibodies, R3 and R4, recognizing domain I and III, respectively. Radioactivity was measured in the precipitates. Both EGF ($P = 0.004$) and colchicine ($P = 0.004$) increased cell lysate content of uPAR, whereas only EGF ($P = 0.004$) and not colchicine increased conditioned medium content of suPAR.

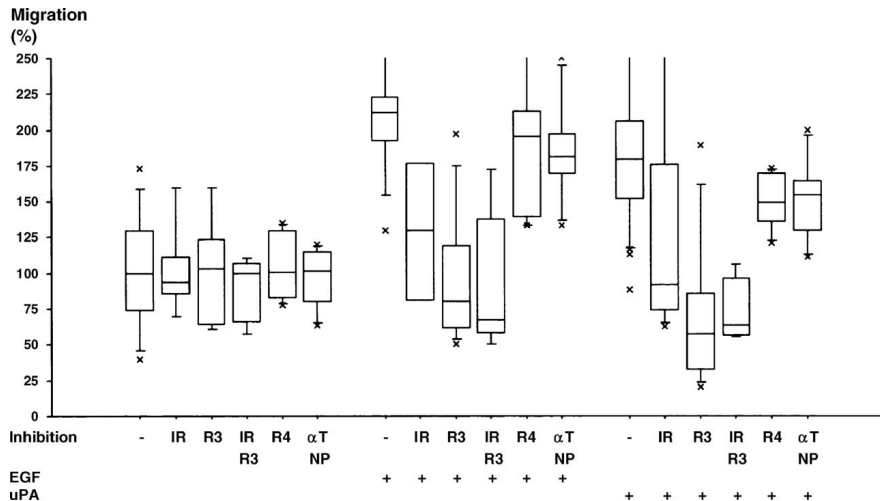


Fig. 11. OVCAR-3 cell migration was stimulated for 24 h with either buffer, EGF 10 ng/mL, or uPA 1 nmol/L, in the absence or presence of inhibitors ($n = 6$). The EGFR inhibitor Iressa (ZD1839) 1 $\mu\text{mol/L}$, the anti-uPAR R3 10 $\mu\text{g/mL}$, the anti uPAR R4 10 $\mu\text{g/mL}$, and anti-TNP 10 $\mu\text{g/mL}$, were added 30 min before the stimulants. All results are given as % of the median in the no stimulant/no inhibitor group. The inhibitors did not affect migration in control wells. Migration in EGF-stimulated wells was greater than in control wells ($P < 0.0001$) and this effect was abrogated by concomitant treatment with Iressa ($P = 0.01$), R3 ($P = 0.002$), and their combination ($P = 0.002$) but not by R4 and anti-TNP. Migration in uPA-stimulated wells were greater than in control wells ($P < 0.0001$) and the increase was inhibited by concomitant treatment with Iressa ($P = 0.04$), R3 ($P = 0.002$), and Iressa + R3 ($P = 0.002$).

internalization. Thus, our finding of decreased degradation of the uPA:PAI-1 complex in EGF-stimulated cells is likely to reflect a real inhibition of the internalization process, which is relevant also for the turnover of uPAR.

Our results suggest that the increased expression of uPAR seen after 24 h stimulation with EGF results both from increased uPAR gene transcription and from decreased internalization of uPAR. In contrast to transcriptional regulation, decreased internalization and degradation of uPAR have to our knowledge not been previously reported in response to EGF. One possible mechanism, which would result in decreased internalization of uPA:PAI-1, would be down-regulation of scavenger receptors involved, e.g. LRP or VLDLR. Down-regulation of LRP in response to a phorbol ester was reportedly accompanied by inhibition of uPA:PAI-1 internalization and degradation [46].

The very early rise in extractable cellular uPAR, which occurred within minutes of EGF stimulation, can neither relate to increased gene transcription nor to decreased internalization/degradation of uPAR. This increase is more likely to result from translocation of uPAR molecules from cryptic domains to the cell surface, where uPAR is accessible for detergent extraction. Stimulation of neutrophils with phorbol esters or cytokines results in rapid up-regulation of cell surface uPAR secondary to translocation from intracellular stores [47]. Depending on the method used, intracellular uPAR has been located in different subcellular compartments. Thus, using ultracentrifugation, uPAR was found in secretory vesicles and specific granules [47], whereas immunoelectron microscopy

identified uPAR in association with primary granules [48], and biochemical characterization located uPAR predominantly in detergent-resistant lipid rafts [49]. Within the lipid rafts, uPAR can occur in non-occupied as well as occupied form. Apparently, the intracellular pool of uPAR mobilized by EGF in ovarian cancer cells is derived from detergent-resistant domains.

In addition to the full-length form, cell surface uPAR and suPAR also occur in a cleaved form. Enzymes including uPA, plasmin, and matrix metallo-proteinases have the capacity to cleave uPAR in the linker region between domains I and II [4,50]. Such cleavage also occurs *in vivo*, and we have previously demonstrated the domain II + III fragment in the cystic fluid from malignant ovarian tumors [51]. Western blot experiments did not detect any domain II + III fragment in the lysates of OVCAR-3 cells, despite the presence of uPA and at least minute amounts of plasmin in the experimental system. It is possible that the actual cleaving enzyme is produced by other cell types, e.g. stromal cells or leucocytes, in ovarian tumors, and thus are not present in our monocultures.

Shedding of uPAR occurs *in vitro* from a variety of cultured cells, and, as shown in the present study, also from ovarian cancer cells. We have previously shown that shedding also occurs *in vivo*, and suPAR is found in tumor fluids of patients with ovarian cancer [51]. The physiological or patho-physiological mechanism of shedding is, however, not known. Possibly, suPAR could represent uPAR molecules cleaved from the cell surface at the trailing edge of migrating cells, or shedding could just be secondary to the accumulation of uPAR

at the cell surface. EGF treated cells display increased migration and accumulation of cell surface uPAR in addition to increased shedding. Cells treated with colchicine have largely deranged cytoskeleton, which inhibits cell migration as well as endocytosis, and decreased internalization of ligated uPAR results in accumulation at the cell surface. These cells also demonstrate extensive shedding of uPAR. Thus, these results suggest that shedding of uPAR is secondary to accumulation of uPAR at the cell surface rather than being dependent on cell migration.

In another set of experiments, however, metabolically labeled uPAR, i.e. newly synthesized molecules, was increased on the cell surface by both EGF and colchicine. In contrast, conditioned medium content of radiolabeled suPAR was increased in EGF treated, but not in colchicine treated cultures. These somewhat divergent results may indicate that migration is needed for shedding of a newly synthesized portion of the uPAR pool. Alternatively, we cannot exclude that colchicine, which has dramatic impact on cells, also has a direct influence on the shedding process of uPAR, at least when uPAR is located within certain cell surface domains, which may not be the case with newly synthesized uPAR molecules. Our results may be interpreted to indicate existence of differential release mechanisms of uPAR, possibly related to location within different cellular compartments.

Also, the function of suPAR is not very well known. The observation that experimentally added suPAR has a restricting effect on tumor cell migration and proliferation suggests scavenging of uPA. However, a recent study found this effect to be uPA independent, and instead a result of suPAR interfering with the interaction between ligated uPAR and adaptor proteins at the cell surface [22]. Another study found suPAR to bind in a paracrine way and thus to be functional in adjacent cells [52,53].

Our results show that OVCAR-3 cells express both EGFR and uPAR and that both these receptors are involved in the migratory response to EGF as well as to uPA. The increase of uPAR in EGF-stimulated cells affected exclusively the endogenously occupied fraction, and not the fraction of available non-occupied uPAR molecules. Presumably, the occupied fraction uPAR translocates on the cell surface to focal contact domains [10]. Activated uPAR associates with several cell surface proteins, among them the β -subunits of some integrin receptors, in multiprotein aggregates during cell migration [7,9,43–45].

Previous reports have concluded that EGFR functions as a transducer of the signal from uPAR activation [21,22]. In agreement with these studies, we found that migration in response to uPA was blocked by inhibition of EGFR activation, but we also found that the response to EGF was inhibited by an anti-uPAR antibody preventing uPA binding. The observation suggests that activations of EGFR and uPAR are steps in the same chain of events, and this is furthermore supported by our finding that blocking both receptors is not more efficient than blocking either of them. We have previously shown similar relation between uPAR and EGFR in endothelial cells [6].

These data taken together with the knowledge that both uPAR and EGFR are able to associate with activated integrin receptors [9,32,45,54], suggest that uPAR and EGFR engage in the same multiprotein signaling complex together with other cell surface proteins and probably several cytoskeleton-associated signaling molecules, at least during some part of the migratory process. Complexity of this cell surface process was indicated in Chinese hamster ovary cells where activation of ERK, but not of STAT5b, in response to uPA, was maintained in EGFR negative cells, although ERK activation is normally EGFR-dependent [55]. Co-immunoprecipitation of uPAR and EGFR was found by some investigators [23], but not by others [56]. Also, β 1 integrin has been co-localized on the cell surface with both uPAR [57] and EGFR [21].

Depending on the activation mechanism, the EGFR is phosphorylated on slightly different tyrosine residues. For example, tyrosine #1173 is phosphorylated after stimulation of the EGFR with EGF, but also after activation of integrin receptors with extracellular matrix proteins [32]. Since activated uPAR presents as a ligand for integrin receptors [8], we were interested to see whether activated uPAR also results in phosphorylation of tyrosine #1173. Using an antibody, which identifies a segment of EGFR containing P-tyrosine #1173, we found that this tyrosine residue is phosphorylated after stimulation with EGF but not after stimulation with uPA. This observation suggests that activated uPAR initiates signaling along a pathway, which is different from that initiated by integrin receptors during matrix adhesion [32], even though activation of uPAR results in association of integrin β -subunits with EGFR [21,32]. EGFR is known to be down-regulated as a result of internalization following stimulation with EGF [58]. We found evidence of EGFR down-regulation at 1 and 6 h after stimulation with EGF in OVCAR-3 cells. In contrast, EGFR down-regulation could not be detected after stimulation with uPA. Our interpretation of these data is that, even though the tyrosine residue #1173 is not phosphorylated, phosphorylation of the EGFR occurs since we inhibited the response to uPA with Iressa, the EGFR phosphorylation inhibitor. Also, EGFR phosphorylation in response to stimulation with uPA has been reported using different antibodies [21,23]. Apparently, even though the EGFR presumably is phosphorylated on some tyrosine residues in response to uPA, it may not be exposed to internalization since down-regulation was not detected.

EGF stimulates migration also in normal ovarian surface epithelial cells. This process is reportedly associated with transition of the epithelial cells to a mesenchymal phenotype [59]. The same authors did however not observe the phenomenon in ovarian cancer cell lines, and our experimental design did not allow evaluation of morphology after the migration experiments.

Acknowledgments

The excellent technical assistance of Li Zhou and Ruth Petersson is gratefully acknowledged. This work was financially supported by EU contract QLK3-CT-2002-02136.

References

- [1] Olayoye MA, Neve RM, Lane HA, Hynes NE. The ErbB signaling network: receptor heterodimerization in development and cancer. *EMBO J* 2000;19:3159–67.
- [2] Schlessinger J. Cell signaling by receptor tyrosine kinases. *Cell* 2000;103:211–25.
- [3] Andreasen PA, Egelund R, Petersen HH. The plasminogen activation system in tumor growth, invasion, and metastasis. *Cell Mol Life Sci* 2000;57:25–40.
- [4] Hoyer-Hansen G, Ploug M, Behrendt N, Ronne E, Dano K. Cell-surface acceleration of urokinase-catalyzed receptor cleavage. *Eur J Biochem* 1997;243:21–6.
- [5] Sandberg T, Casslen B, Gustavsson B, Benraad TJ. Human endothelial cell migration is stimulated by urokinase plasminogen activator: plasminogen activator inhibitor 1 complex released from endometrial stromal cells stimulated with transforming growth factor beta1; possible mechanism for paracrine stimulation of endometrial angiogenesis. *Biol Reprod* 1998;59:759–67.
- [6] Sandberg T, Ehinger A, Casslen B. Paracrine stimulation of capillary endothelial cell migration by endometrial tissue involves epidermal growth factor and is mediated via up-regulation of the urokinase plasminogen activator receptor. *J Clin Endocrinol Metab* 2001;86:1724–30.
- [7] Chapman HA, Chapman HA, Wei Y, Simon DI, Waltz DA. Role of urokinase receptor and caveolin in regulation of integrin signaling. *Thromb Haemost* 1999;82:291–7.
- [8] Tarui T, Mazar AP, Cines DB, Takada Y. Urokinase-type plasminogen activator receptor (CD87) is a ligand for integrins and mediates cell–cell interaction. *J Biol Chem* 2001;276:3983–90.
- [9] Simon DI, Wei Y, Zhang L, et al. Identification of a urokinase receptor–integrin interaction site. Promiscuous regulator of integrin function. *J Biol Chem* 2000;275:10228–34.
- [10] Pollanen J, Stephen R, Salonen EM, Vaheri A. Proteolytic mechanisms operating at the surface of invasive cells. *Adv Exp Med Biol* 1988;233:187–99.
- [11] Fischer-Colbrie J, Witt A, Heinzl H, et al. EGFR and steroid receptors in ovarian carcinoma: comparison with prognostic parameters and outcome of patients. *Anticancer Res* 1997;17:613–9.
- [12] Berchuck A, Rodriguez GC, Kamel A, et al. Epidermal growth factor receptor expression in normal ovarian epithelium and ovarian cancer: I. Correlation of receptor expression with prognostic factors in patients with ovarian cancer. *Am J Obstet Gynecol* 1991;164:669–74.
- [13] Scambia G, Benedetti Panici P, Battaglia F, et al. Epidermal growth factor, oestrogen and progesterone receptor expression in primary ovarian cancer: correlation with clinical outcome and response to chemotherapy. *Br J Cancer* 1995;72:361–6.
- [14] Andreasen PA, Kjoller L, Christensen L, Duffy MJ. The urokinase-type plasminogen activator system in cancer metastasis: a review. *Int J Cancer* 1997;72:1–22.
- [15] Schmalfeldt B, Kuhn W, Reuning U, et al. Primary tumor and metastasis in ovarian cancer differ in their content of urokinase-type plasminogen activator, its receptor, and inhibitors types 1 and 2. *Cancer Res* 1995;55:3958–63.
- [16] Borgfeldt C, Casslen B, Liu CL, Hansson S, Lecander I, Astedt B. High tissue content of urokinase plasminogen activator (u-PA) is associated with high stromal expression of u-PA mRNA in poorly differentiated serous ovarian carcinoma. *Int J Cancer* 1998;79:588–95.
- [17] Borgfeldt C, Hansson SR, Gustavsson B, Masback A, Casslen B. Dedifferentiation of serous ovarian cancer from cystic to solid tumors is associated with increased expression of mRNA for urokinase plasminogen activator (uPA), its receptor (uPAR) and its inhibitor (PAI-1). *Int J Cancer* 2001;92:497–502.
- [18] Kuhn W, Schmalfeldt B, Reuning U, et al. Prognostic significance of urokinase (uPA) and its inhibitor PAI-1 for survival in advanced ovarian carcinoma stage FIGO IIIc. *Br J Cancer* 1999;79:1746–51.
- [19] Borgfeldt C, Bendahl PO, Gustavsson B, et al. High tumor tissue concentration of urokinase plasminogen activator receptor is associated with good prognosis in patients with ovarian cancer. *Int J Cancer* 2003;107:658–65.
- [20] Borgfeldt C, Bendahl PO, Ferno M, Casslen B. High preoperative plasma concentration of tissue plasminogen activator (tPA) is an independent marker for shorter overall survival in patients with ovarian cancer. *Gynecol Oncol* 2003;91:112–7.
- [21] Liu D, Aguirre Ghiso J, Estrada Y, Ossowski L. EGFR is a transducer of the urokinase receptor initiated signal that is required for in vivo growth of a human carcinoma. *Cancer Cell* 2002;1:445–57.
- [22] Jo M, Thomas KS, O'Donnell M, Gonias SI. Epidermal growth factor receptor-dependent and -independent cell-signaling pathways originating from the urokinase receptor. *J Biol Chem* 2003;278:1642–6.
- [23] Guerrero I, Santibanez JF, Gonzalez A, Martinez J. EGF receptor transactivation by urokinase receptor stimulus through a mechanism involving Src and matrix metalloproteinases. *Exp Cell Res* 2004;292:201–8.
- [24] Mahabeleshwar GH, Das R, Kundu GC. Tyrosine kinase, p56lck-induced cell motility, and urokinase-type plasminogen activator secretion involve activation of epidermal growth factor receptor/extracellular signal regulated kinase pathways. *J Biol Chem* 2004;279:9733–42.
- [25] Casslen B, Nordengren J, Gustavsson B, Nilbert M, Lund LR. Progesterone stimulates degradation of urokinase plasminogen activator (u-PA) in endometrial stromal cells by increasing its inhibitor and surface expression of the u-PA receptor. *J Clin Endocrinol Metab* 1995;80:2776–84.
- [26] Thorell JI, Johansson BG. Enzymatic iodination of polypeptides with 125I to high specific activity. *Biochim Biophys Acta* 1971;251:363–9.
- [27] Hunter WM, Greenwood FC. Preparation of iodine-131 labelled human growth hormone of high specific activity. *Nature* 1962;194:495–6.
- [28] Thomas PS. Hybridization of denatured RNA and small DNA fragments transferred to nitrocellulose. *Proc Natl Acad Sci U S A* 1980;77:5201–5.
- [29] Roldan AL, Cubellis MV, Masucci MT, et al. Cloning and expression of the receptor for human urokinase plasminogen activator, a central molecule in cell surface, plasmin dependent proteolysis. *EMBO J* 1990;9:467–74.
- [30] Behrendt N, Ronne E, Ploug M, et al. The human receptor for urokinase plasminogen activator. NH2-terminal amino acid sequence and glycosylation variants. *J Biol Chem* 1990;265:6453–60.
- [31] Riisbro R, Pironen T, Brønner N, Larsen B, Nielsen HJ, Stephens RW, et al. Measurement of soluble urokinase plasminogen activator receptor in serum. *J Clin Ligand Assay* 2002;25:53–6.
- [32] Moro L, Dolce L, Cabodi S, et al. Integrin-induced epidermal growth factor (EGF) receptor activation requires c-Src and p130Cas and leads to phosphorylation of specific EGF receptor tyrosines. *J Biol Chem* 2002;277:9405–15.
- [33] Czekay RP, Kuemmel TA, Orlando RA, Farquhar MG. Direct binding of occupied urokinase receptor (uPAR) to LDL receptor-related protein is required for endocytosis of uPAR and regulation of cell surface urokinase activity. *Mol Biol Cell* 2001;12:1467–79.
- [34] Ronne E, Behrendt N, Ellis V, Ploug M, Dano K, Hoyer-Hansen G. Cell-induced potentiation of the plasminogen activation system is abolished by a monoclonal antibody that recognizes the NH2-terminal domain of the urokinase receptor. *FEBS Lett* 1991;288:233–6.
- [35] Hoyer-Hansen G, Behrendt N, Ploug M, Dano K, Preissner KT. The intact urokinase receptor is required for efficient vitronectin binding: receptor cleavage prevents ligand interaction. *FEBS Lett* 1997;420:79–85.
- [36] Kearney JF, Radbruch A, Liesegang B, Rajewsky K. A new mouse myeloma cell line that has lost immunoglobulin expression but permits the construction of antibody-secreting hybrid cell lines. *J Immunol* 1979;123:1548–50.
- [37] Andreasen PA, Georg B, Lund LR, Riccio A, Stacey SN. Plasminogen activator inhibitors: hormonally regulated serpins. *Mol Cell Endocrinol* 1990;68:1–19.
- [38] Sandberg T, Eriksson P, Gustavsson B, Casslen B. Differential regulation of the plasminogen activator inhibitor-1 (PAI-1) gene expression by growth factors and progesterone in human endometrial stromal cells. *Mol Hum Reprod* 1997;3:781–7.
- [39] Siratsuchi T, Ishibashi H, Shirasuna K. Inhibition of epidermal growth

- factor-induced invasion by dexamethasone and AP-1 decoy in human squamous cell carcinoma cell lines. *Cell Physiol* 2002;193:340–8.
- [40] Nykjaer A, Petersen CM, Møller B, et al. Purified alpha 2-macroglobulin receptor/LDL receptor-related protein binds urokinase plasminogen activator inhibitor type-1 complex. Evidence that the alpha 2-macroglobulin receptor mediates cellular degradation of urokinase receptor-bound complexes. *J Biol Chem* 1992;267:14543–6.
- [41] Battey FD, Gafvels ME, FitzGerald DJ. The 39-kDa receptor-associated protein regulates ligand binding by the very low density lipoprotein receptor. *J Biol Chem* 1994;269:23268–73.
- [42] Olson D, Pollanen J, Hoyer-Hansen G, et al. Internalization of the urokinase-plasminogen activator inhibitor type-1 complex is mediated by the urokinase receptor. *J Biol Chem* 1992;267:9129–33.
- [43] Harder T, Simons K. Caveolae, DIGs, and the dynamics of sphingolipid-cholesterol microdomains. *Curr Opin Cell Biol* 1997;9:534–42.
- [44] Horejsi V, Drbal K, Cebecauer M, et al. GPI-microdomains: a role in signalling via immunoreceptors. *Immunol Today* 1999;20:356–61.
- [45] Wei Y, Lukashev M, Simon DI, et al. Regulation of integrin function by the urokinase receptor. *Science* 1996;273:1551–5.
- [46] Conese M, Blasi F. Urokinase/urokinase receptor system: internalization/degradation of urokinase–serpin complexes: mechanism and regulation. *Biol Chem Hoppe-Seyler* 1995;376:143–55.
- [47] Plesner T, Ploug M, Ellis V, et al. The receptor for urokinase-type plasminogen activator and urokinase is translocated from two distinct intracellular compartments to the plasma membrane on stimulation of human neutrophils. *Blood* 1994;83:808–15.
- [48] Pedersen TL, Plesner T, Horn T, Hoyer-Hansen G, Sorensen S, Hansen NE. Subcellular distribution of urokinase and urokinase receptor in human neutrophils determined by immunoelectron microscopy. *Ultrastruct Pathol* 2000;24:175–82.
- [49] Cunningham O, Andolfo A, Santovito ML, Iuzzolino L, Blasi F, Sidenius N. Dimerization controls the lipid raft partitioning of uPAR/CD87 and regulates its biological functions. *EMBO J* 2003;22:5994–6003.
- [50] Andolfo A, English WR, Resnati M, Murphy G, Blasi F, Sidenius N. Metalloproteases cleave the urokinase-type plasminogen activator receptor in the D1–D2 linker region and expose epitopes not present in the intact soluble receptor. *Thromb Haemost* 2002;88:298–306.
- [51] Wahlberg K, Hoyer-Hansen G, Casslen B. Soluble receptor for urokinase plasminogen activator in both full-length and a cleaved form is present in high concentration in cystic fluid from ovarian cancer. *Cancer Res* 1998;58:3294–8.
- [52] Chavakis T, Kanse SM, Yutzy B, Lijnen HR, Preissner KT. Vitronectin concentrates proteolytic activity on the cell surface and extracellular matrix by trapping soluble urokinase receptor–urokinase complexes. *Blood* 1998;91:2305–12.
- [53] Mizukami IF, Todd III RF. A soluble form of the urokinase plasminogen activator receptor (suPAR) can bind to hematopoietic cells. *J Leukoc Biol* 1998;64:203–13.
- [54] Wei Y, Yang X, Liu Q, Wilkins JA, Chapman HA. A role for caveolin and the urokinase receptor in integrin-mediated adhesion and signaling. *J Cell Biol* 1999;144:1285–94.
- [55] Jo M, Thomas KS, Marozkina N, Amin TJ, Silva CM, Parsons SJ, Gonias SL. Dynamic assembly of the urokinase-type plasminogen activator signaling receptor complex determines the mitogenic activity of urokinase-type plasminogen activator. *J Biol Chem* 2005;280:17449–57.
- [56] Blagoev B, Kratchmarova I, Ong SE, Nielsen M, Foster LJ, Mann M. A proteomics strategy to elucidate functional protein–protein interactions applied to EGF signaling. *Nat Biotechnol* 2003;21:315–8.
- [57] Aguirre-Ghiso JA, Liu D, Mignatti A, Kovalski K, Ossowski L. Urokinase receptor and fibronectin regulate the ERK(MAPK) to p38(MAPK) activity ratios that determine carcinoma cell proliferation or dormancy in vivo. *Mol Biol Cell* 2001;12:63–79.
- [58] Oksvold MP, Thien CB, Widerberg J, Chantry A, Huitfeldt HS, Langdon WY. Serine mutations that abrogate ligand-induced ubiquitination and internalization of the EGF receptor do not affect c-Cbl association with the receptor. *Oncogene* 2003;22:8509–18.
- [59] Salamanca CM, Maines-Bandiera SL, Leung PC, Hu YL, Auersperg N. Effects of epidermal growth factor/hydrocortisone on the growth and differentiation of human ovarian surface epithelium. *J Soc Gynecol Invest* 2004;11:241–51.



Estradiol attenuates EGF-induced rapid uPAR mobilization and cell migration via the G-protein coupled receptor 30 (GPR30) in ovarian cancer cells

E. HENIC*, V. NOSKOVA*, G. HØYER-HANSEN[#], S. HANSSON*, B. CASSLÉN

**Department of Gynecology & Obstetrics, University Hospital, SE-221 85 Lund, Sweden.*

[#]*Finsen Laboratory, Rigshospitalet, DK-2100 Copenhagen Ø, Denmark.*

Abstract. Henic E, Noskova V, Høyer-Hansen G, Hansson S, Casslén B. Estradiol attenuates EGF-induced rapid uPAR mobilization and cell migration via the G-protein coupled receptor 30 (GPR30) in ovarian cancer cells. *Int J Gynecol Cancer*

EGF stimulates proliferation and migration in ovarian cancer cells, and high tumor expression of the EGF system correlates with poor prognosis. EGF up-regulates urokinase plasminogen activator receptor (uPAR) on the cell surface via three distinct mechanisms: rapid mobilization of uPAR from detergent resistant domains, increased mRNA, and decreased degradation. GPR30 is a newly identified membrane estrogen receptor (ER).

The objective of this study was to explore the effects of 17 β -estradiol (E2) on uPAR expression and cell migration in ovarian cancer cells, and further to identify the ER involved.

We used seven ovarian cancer cell lines, cell migration assay, cellular binding of ¹²⁵I-uPA, cellular degradation of ¹²⁵I-uPA:PAI-1 complex, ELISA for uPAR, solid phase EIA for ER α , and qPCR. E2 attenuates the stimulatory effect of EGF on cell migration and uPAR expression. Specifically, E2 reduces the very rapid increase of detergent extractable uPAR, which occurs within minutes of EGF stimulation and probably represents mobilization of uPAR from detergent resistant domains like lipid rafts. E2 influenced neither the amount of uPAR mRNA nor the rate of uPAR degradation or solubilization. The nuclear ER antagonists ICI 182780 and tamoxifen, which are GPR30 agonists, as well as the specifically constructed GPR30 agonist G1, mimicked the effect of E2 on uPAR expression and cell migration. OVCAR-3 cells express mRNA for GPR30.

E2 attenuates EGF-induced mobilization of ligated uPAR from detergent resistant domains and subsequent migration in ovarian cancer cells. The response to various ER ligands indicates that this effect is mediated via the membrane estrogen receptor GPR30.

KEYWORDS: Cell migration. GPR30. Lipid rafts. Membrane ER. OVCAR-3. uPAR.

In addition to the classical pathway of estrogen action via the nuclear receptors ER α and ER β estrogen stimulation results in rapid intracellular increase of second messengers, e.g. cAMP, PiP3, NO, and Ca²⁺ (1-4). This effect is initiated at the cell membrane, but no receptor has so far been recognized. The G-protein coupled membrane receptor GPR30 (5) was recently found to bind E2 with high affinity (6,7) and ligation results in activation of G proteins and subsequent activation of the second messengers. The ER α antagonists ICI

182780 and tamoxifen bind to GPR30, but with agonistic effect (7). Activation of GPR30 may lead to rapid transactivation of epidermal growth factor receptor (EGFR) with subsequent activation of the MAPK pathway (8,9).

Estrogens play a role during carcinogenesis in breast and endometrium, but its role in the ovarian cancer is controversial. Estrogens simulate proliferation of several ovarian cancer cell lines, and this effect is mediated via ER α (10, 11). Furthermore, estrogen reduces

apoptosis in immortalized ovarian surface epithelial cells by Akt mediated up-regulation of bcl-2, an anti-apoptotic gene⁽¹²⁾. Lindgren et al showed that high expression of ER α in poorly differentiated epithelial tumors correlates with lower apoptotic activity⁽¹³⁾. Furthermore, estrogens induce chemo resistance in ovarian cancer cells via phosphorylation of Akt⁽¹⁴⁾. On the other hand, estrogens induce expression of progesterone receptor⁽¹⁵⁾ and high tumor tissue content of progesterone receptor is associated with longer progression-free survival in patients with ovarian cancer^(16, 17).

Urokinase plasminogen activator (uPA) and its receptor (uPAR) play an important role in tumor invasion, since ligand activation of uPAR results in cell migration as well as proteolytic activity focused on the cell surface. Furthermore, activated uPAR is a ligand for several integrin receptors, which promote signaling via ERK1/2⁽¹⁸⁾. Also, uPAR has spatial and functional association with EGFR since EGFR and uPAR co-immuno-precipitate⁽¹⁹⁾ and EGFR mediates intracellular signaling from activated uPAR^(20, 21). The uPAR is attached to the cell membrane by a glycosyl phosphatidyl inositol anchor. It can be shed from the cell surface by cleavage of the anchor. The soluble form of uPAR (suPAR) is increased in peripheral blood of patients with various malignant tumors, but also in cystic fluid from patients with ovarian cancer^(22, 23). The components of the uPA-system are up regulated in a number of malignances and high concentrations correlate with poor prognosis⁽²⁴⁾. We have previously shown that this is the case also in ovarian cancer^(25, 26).

EGF up-regulates the uPA-system in ovarian cancer cells, and we recently reported that EGF increases cell surface expression of uPAR in ovarian cancer cells via three separate mechanisms⁽²⁷⁾. The first very rapid increase presumably results from mobilization of uPAR from detergent resistant domains, such as lipid rafts. Increased expression of uPAR mRNA, and decreased internalization and degradation of uPAR are later effects. Over-expression of EGFR is common in various malignances, and is associated with increased malignant potential and decreased sensitivity for chemotherapy. Increased expression of both EGF and EGFR in ovarian cancer is associated with an aggressive phenotype⁽²⁸⁾, and poor response to chemotherapy⁽²⁹⁾.

Convergence between estrogen and EGF mediated signaling may occur at several levels. Since our preliminary results showed that estrogen alone had no effect on cell migration or surface expression of uPAR, but reduced EGF-stimulated increase of both in several ovarian cancer cell lines, we explored possible mechanisms whereby estrogens may modulate this effect of EGF.

Material and methods

Cell culture

Seven human ovarian adenocarcinoma cell lines were used. The OVCAR-3 cell line derives from ascitic fluid cells from a patient with poorly differentiated papillary ovarian adenocarcinoma. SKOV-3 was also derived from cells in the ascitic fluid associated with a metastatic ovarian adenocarcinoma with unknown histological type. SKOV3-IP derives from SKOV-3 cells but has the ability to form intraperitoneal tumors in mice. HEY cells are derived from a moderately differentiated papillary adenocarcinoma, whereas ES-2 cells and TOV-21G cells are from poorly differentiated clear cell carcinomas⁽³⁰⁾. Finally TOV-112D cells were derived from a patient with poorly differentiated endometrioid carcinoma. OVCAR-3, SKOV-3, TOV-112 D, TOV-21G, SKOV3-IP, and HEY cells were cultured in M199 supplemented with FBS 10 % (20% for OVCAR-3), insulin 10 mg/L, glutamine 2 mmol/L, penicillin 100,000 IU/L, streptomycin 100 mg/L, and fungizone 0.25 mg/L. ES-2 cells were cultured in McCoy's 5A with GlutaMAX™ supplemented with 10% FBS, and same antibiotics. All incubations were performed in humidified air with 5% CO₂ at 37° C. All experiments were performed in serum-free, phenol red-free medium.

Cell migration assay

Cell migration was assayed in 12-well tissue culture plate inserts, which had polyethylene terephthalate track-etched membranes (10.5 mm diameter) with 8 μ m pore diameter (Becton Dickinson, Franklin Lakes, NJ, USA). Cells were suspended in FBS-free, phenol red-free medium (1.5 x 10⁵ cells/mL), and 0.5 mL was added to the insert. The same medium, 1.5 mL, without cells was added to the lower compartment, and chemo-attractants were added here. After 24 hours incubation at 37°C, remaining cells on the upper surface of the

membrane were removed with a cotton swab before the inserts were fixed with methanol for 5 minutes and stained with Giemsa (12.5 %) for 15 minutes. Cells on the lower surface of the membrane were counted at 400x magnification. The mean of four counted fields is given as the result for each membrane. At least six membranes were evaluated in each group.

Cellular binding of ^{125}I -uPA

This assay was performed as previously described using the HMW fraction of uPA labeled with ^{125}I (27, 31).

Cellular degradation of ^{125}I -uPA:PAI-1 complex

Cell cultures were incubated for 2 hours on ice with ^{125}I -uPA:PAI-1 complex in a final concentration 1 nmol/L as previously described (27, 31). After washing x6 with ice-cold HBSS, cultures were transferred to 37°C to allow internalization of the cell surface bound complex. After indicated time periods media were collected, TCA added to a final concentration of 10%, and the samples centrifuged at 3000g for 20 minutes. Radioactivity was measured in the supernatants. The cells were lysed with 1 mol/L NaOH for assay of protein content.

ELISA for uPAR

The conditioned media was collected and cells were lysed with lysis buffer (Tris-HCl 100 mmol/L, EDTA 10 mmol/L, pH 8.1, Triton X-114 1%, phenylmethylsulfonyl fluoride 100 mmol/L, aprotinin 10 mg/L, CHAPS 0.25 %) at 4°C for 10-30 minutes. The total amount of uPAR/suPAR was measured in cell lysates and conditioned media using the uPAR ELISA previously described (32).

Solid phase EIA for ER α

ER α was assayed in cell lysates using a commercial enzyme immunoassay (EIA) kit ABBOTT ER-EIA Monoclonal (ABBOTT Laboratories, North Chicago, IL, USA). The assay used beads coated with a monoclonal anti-ER α . The secondary antibody was also a monoclonal anti-ER α conjugated with horseradish peroxidase. After washings, the beads were incubated with the substrate solution (hydrogen peroxide and o-Phenylenediamine 2 HCl). The reaction was

stopped with 1N sulphuric acid, and the color read at 492 nm. The assay was performed in an Oncology routine lab, and cellular content of ER α was related to the level, which is clinically relevant for breast tumor tissue.

Real time PCR

Total cellular RNA was extracted with Trizol Reagent™ (Life Technologies, Sweden). The quality of RNA samples was analyzed on 1.5% agarose/2% formalin denaturing gel using 1xMOPS buffer (Intergen company). Samples with visible 18S/28S bands using RNA loader (GenHunter, Nashville, TN, USA) were included for further analysis. RNA was reverse transcribed according to protocols from Applied Biosystems (Foster City, CA, USA). Real time PCR amplification (33) used primers and probes from Assays on Demand™ (Applied Biosystems): uPAR (PLAUR): accession # NM_002659, assay on demand # Hs00182181_m1; GPR30 (GPER): accession # NM_001505, assay on demand # Hs00173506_m1; ER α (ESR1): accession # NM_000125.2, assay on demand # Hs00174860_m1; ER β (ESR2): accession # NM_001040275.1, assay on demand # Hs00230957_m1.

Northern blotting for uPAR mRNA

Total RNA was extracted from OVCAR-3 cells, size separated in agarose gels and transferred to GeneScreen Plus nitrocellulose filter. The filters were hybridized with a cDNA probe for uPAR, which had been radiolabelled with ^{32}P -dCTP. In order to correct for unequal loading, the filters were subsequently hybridized with a probe for human β -actin, which had been identically labeled. After autoradiography, signal intensities were measured by computerized densitometric scanning (BioImage Products, Ann Arbor, MI, USA). Signal intensity of the uPAR probe was related to intensity of the β -actin probe. The probe for uPAR, HUR06, was a 584-base pair BamHI fragment of the human uPAR gene subcloned into pBluescript KS.

Statistical Methods

Results are presented as box plots with median and percentiles in the figures. Mann-Whitney U-test for non-paired comparisons was used to evaluate the significance of differences between groups. All tests were two-sided, and a 5% level of significance was used.

Migration of ovarian cancer cells

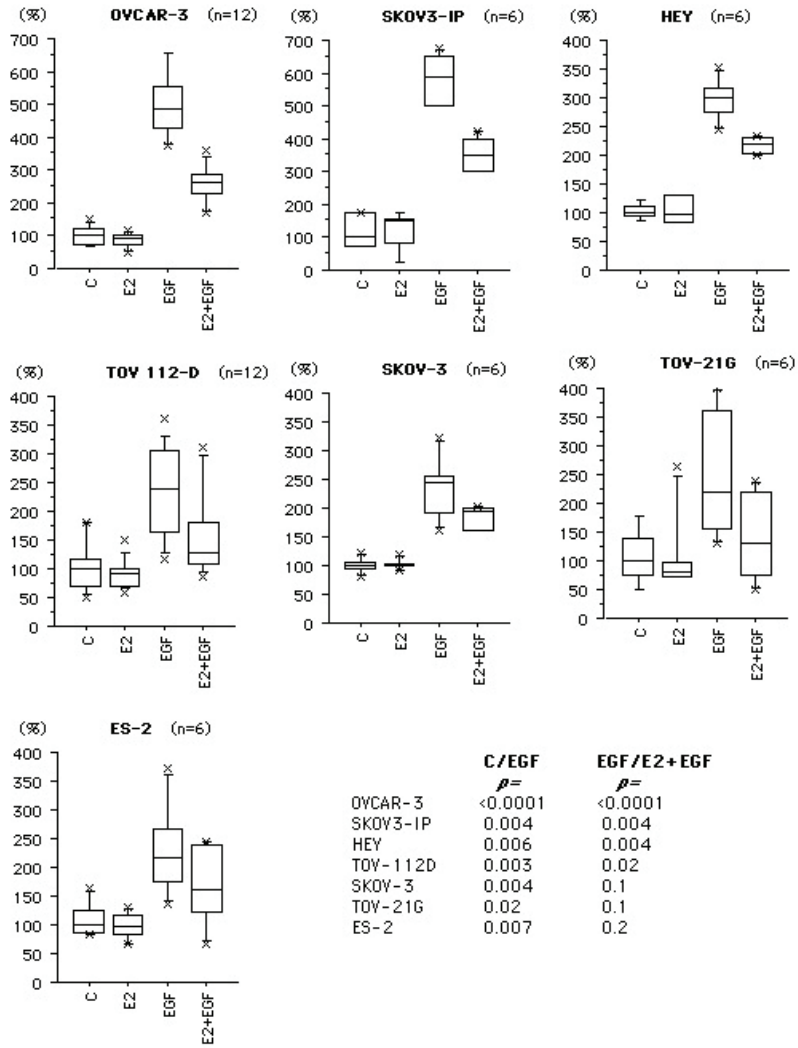


Figure 1.

Cell migration was assayed with tissue culture plate inserts in seven ovarian cancer cell lines. Cells were stimulated for 24 hours with vehicle (C), E2 10 nmol/L, EGF 10 µg/L, or the combination (E2+EGF). EGF stimulated migration in all cell lines. E2 alone did not influence cell migration, but the effect of EGF was reduced by the presence of E2. The level of significance for each cell line is given in the graph.

Results

EGF stimulated cell migration in seven different ovarian cancer cell lines (Fig. 1). Estradiol (E2) had no effect on basal cell migration, but it inhibited EGF-induced migration in four of the cell lines (OVCAR-3, SKOV3-IP, HEY, TOV-112D) and tended to reduce it in the other three (SKOV-3, TOV-21G, ES-2). All following experiments employed the OVCAR-3 cells.

Since cell membrane bound uPAR is crucial for cell migration, we assayed functional binding sites using radiolabelled uPA in OVCAR-3 cells after stimulation with EGF and E2. Neither EGF nor E2 affected the number of free, i.e. unoccupied, receptor sites (data not shown). In contrast, the number of endogenously occupied receptor sites was increased by treatment with EGF, and this effect was attenuated by the presence of E2 (Fig. 2). We subsequently used an ELISA to assay for detergent extractable uPAR in OVCAR-3 cells stimulated with EGF, with or without E2, for 24 hours. EGF increased the content of uPAR in cell lysates ($p < 0.0001$), whereas presence of E2 reduced this effect ($p = 0.03$), a pattern similar to that in figure 2 (data not shown).

Binding of 125 I-uPA (%)

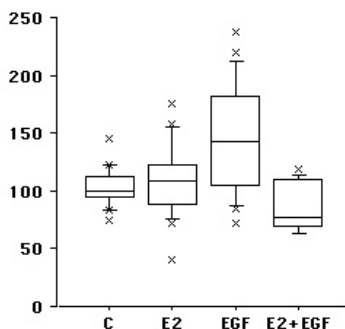


Figure 2.

The endogenously occupied pool of uPAR was assayed in OVCAR-3 cells using 125 I-uPA binding assay ($n = 12$). Cells were pretreated for 24 hours as described in figure 1. E2 alone had no effect. EGF increased the number of occupied receptor sites ($p = 0.002$), and this increase was inhibited by E2 ($p = 0.0004$). Results are given as % of the median in the control group, which was 92 fmol/mg cellular protein.

Since EGF induces increase of cell surface uPAR via three different mechanisms⁽²⁷⁾, we attempted to pinpoint which of these pathways that is attenuated by E2. The first mechanism is an increase of uPAR mRNA. This increase was not significantly modified by E2, neither when evaluated by real-time PCR (Fig. 3) nor by Northern blot (not shown).

uPAR/ β -actin mRNA (%)

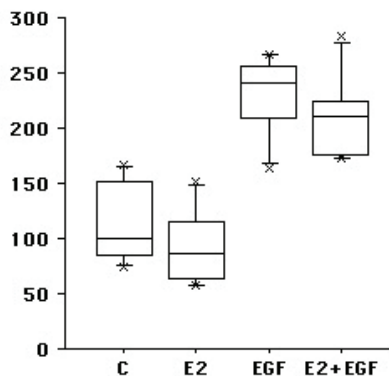


Figure 3.

Real-time PCR analysis of uPAR mRNA in OVCAR-3 cells ($n = 6$), which had been stimulated for 6 hours as described in figure 1. The amount of uPAR mRNA was normalized to β -actin mRNA. The EGF induced increase of uPAR mRNA ($p = 0.007$) was not reduced by E2.

The second mechanism whereby EGF increases uPAR is via reduced internalization and lysosomal degradation, as indicated by the fate of radiolabelled uPA:PAI-1 complex. E2 had no effect on the rate of degradation of the 125 I-uPA:PAI-1 complex, and did not attenuate the decrease caused by EGF (Fig. 4).

Another possible mechanism to explain the decrease of cell surface uPAR in response to E2 could be increased shedding of uPAR from the cell surface. We measured soluble uPAR in conditioned media from confluent OVCAR-3 cultures treated with E2 and EGF for 24 hours. EGF increased the shedding, and this was not further increased by E2 (Fig. 5). Thus, modulation by E2 of the EGF effect on uPAR expression was neither mediated by decreasing the amount of mRNA nor by increasing degradation or shedding of the protein.

The third mechanism, whereby EGF increases uPAR, is an immediate (within

TCA-soluble radioactivity
cpm/ug protein

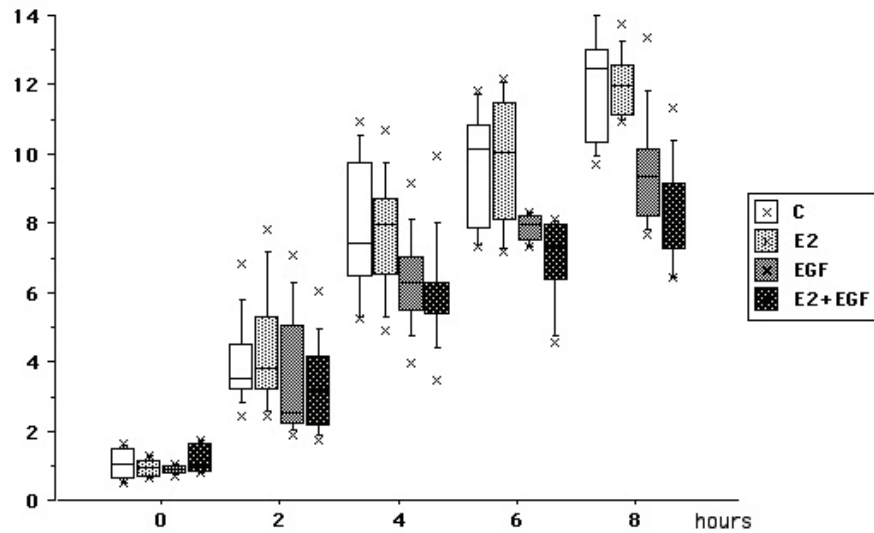


Figure 4.

After binding of ^{125}I -uPA:PAI-1 complex to OVCAR-3 cell cultures at 0°C , degradation of the complex at 37°C was assayed as TCA-soluble radioactivity in the medium after indicated time periods. The cells had been pretreated for 24 hours as described in figure 1. EGF reduced the rate of degradation of the complex ($p=0.004$), and this effect was not reversed by E2.

suPAR in conditioned media
(ng/mg protein)

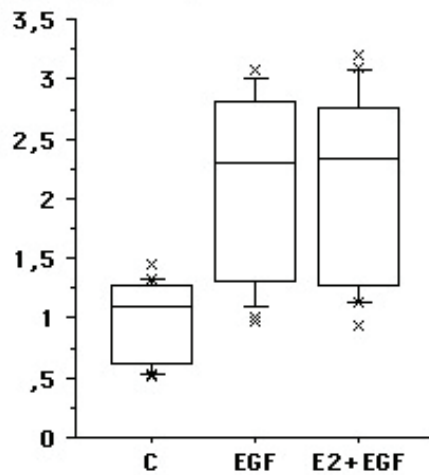


Figure 5.

OVCAR-3 cell cultures ($n=20$) were treated as detailed in figure 1 for 24 hours. Soluble uPAR (suPAR) was quantified in the conditioned media using ELISA. EGF increased the concentration of suPAR ($p<0.0001$), and this effect was not modified by E2.

minutes) effect on the amount of detergent extractable uPAR, probably resulting from recruitment of uPAR from cryptic domains, e.g. lipid rafts. In order to explore whether E2 modifies this effect we stimulated OVCAR-3 cultures briefly for <5 minutes with EGF after pretreatment with either E2 or ICI 182780 (kindly provided by AstraZeneca, Macclesfield, Cheshire, UK) for 30 minutes. Extractable uPAR in cell lysates was measured in an ELISA. Both E2 and ICI 182780 inhibited the EGF stimulated increase of extractable uPAR (Fig. 6).

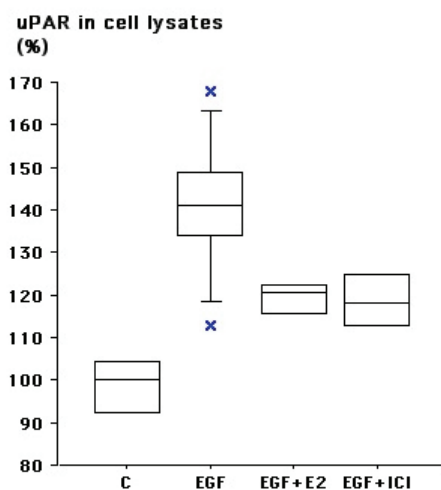


Figure 6. OVCAR-3 cell cultures (n=5) were treated briefly (<5 minutes) with EGF 10 μ g/L, after pretreatment with vehicle, E2 10 nmol/L, or ICI 100 nmol/L for 30 minutes. Cells were lysed with detergent, and the lysate assayed for extractable uPAR using ELISA. Results are given as % of the median in the control group. The immediate effect of EGF on uPAR expression was reduced by both E2 (p=0.01) and ICI (p=0.03).

In order to clarify through which estrogen receptor this effect is mediated, we first studied expression of the membrane bound GPR30 as well as the nuclear ER α and ER β . Human placenta and endometrium reportedly express GPR30⁽⁷⁾, and they were used as reference tissues. GPR30 mRNA was demonstrated with real-time PCR, and the PCR product is shown after agarose gel electrophoresis in figure 7a. The level of GPR30 mRNA in OVCAR-3 cells was lower than in the placenta and endometrium, but clearly detectable (Fig. 7b).

In contrast, ER α mRNA was not detectable in OVCAR-3 cells. Four of the ovarian cancer cell lines, OVCAR-3, SKOV-3, HEY, and SKOV3-IP were analyzed for their content of ER α protein. The content was very low 5, 5, 0, and 16 fmol/mg protein respectively, which is below the cut-off level for clinical relevance in mammary tumor tissue. Thus, since ER α shows no or very low expression during non-estrogenic conditions, we analyzed these cells after E2 stimulation. However, the expression of ER α in OVCAR-3 cells increased neither after 6 hours nor after 24 hours incubation with E2 10 nmol/L (results not shown). Like GPR30 mRNA, ER β mRNA was lower than in placental and endometrial tissue, but clearly detectable (Fig. 7b). Thus, significant expression was found only for GPR30 and ER β in OVCAR-3 cells.

Next, we studied a panel of compounds, which have different effects on GPR30 and nuclear ER, for their effects on EGF induced OVCAR-3 cell migration. ICI 182780 is a pure inhibitor of estrogen effects mediated by nuclear ER, but an agonist to GPR30⁽³⁴⁾. Tamoxifen is also an antagonist for nuclear ER, at least in some tissues, but an agonist for GPR30. G1 (Calbiochem, Darmstadt, Germany) is a specifically designed agonist for GPR30 and does not bind to nuclear ER. G1, ICI 182780, and tamoxifen had all similar effect as E2 on EGF induced cell migration (Fig. 8). Also, the effect of ICI 182780 was similar to that of E2 on EGF induced increase of uPAR in cell lysates (Fig. 6). Furthermore, ICI 182780 did not inhibit the effect of E2 when they were given together (Fig. 8), which would be expected if the effect had been mediated via nuclear ER. 17 α -estradiol, an inactive isomer of 17 β -estradiol (E2), had no effect on EGF stimulated cell migration. These observations taken together strongly indicate that the effect of E2, which we report in this paper, is mediated by GPR30 and not by nuclear ER.

Discussion

We demonstrate in ovarian cancer cells that E2 attenuates the invasive phenotype, which results from EGF stimulation. Cell migration is a crucial component of tumor invasion and is critically dependent on expression of uPAR on the cell surface. In this role, uPAR needs to

retain its ligand binding capacity, since a monoclonal antibody, which blocks uPA binding to uPAR, inhibits the migratory response to EGF⁽²⁷⁾. We have previously shown that within few minutes after EGF stimulation, concomitant with the immediate migratory response, ligated uPAR is recruited from detergent resistant domains, presumably lipid rafts, to detergent extractable domains⁽²⁷⁾. Following chemotactic stimulation, ligated uPAR joins the assembly of proteins at focal adhesion sites⁽³⁵⁾. We show that the increase of detergent extractable uPAR was reduced by E2. This seems to be a general effect of E2 since migration was inhibited to varying degree in all the seven cell lines tested. E2 never caused full inhibition of the EGF effect, presumably because EGF increases uPAR by yet two other mechanisms, i.e. increased content of uPAR mRNA and decreased degradation of uPAR protein, which are not modulated by E2⁽²⁷⁾. Since uPAR in addition is a regulator of pericellular proteolysis, E2 has an anti-tumor effect with respect to the EGF stimulated invasive phenotype. It has yet to be shown whether E2 also modifies the response to other chemotactic stimuli in ovarian or other cancer cells.

The exact mechanism, whereby detergent soluble uPAR is increased within few minutes of EGF stimulation, is not known, but it is very likely that this pool of uPAR molecules is derived from the detergent insoluble pool in lipid rafts. Lipid rafts are specialized, morphologically distinct, membrane microdomains that are enriched in cholesterol and sphingolipids. These highly dynamic domains promote interactions among signaling receptors, and have major impact on the function of these receptors. The lipophilic character of the GPI anchor attracts uPAR to the lipid rafts, and uPAR has been reported to accumulate within these domains also in its ligated form⁽³⁶⁾. This is also supported by our own recent observation, that the ligated, but not the unoccupied, pool of uPAR was recruited after EGF stimulation⁽²⁷⁾. Also, this is the pool of uPAR, which is relevant to cell migration. Pöllänen et al reported that uPAR rapidly re-locates to focal adhesion sites after stimulation with uPA⁽³⁷⁾. Since this process is part of the migratory response, and EGF stimulates cell migration in an uPAR dependent manner in these cells⁽²⁷⁾, it can be

assumed that EGF stimulation causes the same rearrangement in uPAR distribution.

EGFR is abundant in lipid rafts but it is not known whether EGFR molecules leave the rafts together with uPAR after activation. EGFR and uPAR reportedly co-immunoprecipitate under certain conditions⁽¹⁹⁾ suggesting in addition a functional association between these receptors. Furthermore, a specific inhibitor of EGFR phosphorylation blocks the chemotactic response to uPA⁽²⁷⁾, suggesting a close interaction between these two receptors. On the other hand, signaling and internalization of the EGFR can proceed also within the lipid rafts, since these structures are not only platforms to concentrate receptors and assemble the signal transduction machinery, they also recruit several endocytosis proteins⁽³⁸⁾.

In recent years, inter-receptor crosstalk and receptor trans-activation have emerged as general concepts in cellular signaling cascades. In most reports stimulation of a G-protein coupled receptor (GPCR) induces phosphorylation in a receptor tyrosine kinase (RTK), thus combining the broad ligand diversity of GPCRs with the potent signaling capacities of RTKs. Trans-activation of RTKs was first described and is best known for EGFR⁽³⁹⁾, and it can result from activation of various GPCRs, including GPR30^(9, 40). Negative feedback on EGFR signaling has been described for E2 binding to GPR30 via G-protein alpha activation of adenylyl cyclase and cAMP and attenuation of Raf activation⁽⁴¹⁾. GPCR activation results in intracellular release of second messengers, like Ca²⁺ and PiP3, which may act to reduce mobilization of uPAR from lipid rafts after E2 activation of GPR30⁽⁴²⁾. Furthermore, E2 is a potent activator of sphingosine kinase-1, an enzyme, which may potentially influence sphingolipids in the rafts and proteins bound to them⁽⁴³⁾. We found that our OVCAR-3 cells express GPR30. ER α is not expressed at all or in insignificant amounts, whereas ER β is expressed. Since previous reports from other labs suggest that these cells express ER α ^(44, 45), we wanted to explore the possibility that the estrogen free condition was the reason to our finding. However, stimulation with estradiol did not induce expression of ER α . Apparently, our OVCAR-3 cells have developed a variant phenotype, which does not express ER α . The fact that both ICI 182780 and tamoxifen

Gel electrophoresis of the PCR products

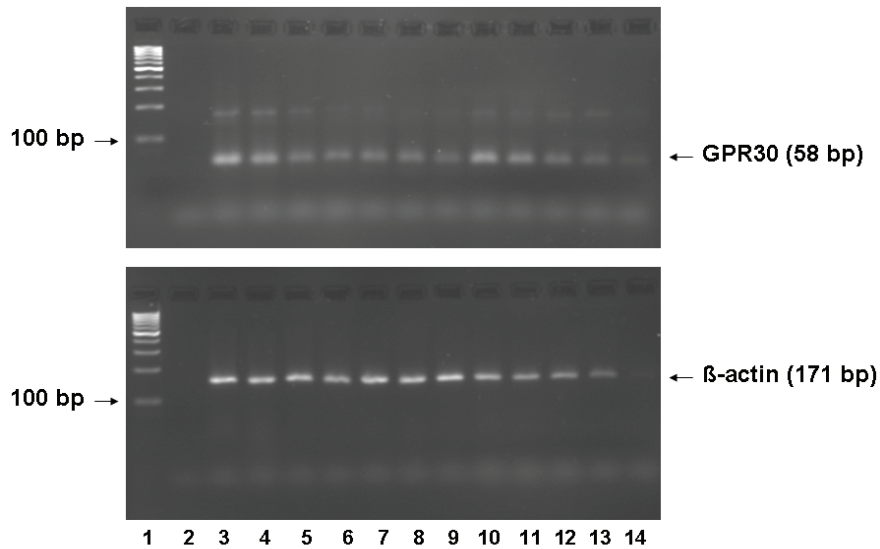
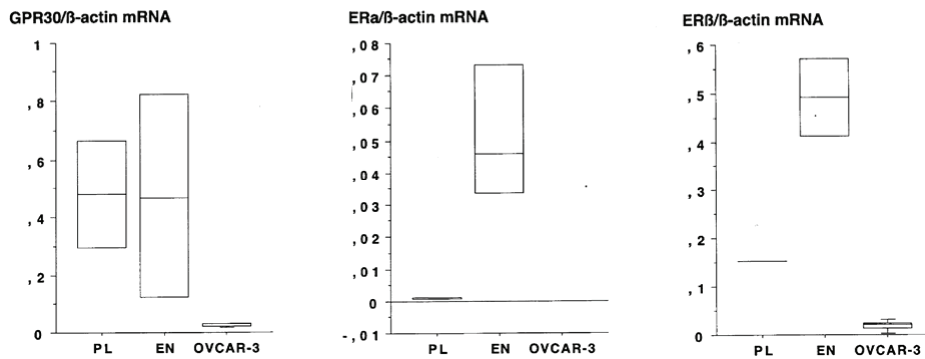


Figure 7.

(a) Agarose gel electrophoresis of the PCR product after amplification of a 58 bp sequence of the GPR30 gene. Upper figure shows GPR30 (58 bp), and lower β -actin (171 bp). The lanes show: DNA ladder (1), negative control (2), human endometrium in mid proliferate (3), late proliferate phase (4), and early secretory (5) phase, OVCAR-3 (6), SKOV-3 (7), SKOV3-IP (8), HEY (9), human placenta extract in dilution 1:1 (10), dilution 1:4 (11), dilution 1:16 (12), dilution 1:64 (13), and dilution 1:256 (14).



(b) Assay of GPR30 mRNA, ER α mRNA and ER β mRNA with real-time PCR in human placenta, human endometrium, and OVCAR-3 cells (n=4). Values were normalized to β -actin. OVCAR-3 cells express GPR30 mRNA and ER β mRNA but not ER α mRNA

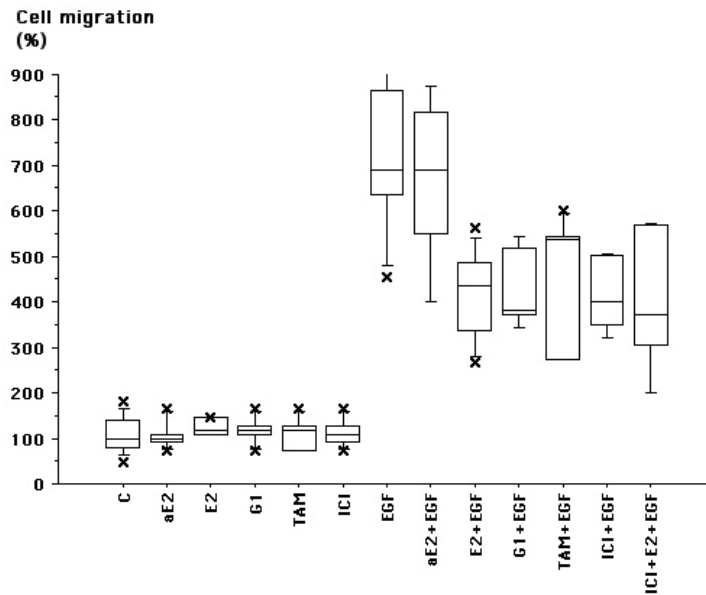


Figure 8.

Cell migration was assayed as in figure 1 after 24 hours stimulation with vehicle (C), 17 α -estradiol (aE2) 10 nmol/L, 17 β -estradiol (E2) 10 nmol/L, G1 100 nmol/L, tamoxifen (TAM) 1 μ mol/L, ICI 182780 (ICI) 100 nmol/L, EGF 10 μ g/L, or combinations (n=12 for C, E2, EGF, and n=6 for the other). All results are expressed in relation to the median of the control group = 100%. EGF stimulated migration was reduced by E2 (p=0.0002), G1 (p=0.006), TAM (p=0.004), and ICI (p=0.006). ICI 182780 did not reverse the effect of E2 (p=0.9). 17 α -estradiol had no effect on EGF stimulated cell migration.

showed agonistic properties with E2 in modulating the response to EGF suggests that this effect is not mediated via nuclear ER, but via GPR30, since these ligands are agonists to GPR30⁽⁴¹⁾. This conclusion is further born out by our finding that a specifically designed GPR30 agonist, G1, inhibited EGF stimulated cell migration in a manner very similar to E2. Also, the observation that ICI 182780, which is a pure inhibitor of E2 binding to nuclear ER, did not antagonize the effect of E2 is further support for this conclusion. All seven ovarian cancer cell lines, which were analyzed, express GPR30, and EGF induced cell migration was inhibited by E2 to some extent in all seven cell lines. All these observations taken together suggest that E2 mediates inhibition of EGF induced cell migration via GPR30, and that this is a common feature in a variety of ovarian cancer cells.

Hormonal therapy has the advantage of very limited side effects. However, only some ovarian tumors respond to hormonal therapy, and responsiveness is difficult to predict⁽⁴⁶⁾. Some authors found no correlation between nuclear ER status and response to hormonal therapy⁽⁴⁷⁾, whereas others showed that tumors with high PR/ER ratio responded better to treatment with high-dose Medroxy-progesterone 17-acetate⁽⁴⁸⁾. The effect of estrogens in ovarian cancer cells is complex. Depending on ER-status, type of estrogenic compound, dosage, cell type, etc. estrogens can influence mitosis, apoptosis, migration, as well as invasion of ovarian cancer cells in different ways. Thus, estrogens can promote tumor growth either by stimulating proliferation or by reducing apoptosis^(11, 12, 49). On other hand, estrogens induce PR expression in ovarian cancer cell lines⁽¹⁵⁾, and high tumor tissue content of PR is positively related to better survival in patients with ovarian cancer^(16, 17). Our present results suggest that E2 inhibits tumor invasion, since it inhibits EGF induced cell migration and uPAR expression. All our data indicate that this effect is mediated by GPR30. Agonist molecules, specifically designed for this receptor, opens up new perspectives for targeted tumor therapy.

Acknowledgement

This work was supported by grants from the Swedish Cancer Fund, the Medical Faculty of Lund University, and the Crafoord's fund.

References

1. Pietras RJ, Szego CM. Specific binding sites for oestrogen at the outer surfaces of isolated endometrial cells. *Nature* 1977;**265**:69-72.
2. Morley P, Whitfield JF, Vanderhyden BC, Tsang BK, Schwartz JL. A new, nongenomic estrogen action: the rapid release of intracellular calcium. *Endocrinology*. 1992;**131**:1305-12.
3. Gu Q, Moss RL. 17 beta-Estradiol potentiates kainate-induced currents via activation of the cAMP cascade. *J Neurosci* 1996;**16**:3620-9.
4. Denninger JW, Marletta MA. Guanylate cyclase and the .NO/cGMP signaling pathway. *Biochim Biophys Acta* 1999;**1411**:334-50.
5. Owman C, Blay P, Nilsson C, Lolait SJ. Cloning of human cDNA encoding a novel heptahelix receptor expressed in Burkitt's lymphoma and widely distributed in brain and peripheral tissues. *Biochem Biophys Res Commun* 1996;**228**:285-92.
6. Revankar CM, Cimino DF, Sklar LA, Arteburn JB, Prossnitz ER. A transmembrane intracellular estrogen receptor mediates rapid cell signaling. *Science* 2005;**307**:1625-30.
7. Thomas P, Pang Y, Filardo EJ, Dong J. Identity of an estrogen membrane receptor coupled to a G protein in human breast cancer cells. *Endocrinology* 2005;**146**:624-32.
8. Filardo EJ, Quinn JA, Bland KI, Frackelton AR. Estrogen-induced activation of Erk-1 and Erk-2 requires the G protein-coupled receptor homolog, GPR30, and occurs via trans-activation of the epidermal growth factor receptor through release of HB-EGF. *Mol Endocrinol* 2000;**14**:1649-60.
9. Filardo E.J. Epidermal growth factor receptor (EGFR) transactivation by estrogen via the G-protein-coupled receptor, GPR30: a novel signaling pathway with potential significance for breast cancer. *J Steroid Biochem Mol Biol* 2002;**80**:231-8.
10. O'Donnell AJ, Macleod KG, Burns DJ, Smyth JF, Langdon SP. Estrogen receptor-alpha mediates gene expression changes

- and growth response in ovarian cancer cells exposed to estrogen. *Endocr Relat Cancer* 2005;**12**:851-66.
11. Langdon SP, Hirst GL, Miller EP et al. The regulation of growth and protein expression by estrogen in vitro: a study of 8 human ovarian carcinoma cell lines. *J Steroid Biochem Mol Biol* 1994;**50**:131-5.
 12. Choi KC, Kang SK, Tai CJ, Auersperg N, Leung PC. Estradiol up-regulates antiapoptotic Bcl-2 messenger ribonucleic acid and protein in tumorigenic ovarian surface epithelium cells. *Endocrinology* 2001;**142**:2351-60.
 13. Lindgren P, Bäckström T, Mählck CG, Ridderheim M, Cajander S. Steroid receptors and hormones in relation to cell proliferation and apoptosis in poorly differentiated epithelial ovarian tumors. *Int J Oncol* 2001;**19**:31-8.
 14. Mabuchi S, Ohmichi M, Kimura A, et al. Estrogen inhibits paclitaxel-induced apoptosis via the phosphorylation of apoptosis signal-regulating kinase 1 in human ovarian cancer cell lines. *Endocrinology* 2004;**145**:49-58.
 15. Langdon SP, Gabra H, Bartlett JM, et al. Functionality of the progesterone receptor in ovarian cancer and its regulation by estrogen. *Clin Cancer Res* 1998;**4**:2245-51.
 16. Hempling RE, Piver MS, Eltabbakh GH, Recio FO. Progesterone receptor status is a significant prognostic variable of progression-free survival in advanced epithelial ovarian cancer. *Am J Clin Oncol* 1998;**21**:447-51.
 17. Munstedt K, Steen J, Knauf AG, Buch T, von Georgi R, Franke FE. Steroid hormone receptors and long term survival in invasive ovarian cancer. *Cancer* 2000;**89**:1783
 18. Kugler MC, Wei Y, Chapman HA. Urokinase receptor and integrin interactions. *Curr Pharm Des* 2003;**9**:1565-74.
 19. Guerrero J, Santibanez JF, Gonzáles A, Martínez J. EGF receptor transactivation by urokinase receptor stimulus through a mechanism involving Src and matrix metalloproteinases. *Exp Cell Res* 2004;**292**:201-8.
 20. Jo M, Thomas KS, O'Donnell DM, Goniás SL. Epidermal growth factor receptor-dependent and -independent cell-signaling pathways originating from the urokinase receptor. *J Biol Chem* 2003;**278**:1642-6.
 21. Liu D, Aguirre Ghiso J, Estrada Y, Ossowski L. EGFR is a transducer of the urokinase receptor initiated signal that is required for in vivo growth of a human carcinoma. *Cancer Cell* 2002;**1**:445-57.
 22. Danø K, Behrendt N, Høyer-Hansen G et al.. Plasminogen activation and cancer. *Thromb Haemost* 2005;**93**:676-81.
 23. Wahlberg K, Hoyer-Hansen G, Casslén B. Soluble receptor for urokinase plasminogen activator in both full-length and a cleaved form is present in high concentration in cystic fluid from ovarian cancer. *Cancer Res* 1998;**58**:3294-8.8.
 24. Andreasen PA, Egelund R, Petersen HH. The plasminogen activation system in tumor growth, invasion, and metastasis. *Cell Mol Life Sci* 2000;**57**:25-40.
 25. Borgfeldt C, Hansson SR, Gustavsson B, Måsbäck A, Casslén B. Dedifferentiation of serous ovarian cancer from cystic to solid tumors is associated with increased expression of mRNA for urokinase plasminogen activator (uPA), its receptor (uPAR) and its inhibitor (PAI-1). *Int J Cancer* 2001;**92**:497-502.
 26. Casslen B, Bossmar T, Lecander I, Åstedt B. Plasminogen activators and plasminogen activator inhibitors in blood and tumour fluids of patients with ovarian cancer. *Eur J Cancer* 1994;**30A**:1302-9.
 27. Henic E, Sixt M, Hansson S, Høyer-Hansen G, Casslén. EGF-stimulated migration in ovarian cancer cells is associated with decreased internalization, increased surface expression, and increased shedding of the urokinase plasminogen activator receptor. *Gynecol Oncol* 2006;**101**:28-39.
 28. Psyrrri A, Kassam M, Bamias A et al. Effect of epidermal growth factor receptor expression level on survival in patients with epithelial ovarian cancer. *Clin Cancer Res* 2005;**11**:8637-43.
 29. Scambia G, Benedetti-Panici P, Ferrandina G et al. Epidermal growth factor, oestrogen and progesterone receptor expression in primary ovarian cancer: correlation with clinical outcome and response to chemotherapy. *Br J Cancer* 1995;**72**:361-6.
 30. Lau DH, Lewis AD, Ehsan MN, Sikic BI., Multifactorial mechanisms associated with broad cross-resistance of ovarian carcinoma cells selected by cyanomorpholino doxorubicin. *Cancer Res* 1991; **51**:5181-7.
 31. Casslen B, Nordengren J, Gustavsson B, Nilbert M, Lund LR. Progesterone stimulates degradation of urokinase plasminogen activator (u-PA) in endometrial stromal cells by increasing its inhibitor and surface expression of the u-

- PA receptor. *J Clin Endocrinol Metab* 1995;**80**:2776-84.
32. Riisbro R, Piironen T, Brünner N et al. Measurement of soluble urokinase plasminogen activator receptor in serum. *J Clin Ligand Assay* 2002;**25**:53-56.
 33. Bottalico B, Larsson I, Brodski J et al. Norepinephrine transporter (NET), serotonin transporter (SERT), vesicular monoamine transporter (VMAT2) and organic cation transporters (OCT1, 2 and EMT) in human placenta from pre-eclamptic and normotensive pregnancies. *Placenta* 2004;**25**:518-29.
 34. Filardo EJ, Thomas P. GPR30: a seven-transmembrane-spanning estrogen receptor that triggers EGF release. *Trends Endocrinol Metab* 2005;**16**:362-7.
 35. Blasi F, Carmeliet P. uPAR: a versatile signalling orchestrator. *Nat Rev Mol Cell Biol* 2002;**3**:932-43.
 36. Cunningham O, Andolfo A, Santovito ML, Iuzzolino L, Blasi F, Sidenius N. Dimerization controls the lipid raft partitioning of uPAR/CD87 and regulates its biological functions. *Embo J* 2003;**22**:5994-6003.
 37. Pöllänen J, Hedman K, Nielsen LS, Danø K, Vaheri A. Ultrastructural localization of plasma membrane-associated urokinase-type plasminogen activator at focal contacts. *J Cell Biol* 1988;**106**:87-95.
 38. Puri C, Tosoni D, Comai R et al. Relationships between EGFR signaling-competent and endocytosis-competent membrane microdomains. *Mol Biol Cell* 2005;**16**:2704-18.
 39. Prenzel N, Zwick E, Daub H et al. EGF receptor transactivation by G-protein-coupled receptors requires metalloproteinase cleavage of proHB-EGF. *Nature* 1999;**402**:884-8.
 40. Sukocheva O, Wadham C, Holmes A et al. Estrogen transactivates EGFR via the sphingosine 1-phosphate receptor Edg-3: the role of sphingosine kinase-1. *J Cell Biol* 2006;**173**:301-10.
 41. Filardo EJ, Quinn JA, Frackelton AR, Bland KI. Estrogen action via the G protein-coupled receptor, GPR30: stimulation of adenylyl cyclase and cAMP-mediated attenuation of the epidermal growth factor receptor-to-MAPK signaling axis. *Mol Endocrinol* 2002;**16**:70-84.
 42. Marinissen MJ, Gutkind JS. G-protein-coupled receptors and signaling networks: emerging paradigms. *Trends Pharmacol Sci* 2001;**22**:368-76.
 43. Sukocheva OA, Wang L, Albanese N, Pitson SM, Vadas MA, Xia P. Sphingosine kinase transmits estrogen signaling in human breast cancer cells. *Mol Endocrinol* 2003;**17**:2002-12.
 44. Kang SK, Choi KC, Tai CJ, Auersperg N, Leung PC. Estradiol regulates gonadotropin-releasing hormone (GnRH) and its receptor gene expression and antagonizes the growth inhibitory effects of GnRH in human ovarian surface epithelial and ovarian cancer cells. *Endocrinology* 2001;**142**:580-8.
 45. Treeck O, Haldar C, Ortmann O. Antiestrogens modulate MT1 melatonin receptor expression in breast and ovarian cancer cell lines. *Oncol Rep* 2006;**15**:231-5.
 46. Perez-Gracia JL, Carrasco EM. Tamoxifen therapy for ovarian cancer in the adjuvant and advanced settings: systematic review of the literature and implications for future research. *Gynecol Oncol* 2002;**84**:201-9.
 47. Schwartz PE, Chambers JT, Kohorn EI et al. Tamoxifen in combination with cytotoxic chemotherapy in advanced epithelial ovarian cancer. A prospective randomized trial. *Cancer* 1989;**63**:1074-8.
 48. Rendina GM, Donadio C, Giovannini M. Steroid receptors and progestinic therapy in ovarian endometrioid carcinoma. *Eur J Gynaecol Oncol* 1982;**3**:241-6.
 49. Perillo B, Sasso A, ABbondanza C, Palumbo G. 17beta-estradiol inhibits apoptosis in MCF-7 cells, inducing bcl-2 expression via two estrogen-responsive elements present in the coding sequence. *Mol Cell Biol* 2000;**20**:2890-901.

III

Manuscript

**EXPRESSION AND REGULATION OF THE ESTROGEN
RESPONSIVE MEMBRANE RECEPTOR GPR30 IN
PRIMARY OVARIAN TUMORS AND OVARIAN
CANCER CELL LINES**

Noskova V, Henic E, Kolkova Z, Ahmadi S, Åsander E, Brommesson S,
Hansson S, Casslén B.

Dep. Gynecology & Obstetrics, University Hospital, Lund, Sweden.

ABSTRACT

Activation of the membrane receptor GPR30 by estradiol modifies invasive properties initiated by EGF in ovarian cancer cells. We analyzed GPR30 gene expression in 44 primary ovarian tumors and in 7 ovarian cancer cell lines. All tumor samples contained GPR30 mRNA. Expression was lower in poorly differentiated malignant tumors than in benign tumors, but peaked in well differentiated malignant tumors. GPR30 mRNA was also found in all seven ovarian cancer cell lines. Expression was up-regulated by estradiol in ES-2, up-regulated by EGF in TOV-21G, but down-regulated by EGF in TOV-112D, SKOV-3ip, Hey-TG, SKOV-3, and OVCAR-3. We subsequently analyzed both primary tumors and cell lines for expression of the nuclear estrogen receptors ER α and ER β for comparison with GPR30. Furthermore, we analyzed expression of components in the EGF system, since EGF contributes to regulation of GPR30 expression and is a marker for poor differentiation and prognosis in ovarian cancer. The content of mRNA for ER α , EGF, and HER2 was higher in malignant than in benign tumors. In contrast, mRNA for ER β and EGFR1 were lower in malignant than in benign samples. HB-EGF mRNA was equally expressed in all tumor groups. All these genes were variably expressed in the cell lines, with few exceptions of undetectable amounts of mRNA. GPR30 mRNA may be reduced in poorly differentiated tumors as a result of increased expression of EGF, since EGF down-regulated GPR30 mRNA in most ovarian cancer cells. GPR30 protein was detected with Western Blot in all 7 ovarian cancer cell lines as well as in all ovarian tumor tissues examined. The bands were stronger in samples from malignant than from benign tumors, thereby suggesting discordant expression patterns between GPR30 protein and GPR30 mRNA.

INTRODUCTION

Even though development and progression of ovarian tumors are not generally considered estrogen-sensitive from a clinical perspective, as is the case for breast cancer and endometrial cancer, estrogens may still have an impact on ovarian tumor progression. Patients with ovarian tumors have elevated blood levels of estradiol, and nuclear estrogen receptors are present in normal ovarian surface epithelial cells as well as in ovarian tumors and ovarian cancer cells [1-5] [6-8]. Estrogenic steroids stimulate proliferation in several ovarian cancer cell lines, and this effect seems to be mediated via the nuclear estrogen receptor α (ER α) [9, 10]. Lindgren et al found overlapping tissue distribution between ER α and a marker for cell proliferation in malignant ovarian tumors [11]. Furthermore, apoptosis was reduced by estradiol in immortalized ovarian surface epithelial cells via Akt mediated up-regulation of bcl-2, an anti-apoptotic gene [12], and regional expression of ER α correlated with lower apoptotic activity in poorly differentiated malignant ovarian tumors [11]. In addition to these observations, epidemiologic data indicate a correlation between estradiol taken as hormone replacement therapy and increased risk of ovarian cancer [13-15].

Our studies on the effect of estradiol on cell migration in seven ovarian cancer cell lines found that estradiol by itself did not influence cell migration but consistently attenuated the stimulatory effect of EGF [16]. We also reported that this effect of estradiol resulted from inhibited mobilization of the urokinase plasminogen activator receptor (uPAR) from detergent resistant domains, possibly lipid rafts, to detergent sensitive domains, presumably focal adhesion sites at the cell surface. Finally, this effect appeared to be mediated by the recently identified estrogen responsive G-protein coupled receptor 30 (GPR30).

GPR30, which belongs to the large family of G-protein coupled seven spanning transmembrane receptors, was originally cloned by several independent research groups as an orphan receptor [17, 18]. However, the receptor was subsequently reported to bind estradiol with high affinity, and also to bind a number of nuclear ER antagonists and modulators with agonistic effect [19-21]. Since expression of the EGF system in ovarian tumors relates to poor prognosis and poor response to chemotherapy [22-24], and estradiol mediated activation of GPR30 attenuates the invasive properties

resulting from EGF stimulation [16], GPR30 may potentially be targeted with an agonist for therapeutic purpose in patients with ovarian cancer.

In this paper we assayed GPR30 expression in primary ovarian tumors and ovarian cancer cell lines. The mRNA species for nuclear estrogen receptors were quantified for comparison. Furthermore, we assayed expression of components of the EGF system, which is significant in the GPR30 story for several reasons. GPR30 activation can modify down-stream events from the EGF receptor [16], but can also transactivate the EGF receptor [25, 26]. In addition, this study found EGF to take part in regulation of GPR30 gene expression in ovarian cancer cells.

MATERIALS AND METHODS

Tumor tissue samples

Ovarian tumor tissue was obtained during operations at the Department of Obstetrics and Gynecology, Lund University Hospital, 2001-2007. As soon as the tumor was removed from the patient, samples of tumor tissue, 5x5x5 mm, were prepared and quick frozen on dry ice. The tissue samples were subsequently stored in -80 °C until used. The Ethical Review Board at the Lund University Hospital approved the study. All tumors were classified by histo-pathological diagnosis (Table 1). Tumor grade was classified as benign (BE), borderline (BO), well differentiated malignant (WD), moderately differentiated malignant (MD), and poorly differentiated malignant (PD). Tumor types included serous, mucinous, and endometrioid.

	Serous	Mucinous	Endometrioid	Total
Benign	4	5		9
Borderline	6	5		11
Well diff.	6	2		8
Moderately diff.		1	3	4
Poorly diff.	7		5	12
Total	23	13	8	44

Table 1. Distribution of 44 ovarian tumor samples according to histological type and differentiation.

Ovarian cancer cell lines

Seven different human ovarian cancer cell lines were used in this study. All of them were derived from epithelial ovarian adenocarcinomas. Cells were cultured on uncoated plastic at 37°C in humidified atmosphere with 5% CO₂. Media were supplemented with fetal bovine serum (FBS), Penicillin (100 U/mL), Streptomycin (100 µg/mL), and Amphotericin B (0.25 µg/mL). All culture media and supplements were from Invitrogen, Gibco (Carlsbad, CA, USA). Characteristics of each cell line, relevant to issues addressed by this study, are given below together with culture conditions. The doubling time, which is given for each cell line, has been determined in our laboratory.

The ES-2 cell line derives from a poorly differentiated clear cell cancer. ES-2 cells were cultured in McCoy's 5A medium with 10% FBS according to ATCC recommendations. Doubling time is 13 hours.

The Hey-TG cell line (gift from M.D. Anderson Cancer Institute, Houston, TX, USA) is one of several aggressive cell lines derived from HEY cells, which originate from an intermediately differentiated serous tumor. Hey-TG cells were cultured in M199 medium with 10% FBS. Doubling time is 28 hours.

The OVCAR-3 cell line derives from ascitic fluid cells from a patient with poorly differentiated papillary tumor. The cells are tumorigenic in mice. OVCAR-3 cells were cultured in RPMI 1640 medium with insulin 0.01 mg/mL and 20% FBS according to ATCC recommendations. Doubling time is 21 hours.

The SKOV-3 cell line derives from a metastasis of an ovarian cancer with unknown histology. Those cells form intermediately differentiated tumors when injected subcutaneously in mice. The cells are reportedly ER β positive, but ER α negative due to inactivating mutation, which renders the cells insensitive to estrogen in terms of cell proliferation and gene induction [4, 27]. SKOV-3 cells were cultured in McCoy 5A medium with 10% FBS according to ATCC recommendations. Doubling time is 25 hours.

The SKOV-3ip cell line (gift from Tumor Immunology, Lund University, Sweden) is derived from SKOV-3 cells. These cells form intra-peritoneal metastases in mice. They were cultured in M199 medium with 10% FBS. Doubling time is 22 hours.

The TOV112D cell line derives from a poorly differentiated endometrioid carcinoma. The cells were cultured in D-MEM medium with 10% FBS according to ATCC recommendations. Doubling time is 32.5 hours.

The TOV21G cell line derives from a poorly differentiated clear-cell carcinoma. The cells were cultured in D-MEM medium with 10% FBS according to ATCC recommendations. Doubling time is 28 hours.

Regulation of GPR30 mRNA by EGF and estradiol

In order to study regulation of GPR30 gene expression, each cell type was grown in serum-free medium, and when confluent cells were stimulated with vehicle, estradiol 10 nmol/L, EGF 10 μ g/L, or the combination of estradiol and EGF for 6 hours. Estradiol was added 30 minutes before EGF.

Extraction of total RNA

Ovarian tumor tissue. Total RNA was extracted from frozen tissue using Trizol (Invitrogen, Carlsbad, CA) according to the manufacture's instructions. Briefly, frozen tissue was weighed and about 125 mg was placed in Trizol (1 mL per 50 mg of tissue) and homogenized using rotating-knives (Polytron). Following centrifugation at 12000g for 10 minutes at 4°C in order to remove debris, the supernatant was split in three tubes with each 0.8 mL, kept for 5 minutes at room temperature before 0.18 mL chloroform per tube was added. Samples were vortexed for 15 seconds, and then centrifuged 12000g for 15 minutes at 4°C. The chloroform phases were transferred to new tubes, and in order to remove proteoglycans and polysaccharides, a high-salt precipitation was performed using isopropanol (0.2 mL per tube) and salt solution (Na-citrate 0.8 mol/L, NaCl 1.2 mol/L) (0.2 mL per tube). After incubation for 10 minutes at room temperature, samples were centrifuged 12000g for 10 minutes at 4°C. The pellet was washed with 75% ethanol, 0.8 mL per tube, centrifuged 7500 g for 5 minutes at 4°C, air-dried, and diluted in RNase-free water 20 μ L per tube. The three tubes were pooled, incubated at 60°C for 10 minutes, and subsequently cooled down and frozen at -80° C until further used.

Ovarian cancer cell lines. Total RNA was extracted from harvested cells using EZNA Total RNA Kit™ according to instructions of the manufacturer (OMEGA Bio-Tec, Doraville, GA, USA).

The concentration and purity of all the extracted RNA samples was evaluated by spectrophotometry. The quality of each RNA sample was verified by 2% agarose gel electrophoresis with running buffer 1x MOPS at 70V for ~2 hours. If the total RNA had been successfully extracted, two bands could be detected under UV light, representing the 18S and 28S ribosome subunits. The samples with successfully extracted total RNA were further used in reverse transcription qPCR.

Synthesis of cDNA

Intact RNA was converted to cDNA using Taqman Reverse Transcription Reagents (Applied Biosystems, Foster City, CA, USA). According to protocol from manufacture one 20 μ L reaction contained 0.2 μ g total RNA, final concentration of 1x Taqman RT buffer, 2.2 mmol/L MgCl₂, 200 μ mol/L dNTP, 1 μ mol/L random hexamers, 0.4 IU/ μ L RNase inhibitor and 0.5 IU/ μ L Multiscribe reverse transcriptase. The mix was incubated at 25°C for 10 minutes, at 48°C for 30 minutes, and then 5 minutes of inactivation at 95°C. The final concentration of cDNA was 10 ng/ μ L. The samples were stored at -20°C until further use.

Quantification of specific mRNA species

Gene transcripts were quantified using real-time PCR on ABI Prism 7000 sequence detection system (Applied Biosystems, Foster City, CA, USA). All transcripts were analyzed with pre-manufactured primers and probes (Applied Biosystems). Primers were located on exons of investigated genes in order to avoid contamination with genomic DNA. Oligonucleotide probes (Table 2) were labeled with fluorogenic dye, 6-carboxyfluorescein (Fam). PCR reactions were carried out in a 25 μ L final volume containing final concentrations: 1x Taqman Universal PCR Master Mix (Applied Biosystems), 1x Assaymix (Applied Biosystems), 0.25 μ mol/L probe, 0.9 μ mol/L of forward and reverse primers, respectively, and 1 μ L of 10 ng/ μ L DNA aliquot. The thermal cycling conditions were initiated by an initial uracil DNA glycosylase (UNG) activation at 50°C for 2 minutes, denaturation at 95°C for 10 minutes followed by 40 cycles at 95°C for 15 seconds and annealing at 60°C for 1 minute. Two negative controls, without template, were included in each amplification. Each reaction was carried out in duplicate. Transcripts for β -actin, as a housekeeping gene, were

quantified as endogenous RNA of reference to normalize each sample. Quantification was achieved through a calibration curve obtained by serial 10-fold dilutions of the template DNA (80 – 0.08 ng). Results are expressed as relative values.

mRNA	Accession number	Size (NT)	Pre-manufactured Assay number
GPR30	NM_001505.	<15	Hs00173506_m1
ERα	NM_001122740.1	<150	Hs00174860_m1
ERβ	NM_001040275.1	<150	Hs00230957_m1
EGF	NM_001963.3	<150	Hs00153181_m1
HB-EGF	NM_001945.1	<150	Hs00181813_m1
EGFR1	NM_005228.3	<150	Hs00193306_m1
EGFR2	NM_001005862.1	<150	Hs00170433_m1
β-actin	NM_001101.3	<150	Hs99999903_m1

Table 2. Data on primers and probes used for qPCR amplification.

Membrane protein extraction and Western blot analysis

Ovarian tumor tissue (65-75 mg) was disintegrated in homogenizing buffer containing sucrose 1.25 mol/L, HEPES 200 mmol/L (pH 7.5), EGTA 10 mmol/L, DTT 100 mmol/L, soybean trypsin inhibitor 1 mg/mL, leupeptin 1 mg/mL, and aprotinin 1 mg/mL at 4°C using QIAGEN TissueLyser (Retsch Technology GmbH, Haan, Germany). Tissue debris and nuclei were removed by spinning the lysates at 1000 g for 10 minutes at 4°C. Supernatants were filtered through one layer of gauze and subsequently centrifuged at 40 000 g for 45 minutes at 4°C, in order to obtain the membrane fraction. The pellet was washed, re-suspended in buffer containing Tris-HCl 500 mmol/L (pH 7.4), EGTA 10 mmol/L, PMSF (phenyl-methyl-sulfonyl-fluoride) 100 mmol/L, and soybean trypsin inhibitor 1 mg/mL, and sonicated for 5 seconds with the Ultrasonic processor UP50H (Hielscher Ultrasonics, GmbH, Teltow, Germany). The total protein concentration was determined by the BCATM protein

assay kit (Pierce Biotechnology, Rockford, IL, USA). Samples were stored at -20°C until used.

Each sample of membrane fraction (10-20 µg total protein) was mixed with LDS sample buffer (Invitrogen, Carlsbad, CA, USA) and DTT 0.5 mol/L, and incubated for 10 minutes at 70°C before they were subjected to SDS-PAGE on a 12% NuPage™ 12 lanes Bis-Tris gel (Invitrogen) using XCell Surelock™ MiniCell (Invitrogen). Proteins were transferred to polyvinylidene difluoride membranes (Bio-Rad, Hercules, CA, USA) by semi-dry electroblotting. Membranes were subsequently blocked with Non-Fat Dry Milk (Bio-Rad) in TBS-Tween containing TRIS 20 mmol/L and Tween-20 0.1 % at 4°C overnight. Next day, the membranes were incubated for 1 hour with a rabbit antibody against human GPR30, LS-A4290 (Life Span Biosciences, Seattle, WA, USA) diluted 1:1000. After washing 1 x 15 minutes and then 3 x 5 minutes in TBS-Tween, the membranes were further incubated for 1 hour with a secondary antibody, i.e. goat antibody against rabbit IgG labeled with horseradish peroxidase (Santa Cruz Biotechnology Inc., CA, USA) diluted 1:10000. Membranes were again washed in TBS-Tween supplemented with sodium chloride 0.2 mol/L. Immune-complexes were detected by the ECL Plus Western Blotting Detection System (GE Healthcare, Amersham, Little Chalfont, UK) and membranes were exposed to Hyperfilm™ ECL (GE Healthcare) for 30 minutes.

Statistical methods

Data are presented as scatter plots with median and percentiles. The Mann-Whitney test was used to evaluate the significance of differences between groups. The test was two-sided and 5% level of significance was used. Trends to changed expression in relation to histological differentiation were analyzed for statistical significance using Chi square test for trend. Fisher's exact test was used to compare number of samples with over-expression between groups.

RESULTS

Ovarian tumors invariably expressed GPR30 mRNA (Fig. 1). Serous, mucinous, and endometrioid tumors were analyzed together, since no apparent difference was found between these types within each differentiation group. The group of well differentiated malignant tumors had significantly increased number of samples with high expression of GPR30 mRNA. Well differentiated tumors with high levels were both serous and mucinous. However, when altogether six samples with concentrations above the arbitrary level 0.3 were disregarded, there was a gradual decrease of GPR30 mRNA content from benign to poorly differentiated malignant tumors (test for trend $p=0.01$).

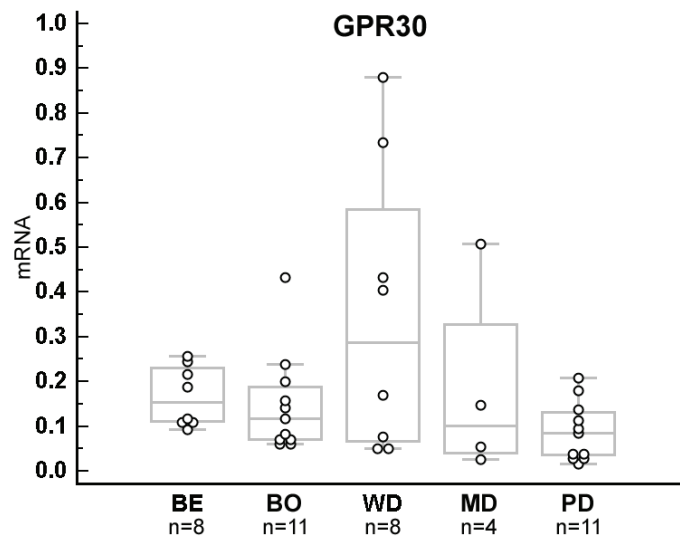


Figure 1

GPR30 mRNA was assayed in ovarian tumor tissue samples, and normalized to corresponding β -actin mRNA. Tumors were classified according to histological differentiation as benign (BE), borderline (BO), and malignant. The malignant tumors were sub-grouped as well (WD), moderately (MD), and poorly (PD) differentiated. The number of tumor tissue samples (n) in each group is indicated in the figure. GPR30 mRNA levels were lower in poorly differentiated tumors than in benign ($p=0.02$) and well differentiated ($p=0.05$) tumors. The number of samples with GPR30 mRNA levels above the arbitrary cut-off 0.3 was higher in well differentiated than in benign ($p=0.03$) and poorly differentiated ($p=0.02$) tumors using Fisher's exact test. When altogether six samples with levels above the arbitrary cut-off 0.3 were excluded, the content of GPR30 mRNA decreased gradually from benign to poorly differentiated tumors (test for trend $p=0.01$).

For comparison, the same set of samples was analyzed for ER α and ER β mRNA (Fig. 2). ER α mRNA was higher in truly malignant tumors than in benign and borderline tumors whereas the opposite was true for ER β . Thus, a peak of expression in well differentiated tumors seems to be a unique feature for GPR30 mRNA.

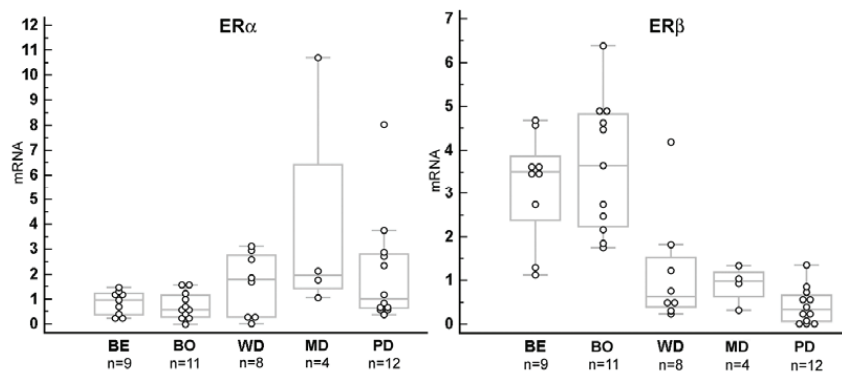


Figure 2

ER α mRNA and ER β mRNA in ovarian tumor tissue samples. See figure 1 legend for details. The content of ER α mRNA was higher in malignant samples than in benign and borderline samples ($p=0.01$), whereas the content of ER β mRNA was lower in malignant samples than in benign and borderline samples ($p<0.0001$).

Since EGF regulates the expression of GPR30 mRNA in ovarian cancer cell lines (see below), we also analyzed mRNA for members of the EGF system in this set of ovarian tumor tissue samples (Fig. 3). The amount of EGF mRNA and HER2 mRNA increased in malignant groups, whereas EGFR-1 mRNA decreased in these groups. In contrast, the level of HB-EGF mRNA was not different between the groups. There was a weak positive correlation between GPR30 and ER α ($r^2=0.13$, $p=0.049$) including benign tumors to moderately differentiated tumors, i.e. when poorly

differentiated tumors were excluded. There were no other, positive or negative, correlations between the parameters.

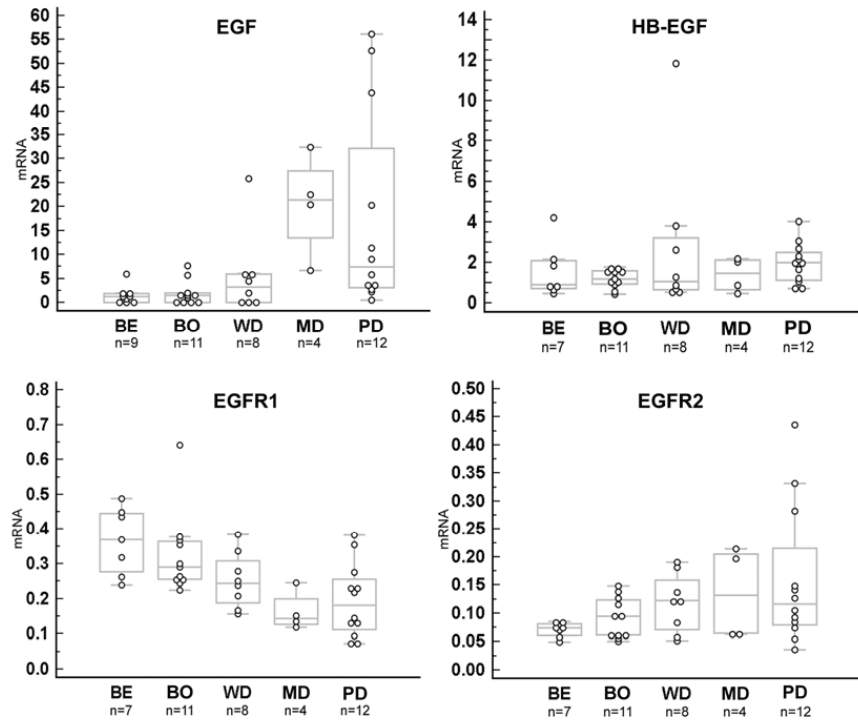


Figure 3

Ovarian tumor tissue content of mRNA for EGF, HB-EGF, EGFR-1, and EGFR-2 (HER2). See figure 1 legend for details. EGF mRNA was higher in malignant tumors than in benign and borderline tumors ($p=0.0005$), whereas HB-EGF mRNA was not different between these groups. EGFR-1 mRNA was gradually down-regulated (test for trend $p=0.0001$), whereas EGFR-2 (HER2) mRNA was gradually up-regulated (test for trend $p=0.007$) between benign tumors and poorly differentiated malignant tumors.

We screened seven ovarian cancer cell lines for their expression of estrogen receptors, EGF receptors, and EGF receptor ligands, before using them to study regulation of GPR30 gene expression by estradiol and EGF. All seven cell lines expressed GPR30 mRNA (Fig. 4). Highest expression was seen in TOV-112D and TOV-21G, whereas the other five cell lines were roughly on the same level. Expression of ER α mRNA was very variable among the cell lines (Fig. 4). Highest expression was seen in Hey-TG and SKOV-3ip. The message was barely detectable in OVCAR-3, and not

detectable in TOV-112D and TOV-21G. The pattern of ER β mRNA expression had similarities to that of GPR30 mRNA (Fig. 4). Highest expression was found in TOV-112D, followed by TOV-21G. The other six cell lines expressed ER β mRNA roughly on the same level.

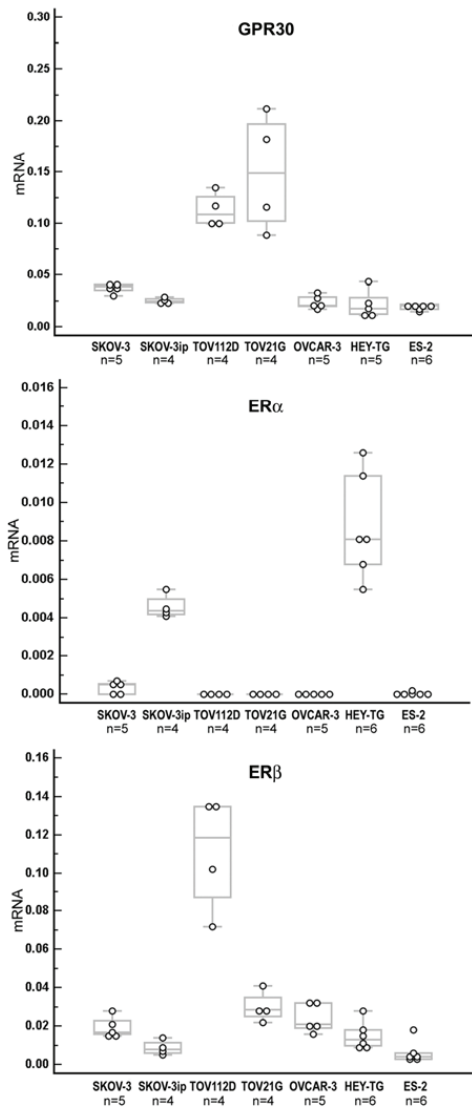


Figure 4
Expression of mRNA for GPR30, ER α , and ER β was assayed in seven ovarian cancer cell lines, and normalized to corresponding β -actin mRNA. The number of wells (n) in each group is indicated in the figure.

Highest expression of EGF mRNA was seen in Hey-TG cells, followed by ES-2 cells (Fig. 5). TOV-21G had low and TOV-112D had no expression of EGF mRNA. Expression of HB-EGF mRNA was detected in all cell lines (Fig. 5). It was highest in ES-2 cells and lowest in TOV-112D cells. EGFR-1 mRNA was detected in all seven cell lines (Fig. 5). Expression was low in TOV-112D and in TOV-21G, but on a similar higher level in the other five cell lines. The level of HER2 mRNA was high in Hey-TG cells and low in TOV-112D and TOV-21G cells (Fig. 5). ES-2 cells expressed the message in very low quantities.

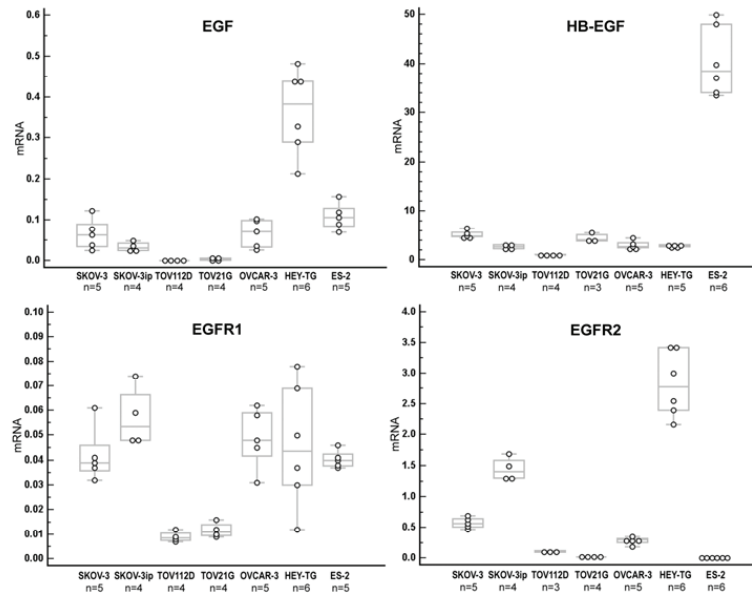


Figure 5
Expression of mRNA for EGF, HB-EGF, EGFR1, and EGFR2 (HER2) in seven ovarian cancer cell lines. See figure 4 legend for details.

Either estradiol or EGF regulated expression of the GPR30 gene in all seven cell lines (Fig. 6). We identified three patterns of regulation, i.e. up-regulation by estradiol in ES-2 cells, up-regulation by EGF in TOV-21G cells, and down-regulation by EGF in the other cell lines TOV-112D, SKOV-3ip, Hey-TG, SKOV-3, and OVCAR-3.

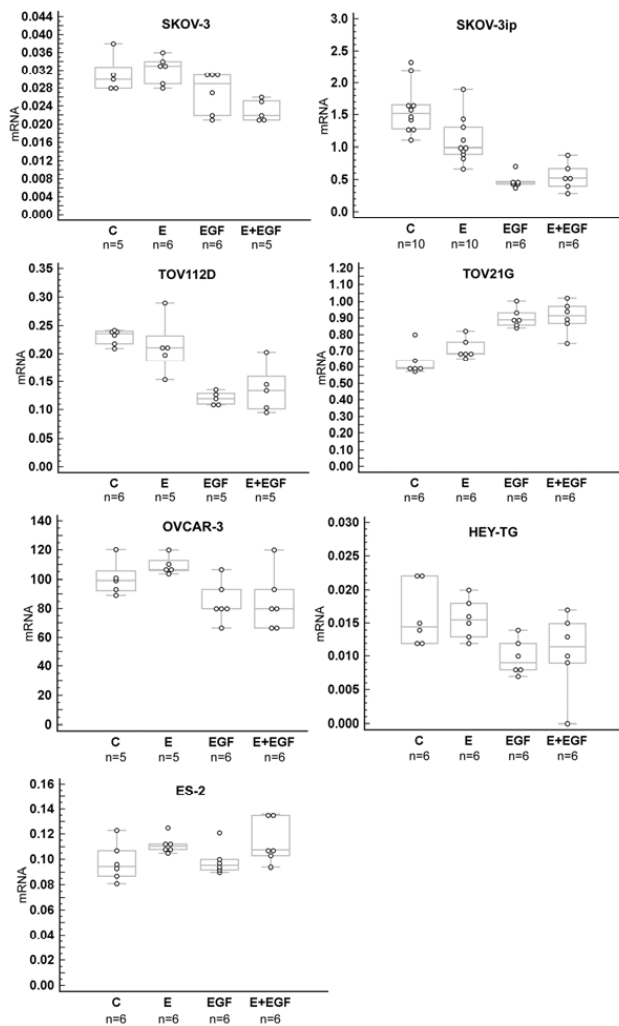


Figure 6 GPR30 mRNA normalized to β -actin mRNA in ovarian cancer cells stimulated with estradiol E (10^{-8} mol/L), EGF ($10\mu\text{g/L}$), the combination E+EGF, or vehicle C for 6 hours. GPR30 mRNA was up-regulated by estradiol (E and E+EGF vs. C and EGF) in ES-2 cells ($p=0.007$), and by EGF (EGF and E+EGF vs. C and E) in TOV-21G cells ($p=0.0001$), but was down-regulated by EGF (EGF and E+EGF vs. C and E) in TOV-112D cells ($p<0.0001$), SKOV-3ip cells ($p<0.0001$), Hey-TG cells ($p=0.005$), SKOV-3 cells ($p=0.003$), and OVCAR-3 cells ($p=0.005$).

Western blots demonstrated GPR30 protein in benign tumors as well as in malignant tumors of different histological differentiation (Fig. 7). The bands were stronger in malignant than in benign tumors. Also, all seven ovarian cancer cell lines had GPR30 protein. A band at 38 kDa predominated in tumor tissue as well as in the cell lines. In addition, tumor tissue samples had bands at 34 kDa and 44 kDa.

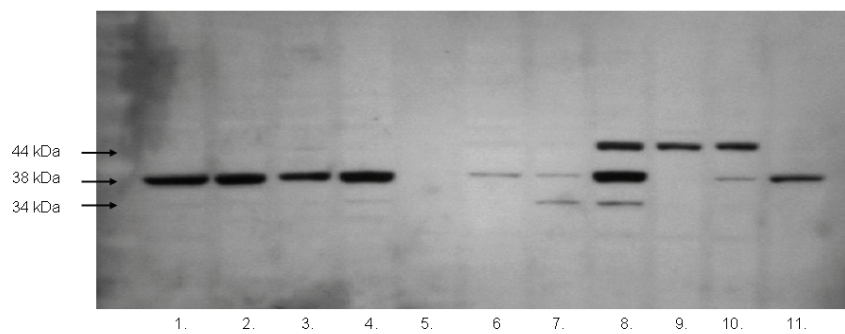


Figure 7

Western blot analysis of ovarian cancer cell lines TOV21G, OVCAR-3, SKOV-3ip, SKOV-3 (1, 2, 3, 4), HEK 293 cells as negative control (5), and tissue samples from benign (6,7), well differentiated (8, 9) and poorly differentiated (10, 11) malignant tumors. Ovarian cancer cell lines had a band at 38 kDa. Ovarian tumor tissue showed bands at 44 kDa, 38 kDa, and a weaker band at 34 kDa. No bands were visible in the negative control (HEK 293 cells).

DISCUSSION

This is to our knowledge the first report on expression of GPR30 in primary ovarian tumors. Two previous immune-histochemical studies have reported on tissue localization and expression of GPR30 protein in primary breast and endometrial cancer [28, 29]. GPR30 is also expressed in a variety of cell lines originating in hormone producing or dependant tumors, like breast cancer [30] [25] [21] [20], endometrial cancer [20] [31], choriocarcinoma [20], and thyroid cancer [32].

All primary ovarian tumors in our study expressed GPR30 mRNA, and expression was lower in poorly differentiated malignant tumors than in benign tumors. However, in addition to this decline, which seemed to accompany loss of histological differentiation, there was a peak in well differentiated malignant tumors, which created a bi-phasic pattern. This pattern, which is unlike the other genes we examined in this set of tumors, suggests one mechanism which up-regulates GPR30 gene expression in well differentiated tumors, but also another mechanism which down-regulates gene expression in poorly differentiated tumors.

ER α mRNA had a weak positive correlation with GPR30 mRNA and samples with high GPR30 levels tended to have higher levels of ER α , when poorly differentiated tumors were excluded. This may indicate either that expression of GPR30 is up-regulated by ER α , or that both receptors are co-regulated by yet another mechanism. A significant but incomplete association between GPR30 and ER α has also been described in breast carcinomas [28]. We found that expression of the GPR30 gene was down-regulated by EGF in five out of seven ovarian cancer cell lines. Since GPR30 gene expression was significantly down-regulated in poorly differentiated ovarian tumors, where expression of EGF and HER2 was up-regulated, it is possible that the EGF system actually is involved in down-regulation of the GPR30 gene in poorly differentiated malignant tumors, although we found no statistical correlation between mRNA for GPR30 and members of the EGF system in this set of ovarian tumors.

However, correlation between GPR30 mRNA and GPR30 protein is inconsistent, since our Western blot results indicate that poorly differentiated tumors contain considerably more GPR30 protein than benign tumors. Well differentiated tumors expressed at least as much GPR30 protein as poorly differentiated tumors. Thus, our GPR30 protein data suggest a different expression pattern between benign and malignant tumors than that suggested by our GPR30 mRNA results. Possible explanations include more efficient translation of the mRNA or reduced turnover of the protein in malignant samples. Alternatively, since the probe used for qPCR is rather short and covers only one exon-intron border, the low levels of GPR30 mRNA detected in poorly differentiated tumors, do not exclude the presence other molecular forms of GPR30 mRNA. We have actually observed different molecular forms of GPR30 protein in Western blots of ovarian tumor tissue.

Immuno-histochemistry performed in a large number of malignant breast tumors found that over-expression of GPR30 protein was associated with poor prognostic parameters, like large tumor size, distant metastases, and over-expression of HER2 [28]. Interestingly, however, a subsequent study of GPR30 mRNA in breast carcinomas failed to identify similar correlations [33]. In addition, another immunohistochemical study of primary endometrial cancer reported similar findings as the above mentioned, i.e. over-expression of GPR30 protein in the tumor tissue associated with poor differentiation, aggressive subtype, and advanced clinical stage [29]. The discrepancy between GPR30 mRNA and protein in breast cancer seems to parallel what we report for ovarian cancer in this paper.

Proliferation in ovarian cancer cells is influenced by estrogen. BG-1 ovarian cancer cells, which express both GPR30 and ER α , respond to both estradiol and to a selective GPR30 agonist G-1 with induced expression of c-fos and cyclins D1, E, and A [34]. For comparison, only estradiol enhanced expression of the progesterone receptor as well as an estrogen response element reporter gene. Interestingly, expression of both GPR30 and ER α was needed for the response, also when cells were stimulated with G1. Furthermore, inhibition of the EGFR transduction pathway inhibited c-fos stimulation and ERK activation by either of the ligands, supporting previous reports that GPR30 activation and signaling involves trans-activation of the

EGFR [25]. Thus, both GPR30 and ER α expression along with intact EGFR signaling are required for estradiol stimulated as well as G1 stimulated proliferation of these ovarian cancer cells.

Cell migration has been studied in ovarian cancer cell lines. Park et al reported that migration in BG-1 ovarian cancer cells was stimulated by estradiol, in a scratch assay [35]. They did not consider possible involvement of GPR30, but concluded that the effect was mediated via ER α . This is unfortunate, since Albanito et al reported, also in BG-1 ovarian cancer cells, that both GPR30 and ER α expression along with active EGF receptor signaling were required for estradiol stimulated as well as G-1 stimulated proliferation in these cells [34]. Also, previously we used a scratch assay to measure cell migration [36], but more recently we have preferred a trans-membrane migration assay, which gives more reproducible results. Using this migration assay, we have examined seven different ovarian cancer cell lines for their response to EGF and estradiol. However, these seven cell lines did unfortunately not include BG-1 cells. We found that EGF stimulates cell migration in all seven cell lines, and that this resulted from increased cell surface expression of ligand-activated uPAR [37]. Dissecting cellular mechanisms whereby EGF could possibly achieve this result, we managed to identify at least three such mechanisms. Apart from increased expression of uPAR mRNA and decreased internalization and degradation of uPAR, which both contribute to the late effect on uPAR expression, we also found a very rapid, almost instant, recruitment of endogenously occupied uPAR from detergent resistant domains. In contrast to Park et al [35], we did not find a direct effect of estradiol on migration in any of the seven ovarian cancer cell lines [16]. However, estradiol attenuated the stimulatory effect of EGF on migration in all seven cell lines. Analyzing possible influence on the three mechanisms described above, we found that estradiol affects neither the increase of uPAR mRNA, nor the decrease of internalization and degradation. However, the immediate increase of ligated uPAR in response to EGF was reduced in cells pre-treated with estradiol. This effect of estradiol was furthermore mimicked by ICI 182780, an antagonist to nuclear ERs, and G-1, a specific agonist to GPR30. In conclusion, our results strongly suggest that the estrogen induced modification of the EGF effect involves GPR30, but not ER α .

Expression of the two nuclear estrogen receptors ER α and ER β mRNA had opposite patterns in the tumors, i.e. ER α mRNA was increased whereas ER β mRNA was decreased in malignant as compared to benign tumors. In fact, our results confirm very similar findings in a previous mRNA study of ER α and ER β in ovarian tumors [38]. Furthermore, these authors show a good correlation between mRNA and protein for both ER α and ER β . Thus, mRNA data as well as protein data suggest that over-expression of ER α as well as loss of ER β expression parallels malignant transformation in ovarian tumors. Differential expression of ER α and ER β in malignant tumors compared to benign tumors and normal tissue have previously been reported also in other estrogen dependent tumors such as breast and prostate cancer [39-41]. The relation of ER α and ER β respectively to malignant progression is furthermore highlighted by the following observations. Experiments using over-expression as well as knockdown of ER α and ER β demonstrate that estradiol up-regulates via ER α but down-regulates via ER β molecular markers for an invasive pro-metastatic phenotype in ovarian cancer cells [35]. High ER α expression in poorly differentiated ovarian tumors co-localize histologically with a high proliferation index and a low apoptotic activity [11]. Finally, Skliris et al found that high ER β expression was an independent predictor for disease-free survival as well as overall survival in multivariate analysis of patients with malignant ovarian tumors [39].

REFERENCES

1. Aiman, J., J.P. Forney, and C.R. Parker, *Androgen and estrogen secretion by normal and neoplastic ovaries in premenopausal women*. *Obstet Gynecol*, 1986. **68**(3): p. 327-32.
2. Bai, W., et al., *Estrogen stimulation of ovarian surface epithelial cell proliferation*. *In Vitro Cell Dev Biol Anim*, 2000. **36**(10): p. 657-66.
3. Kitayama, S. and R. Nakano, *Peripheral and ovarian venous concentrations of estradiol and progesterone in postmenopausal women with "non-endocrine" ovarian tumors*. *Acta Obstet Gynecol Scand*, 1990. **69**(3): p. 245-8.
4. Lau, K.M., S.C. Mok, and S.M. Ho, *Expression of human estrogen receptor-alpha and -beta, progesterone receptor, and androgen receptor mRNA in normal and malignant ovarian epithelial cells*. *Proc Natl Acad Sci U S A*, 1999. **96**(10): p. 5722-7.
5. Lindgren, P.R., et al., *The pattern of estradiol and progesterone differs in serum and tissue of benign and malignant ovarian tumors*. *Int J Oncol*, 2002. **21**(3): p. 583-9.
6. Emons, G. and J.J. Kavanagh, *Hormonal interactions in ovarian cancer*. *Hematol Oncol Clin North Am*, 1999. **13**(1): p. 145-61, ix.
7. Jeppsson, S., S. Karlsson, and S. Kullander, *Gonadal steroids, gonadotropins and endometrial histology in postmenopausal women with malignant ovarian tumors*. *Acta Obstet Gynecol Scand*, 1986. **65**(3): p. 207-10.
8. Mahlck, C.G., T. Backstrom, and O. Kjellgren, *Plasma level of estradiol in patients with ovarian malignant tumors*. *Gynecol Oncol*, 1988. **30**(3): p. 313-20.
9. O'Donnell, A.J., et al., *Estrogen receptor-alpha mediates gene expression changes and growth response in ovarian cancer cells exposed to estrogen*. *Endocr Relat Cancer*, 2005. **12**(4): p. 851-66.
10. Langdon, S.P., et al., *The regulation of growth and protein expression by estrogen in vitro: a study of 8 human ovarian carcinoma cell lines*. *J Steroid Biochem Mol Biol*, 1994. **50**(3-4): p. 131-5.
11. Lindgren, P., et al., *Steroid receptors and hormones in relation to cell proliferation and apoptosis in poorly differentiated epithelial ovarian tumors*. *Int J Oncol*, 2001. **19**(1): p. 31-8.
12. Choi, K.C., et al., *Estradiol up-regulates antiapoptotic Bcl-2 messenger ribonucleic acid and protein in tumorigenic ovarian surface epithelium cells*. *Endocrinology*, 2001. **142**(6): p. 2351-60.
13. Gambacciani, M., et al., *Hormone replacement therapy and endometrial, ovarian and colorectal cancer*. *Best Pract Res Clin Endocrinol Metab*, 2003. **17**(1): p. 139-47.
14. Greiser, C.M., E.M. Greiser, and M. Doren, *Menopausal hormone therapy and risk of ovarian cancer: systematic review and meta-analysis*. *Hum Reprod Update*, 2007. **13**(5): p. 453-63.
15. Rao, B.R. and B.J. Slotman, *Endocrine factors in common epithelial ovarian cancer*. *Endocr Rev*, 1991. **12**(1): p. 14-26.
16. Henic, E., et al., *Estradiol attenuates EGF-induced rapid uPAR mobilization and cell migration via the G-protein coupled receptor 30 (GPR30) in ovarian cancer cells*. *International Journal of Gynecological Cancer*.
17. Owman, C., et al., *Cloning of human cDNA encoding a novel heptahelix receptor expressed in Burkitt's lymphoma and widely distributed in brain and peripheral tissues*. *Biochem Biophys Res Commun*, 1996. **228**(2): p. 285-92.
18. Carmeci, C., et al., *Identification of a gene (GPR30) with homology to the G-protein-coupled receptor superfamily associated with estrogen receptor expression in breast cancer*. *Genomics*, 1997. **45**(3): p. 607-17.
19. Filardo, E., et al., *Activation of the novel estrogen receptor G protein-coupled receptor 30 (GPR30) at the plasma membrane*. *Endocrinology*, 2007. **148**(7): p. 3236-45.
20. Revankar, C.M., et al., *A transmembrane intracellular estrogen receptor mediates rapid cell signaling*. *Science*, 2005. **307**(5715): p. 1625-30.
21. Thomas, P., et al., *Identity of an estrogen membrane receptor coupled to a G protein in human breast cancer cells*. *Endocrinology*, 2005. **146**(2): p. 624-32.
22. Berchuck, A., et al., *Epidermal growth factor receptor expression in normal ovarian epithelium and ovarian cancer. I. Correlation of receptor expression with prognostic factors in patients with ovarian cancer*. *Am J Obstet Gynecol*, 1991. **164**(2): p. 669-74.
23. Fischer-Colbrie, J., et al., *EGFR and steroid receptors in ovarian carcinoma: comparison with prognostic parameters and outcome of patients*. *Anticancer Res*, 1997. **17**(1B): p. 613-9.

24. Scambia, G., et al., *Epidermal growth factor, oestrogen and progesterone receptor expression in primary ovarian cancer: correlation with clinical outcome and response to chemotherapy*. Br J Cancer, 1995. **72**(2): p. 361-6.
25. Filardo, E.J., et al., *Estrogen-induced activation of Erk-1 and Erk-2 requires the G protein-coupled receptor homolog, GPR30, and occurs via trans-activation of the epidermal growth factor receptor through release of HB-EGF*. Mol Endocrinol, 2000. **14**(10): p. 1649-60.
26. Filardo, E.J., *Epidermal growth factor receptor (EGFR) transactivation by estrogen via the G-protein-coupled receptor, GPR30: a novel signaling pathway with potential significance for breast cancer*. J Steroid Biochem Mol Biol, 2002. **80**(2): p. 231-8.
27. Hua, W., et al., *SKOV3 ovarian carcinoma cells have functional estrogen receptor but are growth-resistant to estrogen and antiestrogens*. J Steroid Biochem Mol Biol, 1995. **55**(3-4): p. 279-89.
28. Filardo, E.J., et al., *Distribution of GPR30, a seven membrane-spanning estrogen receptor, in primary breast cancer and its association with clinicopathologic determinants of tumor progression*. Clin Cancer Res, 2006. **12**(21): p. 6359-66.
29. Smith, H.O., et al., *GPR30: a novel indicator of poor survival for endometrial carcinoma*. Am J Obstet Gynecol, 2007. **196**(4): p. 386 e1-9; discussion 386 e9-11.
30. Carmeci, C., et al., *Analysis of estrogen receptor messenger RNA in breast carcinomas from archival specimens is predictive of tumor biology*. Am J Pathol, 1997. **150**(5): p. 1563-70.
31. Vivacqua, A., et al., *The G protein-coupled receptor GPR30 mediates the proliferative effects induced by 17beta-estradiol and hydroxytamoxifen in endometrial cancer cells*. Mol Endocrinol, 2006. **20**(3): p. 631-46.
32. Vivacqua, A., et al., *17beta-estradiol, genistein, and 4-hydroxytamoxifen induce the proliferation of thyroid cancer cells through the g protein-coupled receptor GPR30*. Mol Pharmacol, 2006. **70**(4): p. 1414-23.
33. Kuo, W.H., et al., *The interactions between GPR30 and the major biomarkers in infiltrating ductal carcinoma of the breast in an Asian population*. Taiwan J Obstet Gynecol, 2007. **46**(2): p. 135-45.
34. Albanito, L., et al., *G protein-coupled receptor 30 (GPR30) mediates gene expression changes and growth response to 17beta-estradiol and selective GPR30 ligand G-1 in ovarian cancer cells*. Cancer Res, 2007. **67**(4): p. 1859-66.
35. Park, S.H., et al., *Estrogen regulates Snail and Slug in the down-regulation of E-cadherin and induces metastatic potential of ovarian cancer cells through estrogen receptor alpha*. Mol Endocrinol, 2008. **22**(9): p. 2085-98.
36. Sandberg, T., A. Ehinger, and B. Casslen, *Paracrine stimulation of capillary endothelial cell migration by endometrial tissue involves epidermal growth factor and is mediated via up-regulation of the urokinase plasminogen activator receptor*. J Clin Endocrinol Metab, 2001. **86**(4): p. 1724-30.
37. Henic, E., et al., *EGF-stimulated migration in ovarian cancer cells is associated with decreased internalization, increased surface expression, and increased shedding of the urokinase plasminogen activator receptor*. Gynecol Oncol, 2005.
38. Chan, K.K., et al., *Estrogen receptor subtypes in ovarian cancer: a clinical correlation*. Obstet Gynecol, 2008. **111**(1): p. 144-51.
39. Skliris, G.P., et al., *Reduced expression of oestrogen receptor beta in invasive breast cancer and its re-expression using DNA methyl transferase inhibitors in a cell line model*. J Pathol, 2003. **201**(2): p. 213-20.
40. Iwao, K., et al., *Quantitative analysis of estrogen receptor-beta mRNA and its variants in human breast cancers*. Int J Cancer, 2000. **88**(5): p. 733-6.
41. Horvath, L.G., et al., *Frequent loss of estrogen receptor-beta expression in prostate cancer*. Cancer Res, 2001. **61**(14): p. 5331-5.

IV

Cleaved Forms of the Urokinase Plasminogen Activator Receptor in Plasma Have Diagnostic Potential and Predict Postoperative Survival in Patients with Ovarian Cancer

Emir Henić,¹ Christer Borgfeldt,¹ Ib Jarle Christensen,² Bertil Caslén,¹ and Gunilla Høyer-Hansen²

Abstract Purpose: To evaluate the plasma level of different forms of soluble urokinase plasminogen activator receptor (suPAR) as discriminators between malignant, borderline, and benign ovarian tumors and as prognostic markers in patients with ovarian cancer.

Experimental Design: The different suPAR forms were measured in preoperative plasma samples obtained from 335 patients with adnexal lesions using three different time-resolved fluorescence assays (TR-FIA): TR-FIA 1 measuring intact suPAR, suPAR(I-III), TR-FIA 2 measuring the total amount of suPAR(I-III) and the cleaved form, suPAR(II-III), and TR-FIA 3 measuring the liberated uPAR(I). Tumors were classified as benign ($n = 211$), borderline (possibly malignant; $n = 30$), and well ($n = 19$), moderately ($n = 15$), and poorly ($n = 60$) differentiated malignant.

Results: All uPAR forms as well as CA125 were statistically significant in univariate analysis discriminating between benign, borderline, and invasive tumors. Restricting the analysis of invasive tumors to early stage (I and II) showed similar results. A combination of CA125 and suPAR(I-III) + suPAR(II-III) discriminated between malignant (all stages) and benign tumors [AUC, 0.94; 95% confidence interval (95% CI), 0.90-0.98] as well as borderline and benign tumors (AUC, 0.78; 95% CI, 0.67-0.89). All suPAR forms were markers for poor prognosis in univariate analyses, and high preoperative plasma level of uPAR(I) is an independent predictor of poor prognosis (hazard ratio, 1.84; 95% CI, 1.15-2.95; $P = 0.011$) in multivariate analyses including age and CA125.

Conclusions: High concentration of plasma uPAR(I) is an independent preoperative marker of poor prognosis in patients with ovarian cancer. The combination of plasma suPAR(I-III) + suPAR(II-III) and CA125 discriminates between malignant and benign tumors with an AUC of 0.94.

Ovarian cancer is the third leading cause of death in cancer among women ages 45 to 64 years in Sweden, and the incidence in Sweden is comparable with other western countries (1). Due to mild symptoms, the majority of patients with ovarian cancer are not diagnosed until the disease is in advanced stages, which is consequently reflected in poor outcome (2). In contrast, early-stage ovarian cancer (before the tumor has spread in the peritoneal cavity) has excellent curability. Thus, any marker, which could be used for screening of asymptomatic women in age groups at risk, would promote early detection and thus increase curability. Several tumor

markers have been tried, either alone or in combinations. However, even the most useful one, CA125, is not reliable due to low sensitivity in patients with early-stage ovarian cancer (3-8). Gynecologic ultrasound has high sensitivity and acceptable specificity but is too labor intense to be employed for screening.

The urokinase plasminogen activator (uPA) system is involved in tissue remodeling processes, such as wound healing and cancer cell invasion. In addition, the components of the uPA system are up-regulated in many types of malignant tumors (9). The uPA receptor (uPAR) has a central function in these processes, because binding of the zymogen pro-uPA initiates activation of plasminogen leading to other proteolytic events in the extracellular matrix. Intact uPAR, uPAR(I-III), consists of three domains denoted uPAR(I), uPAR(II), and uPAR(III) connected by two linker regions and uPAR(III) is attached to cell membrane by a glycosylphosphatidylinositol anchor. Two crystal structures of soluble forms of the human uPAR(I-III) have recently been reported (10, 11). Intact uPAR is required for efficient binding of ligands like uPA and vitronectin (12-14). uPAR(I-III) can be cleaved in the linker region between domains I and II by uPA, liberating uPAR(I) and leaving the cleaved form, uPAR(II-III), on the cell surface (15, 16). *In vivo* uPA has been shown to be responsible for cleavage of uPAR (17, 18), but *in vitro* uPAR can also be cleaved

Authors' Affiliations: ¹Department of Obstetrics and Gynecology, University Hospital Lund, Lund, Sweden and ²Finsen Laboratory, Copenhagen, Denmark

Received 1/15/08; revised 5/22/08; accepted 5/26/08.

Grant support: EU contract LSHC-CT-2003-503297, Danish Cancer Society, and Aase and Einar Danielsens Fund.

The costs of publication of this article were defrayed in part by the payment of page charges. This article must therefore be hereby marked *advertisement* in accordance with 18 U.S.C. Section 1734 solely to indicate this fact.

Requests for reprints: Christer Borgfeldt, Department of Obstetrics and Gynecology, University Hospital Lund, SE-221 85 Lund, Sweden. Phone: 46-46-17-10-00; Fax: 46-46-15-78-68; E-mail: christer.borgfeldt@med.lu.se.

© 2008 American Association for Cancer Research.

doi:10.1158/1078-0432.CCR-08-0096

Translational Relevance

Ovarian cancer is the leading cause of death among gynecologic malignancies. Due to mild symptoms, the majority of patients are already in advanced stage at diagnosis, facing poor long-term survival despite radical surgery and improved chemotherapy. In contrast, early-stage ovarian cancer has excellent curability. Early diagnosis is the only measure that can radically improve prognosis in patients with ovarian cancer. Unfortunately, there is no reliable marker to be used in screening for early-stage ovarian cancer. CA125 has too low sensitivity for early-stage tumors, and gynecologic ultrasound is too labor intense to be employed in screening. We show that plasma levels of suPAR (I-III) + suPAR (II-III) have diagnostic potential in patients with ovarian cancer. The product of suPAR (I-III) + suPAR (II-III) and CA125 detects early-stage tumors more accurately than each marker separately. This variable may help to identify early-stage ovarian tumors among the numerous ovarian cysts detected by transvaginal ultrasonography. In addition, uPAR (I) is an independent marker for postoperative survival in patients with ovarian cancer. It is available already preoperatively and can be used to guide the effort of surgery as well as to individualize chemotherapy.

in the linker region by other proteases (19). uPAR is also shed from the cell surface and soluble forms of suPAR: suPAR (I-III), suPAR (II-III), and uPAR (I) have been detected in blood (20, 21) and in cystic fluid from patients with ovarian cancer (22). Although the mechanism of suPAR shedding is not clarified, evidence has been provided that the glycolipid (glycosylphosphatidylinositol) anchor can be cleaved by endogenous cellular glycosylphosphatidylinositol-specific phospholipase D (23). Whereas glycosylphosphatidylinositol-anchored uPAR (I-III) is readily cleaved by uPA, suPAR cannot be cleaved by uPA in the linker region between domains I and II (24). The function of suPAR (I-III) is not fully elucidated, but it has been shown to act as a scavenger on free uPA and reduces growth and metastasis of breast and ovarian cancer cells (25, 26). However, whereas no functional role has been assigned to uPAR (II-III), its soluble counterpart has been shown to be a strong chemoattractant important for the migration of different cell types (27, 28).

Increased levels of the collective amounts of suPAR forms in blood have been reported in patients with malignant tumors including ovarian, endometrial, and cervical cancers (22, 29), non-small cell lung cancer (30), and colon cancer (31). In addition, high preoperative concentration of suPAR forms in blood from patients with breast and colorectal cancer correlate with poor prognosis (32, 33).

Malignant ovarian tumors have up-regulated expression of the genes for uPAR, uPA, and its inhibitor-1 (plasminogen activator inhibitor-1; ref. 34). Plasminogen activator inhibitor-1 and uPA proteins are also increased (35). In this study, we wanted to quantify the individual forms of suPAR in preoperatively taken peripheral blood from patients hospitalized for ovarian tumors using specific immunoassays. The aim was to evaluate the possibility to use these variables as diagnostic and/or prognostic markers in patients with ovarian cancer.

Materials and Methods**Patients and Treatment**

Peripheral blood samples were obtained preoperatively in 335 patients admitted for primary surgery because of adnexal masses at the Department of Obstetrics and Gynecology in Lund from 1993 to 2005. Blood was collected in citrate tubes and centrifuged, and the plasma was stored at -20°C until analyzed. The standard surgical procedure included resection of the cyst or unilateral oophorectomy in benign cases and abdominal hysterectomy, bilateral salpingo-oophorectomy, and infracolic omentectomy in the malignant cases. Cytologic analyses of ascitic fluid, or when absent, of peritoneal washing were done. All diagnoses were verified by histopathology of the tumors. Histopathologic grade and stage of the disease (FIGO) were available in all malignant cases as shown in Tables 1 and 2. Postoperative adjuvant treatment was given according to clinical standards in patients with invasive cancer. Patients with stage Ic or higher stage received platinum-based chemotherapy, either alone or combined with paclitaxel or cyclophosphamide. Survival status of all patients (alive or dead including date of death) was obtained on September 27, 2006 from the Swedish Population Register (Tumor Registry Center in Lund). For patients with benign cysts, the median age was 50 years (range, 16.6-88); for borderline patients, the median age was 52.2 years (range, 30.6-85.7); and for ovarian cancer patients, the median age was 62.6 years (range, 31-88). The median follow-up time for patients alive on September 27, 2006 was 64 months (range, 20-154).

The study was approved by the Regional Ethical Board, Faculty of Medicine, University of Lund.

Immunoassays

uPAR. Three uPAR immunoassays, time-resolved fluorescence assays (TR-FIA) 1 to 3, have been designed for the specific measurement of uPAR (I-III), uPAR (I-II) + uPAR (II-III), and uPAR (I), respectively (21). The detection limits were 0.3 pmol/L suPAR (I-III) for TR-FIA 1 and 2 and 1.9 pmol/L uPAR (I) for TR-FIA 3. The assays were previously validated for use in citrate plasma diluted 1:10 (21). Because the amounts of uPAR (I) in citrate plasma diluted 1:10 is close to the limit of quantification, we decided to only dilute our samples 1:5 in assay buffer (DELFA assay buffer 1244-111). The assays were therefore validated for their use in citrate plasma diluted 1:5. The limit of quantification was determined by spiking suPAR-depleted citrate plasma with purified suPAR and examining the coefficient of variation (CV). suPAR depletion of plasma diluted 1:5 was achieved as described previously (21). The depleted plasma was spiked with a concentration range from 0.016 to 10 µg/L purified standards [0.5-325 pmol/L suPAR (I-III) and 1.5-961 pmol/L uPAR (I)]. The limit of quantification was defined as the concentration at which CV exceeded 20%.

Intra-assay precision was determined by measuring the donor citrate plasma pool in TR-FIA 1 ($n = 26$) and TR-FIA 2 ($n = 28$) and calculating the CVs. For TR-FIA 3 ($n = 27$), we used donor citrate plasma pool spiked with 480 pmol/L uPAR (I). The same samples were employed for determination of interassay precision ($n = 24$).

The amount of suPAR (II-III) was obtained by subtracting the moles of suPAR (I-III) measured in TR-FIA 1 from those of suPAR (I-III) and suPAR (II-III) measured in TR-FIA 2.

CA125. Preoperative plasma samples were routinely assayed for CA125 using a commercial electrochemiluminescence immunoassay Elecsys CA125 kit (Roche). The assay was done according to the manufacturer's instructions.

Statistical Methods

Descriptive statistics for the plasma content of the different suPAR forms and CA125 stratified by the histopathologic group and stage are presented by box-whisker plots showing their medians, quartiles, and extreme values. Tests for location comparing the histopathologic groups have been done using the Kruskal-Wallis test, and if significant, pairwise

Table 1. Histopathologic diagnoses in relation to differentiation and grade of the ovarian tumor

Differentiation	Histopathologic diagnose							Total
	Serous	Mucinous	Endometrioid	Clear cell	Functional	Endometriosis	Teratoma	
Benign	91	40	0	0	16	39	25	211
Borderline	17	12	1	0	0	0	0	30
Well	8	6	5	0	0	0	0	19
Moderately	9	2	4	0	0	0	0	15
Poor	41	4	12	3	0	0	0	60
Total	166	64	22	3	16	39	25	335

comparisons have been done using the Mann-Whitney *U* test. The component uPAR(I) was lower than the detection limit in 75% of the analyzed samples; therefore, we chose to dichotomize uPAR(I) at the detection limit considering uPAR(I) levels above the limit to be elevated. Tests for independence between the histopathologic groups and uPAR(I) were done using the χ^2 test. Trend tests for ordered groups were done using linear regression with the dependent variable log transformed. Spearman's rank correlation has been used as a measure of association between the studied biomarkers.

Analysis of discrimination between the benign, borderline, and invasive has been done using a proportional odds model with biomarkers either log transformed or dichotomized. Backwards selection was used to identify the significant biomarkers (<5%). The initial model did not include suPAR(II-III), as this marker is highly correlated to suPAR(I-III) + suPAR(II-III). Results are presented by the respective odds ratios and 95% confidence intervals (95% CI). The receiver operating characteristic (ROC) curve and the area under the ROC curve with 95% CI are presented for comparison of borderline and invasive tumors to benign tumors. Furthermore, the specificity for fixed sensitivities of 85%, 90%, and 95% was calculated for the combination of suPAR(I-III) + suPAR(II-III) and CA125 as well as the false-positive and false-negative rates computed as posterior probabilities using Bayes' theorem. The Cox proportional hazards model was used for univariate and multivariate analysis. The uPAR variants and CA125 were entered as a continuous covariate on the log scale. uPAR(I) levels below the detection limit have been set at the limit for the analysis of continuous levels. Point estimates are reported as hazard ratios (HR) with 95% CI. Assumptions of proportional hazards were checked using Schoenfeld's test or verified graphically where applicable. Significant departures from proportionality were not observed for dichotomized soluble uPAR forms or for other covariates used in the Cox regression. For graphical presentation of overall survival, probabilities were estimated using the Kaplan-Meier method, dichotomizing biomarker levels by their respective medians. Multivariate analysis of the suPAR components using backwards selection was used to identify a model for use in a final model including CA125, grade, stage, age, and residual tumor, all significant in univariate analysis. Histology type was not significant in univariate analysis and is therefore not included in the multivariate analysis. The final model was also reduced using backwards selection.

All comparisons were two sided, and a 5% level of significance was used. The statistical analyses were done using SPSS (11.5.1) and SAS (v9.1; SAS Institute).

Results

The limit of quantification was determined in suPAR-depleted citrate plasma pool spiked with the analytes and was for suPAR(I-III) <1.3 pmol/L in TR-FIA 1 and 1.3 pmol/L in TR-FIA 2. For uPAR(I) in TR-FIA 3, the limit of quantification was 2.9 pmol/L. The CVs calculated for the intra-assay precision was 4.9% for TR-FIA 1, 6.4% for TR-FIA 2, and 7.9% for TR-FIA 3. The CVs for the interassay precision of TR-FIA 1 and TR-FIA 2

were 10.2% and 7.3%, respectively, whereas the CV for TR-FIA 3 was 10.6%. Accuracy was previously determined and the recoveries in 20% citrate plasma of TR-FIA 1 to 3 were 93%, 101%, and 95%, respectively (21).

The plasma levels of suPAR(I-III) + suPAR(II-III) were higher in patients with borderline ($P < 0.0001$) and invasive ($P < 0.0001$) tumors than in those with benign tumors (Fig. 1; Table 3). Furthermore, the levels were higher in patients with invasive tumors than in those with borderline tumors ($P = 0.03$). It was, however, not significantly different between the grades of invasive tumors. The plasma concentrations of suPAR(I-III) + suPAR(II-III) were not different in patients with different clinical stages of invasive tumors (data not shown).

The content of suPAR(I-III) in plasma was higher in patients with malignant ($P < 0.0001$) and borderline ($P = 0.0002$) tumors than in those with benign tumors. However, the levels of suPAR(I-III) in samples from patients with borderline and malignant tumors were not different ($P = 0.36$), and there was no difference between the histologic grades of invasive tumors. Also, the levels of suPAR(I-III) were not different between the clinical stages of the disease.

The calculated plasma levels of suPAR(II-III) were higher in patients with malignant ($P < 0.0001$) and borderline ($P < 0.0001$) tumors compared with patients with benign tumors. The levels were also higher in patients with malignant compared with those with borderline tumors ($P = 0.009$) and were not vary with the clinical stages of the disease.

The number of patients with uPAR(I) above detection limit was 47% in the malignant group, 50% in the borderline group, and 12% in the benign group. Concentrations were significantly higher in the malignant ($P < 0.0001$) and borderline ($P < 0.0001$) groups than in the benign group, but there was no difference between plasma samples from patients with malignant and borderline tumors ($P = 0.76$). There was also no difference between the histologic grades or clinical stages within the malignant group.

Table 2. Histopathologic grade differentiation in relation to stage

Differentiation	Stage				Total
	I	II	III	IV	
Borderline	27	1	2	0	30
Well	12	2	4	1	19
Moderately	5	2	7	1	15
Poor	5	6	44	5	60
Total	49	11	57	7	124

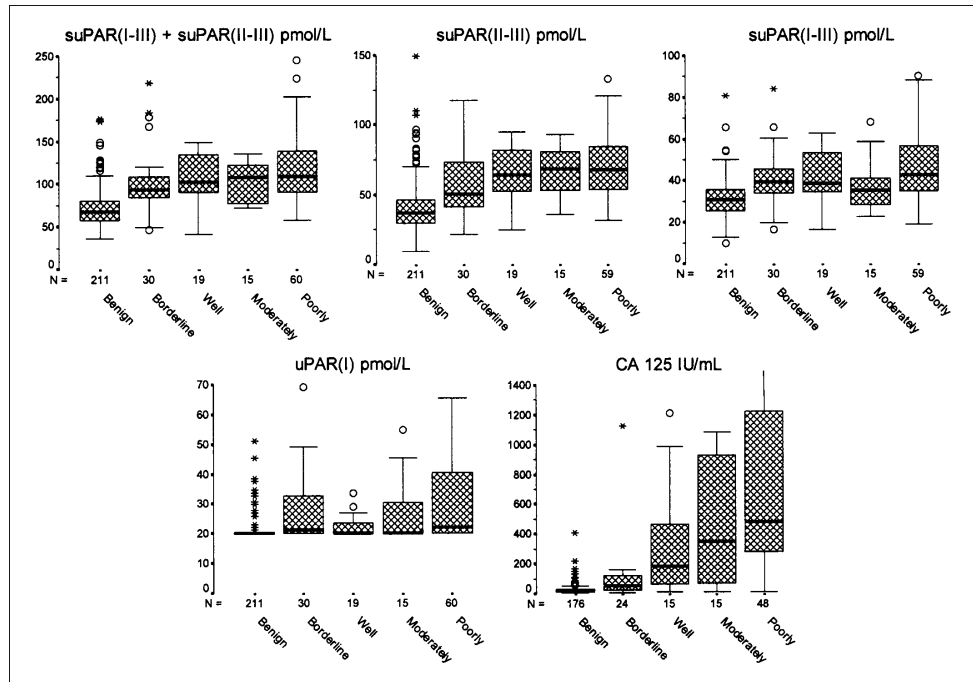


Fig. 1. Peripheral blood concentrations of suPAR(I-III) + suPAR(II-III), suPAR(I-III), suPAR(II-III), uPAR(I) ($n = 335$), and CA125 ($n = 278$) obtained preoperatively in patients with adnexal lesions. Boxes represent the 25th, 50th, and 75th percentiles. Bars include highest and lowest values, except outliers (○), which are 1.5 to 3 box lengths from the end of the box, and extremes (*), which are more than 3 box lengths from the end of the box.

The content of CA125 in plasma was evaluated in 278 patients only, because this variable is missing in 35 patients with benign tumors, 6 patients with borderline tumors, and 16 patients with malignant tumors. The concentration was higher in patients with malignant ($P < 0.0001$) and borderline ($P < 0.0001$) tumors compared with those with benign tumors. Also, the concentration was higher in patients with well ($P = 0.02$), moderately ($P = 0.008$), and poorly ($P < 0.0001$) differentiated tumors compared with those with borderline tumors. Plasma CA125 increased with loss of histologic differentiation ($P_{\text{trend}} < 0.001$). Patients with endometriosis had significantly higher CA125 values compared with other benign cysts ($P < 0.001$). In contrast, however, there were no differences in plasma levels of suPAR(I-III) + suPAR(II-III), suPAR(I-III), or uPAR(I) between patients with endometriosis and other benign ovarian cysts.

The Spearman rank correlation coefficients between different uPAR forms range from 0.40 to 0.70, except that between suPAR(I-III) + suPAR(II-III) and suPAR(II-III), which is 0.94. Correlation coefficients between uPAR forms and CA125 range from 0.32 to 0.50. All correlations are significantly different from 0.

Univariate analysis using the proportional odds model showed that all uPAR forms were statistically significant

($P < 0.0001$) with suPAR(I-III) + suPAR(II-III) as the best discriminator. In addition, CA125 was also significant ($P < 0.0001$). The results of the proportional odds model discriminating the three ordered categories showed that suPAR(I-III) + suPAR(II-III) and CA125 were retained in the final model ($P = 0.0002$ and $P < 0.0001$, respectively). The score test for the proportional odds assumption yielded $P = 0.46$, showing that the assumption could not be rejected. The odds ratios were 7.94 (95% CI, 2.64-23.85) for suPAR(I-III) + suPAR(II-III) and 3.46 (95% CI, 2.59-4.61) for CA125. Note that these odds are on the log scale (natural) showing the odds comparing patients differing by one unit on the log scale. Restricting the analysis to include only early invasive cancers (stages I and II) also showed suPAR(I-III) + suPAR(II-III) to be significant (odds ratio, 6.41; 95% CI, 2.12-19.42) as well as CA125 (odds ratio, 2.34; 95% CI, 1.70-3.24). Further analysis using the ROC curve comparing benign with invasive tumors yields an AUC of 0.94 (95% CI, 0.90-0.98) and between benign and borderline the AUC is 0.78 (95% CI, 0.67-0.89; Fig. 2). From this model, the specificities for borderline versus benign were 11.9%, 19.9%, and 23.9% when the sensitivity was set at 95%, 90%, and 85%, and increased to 52.3%, 82.4%, and 89.2% when invasive versus

benign was analyzed (Table 4). Restricting the invasive group to early stage, stages I and II ($n = 32$ and $n = 25$ with CA125 available) resulted in 44.9%, 48.9%, and 68.2% specificities at 95%, 90%, and 85% sensitivities. The AUC of this model is 0.87 (95% CI, 0.78-0.96).

Overall survival was analyzed in patients with invasive malignant tumors ($n = 94$), thus excluding borderline tumors. The different variables of plasma suPAR were dichotomized at the median to discriminate between high and low risk for poor overall survival using univariate Cox regression analysis and Kaplan-Meier curves (Fig. 3A-D; P values are for the log-rank test; the HR and 95% CI estimated using the Cox model are shown). Using backwards selection in multivariate analysis including all variants of suPAR dichotomized by their respective medians, uPAR(I) was selected as the only covariate (HR, 2.49; 95% CI, 1.40-4.41; $P = 0.002$). A similar analysis using the log-transformed values resulted in uPAR(I) being retained (HR, 2.38; 95% CI, 1.58-3.57; $P < 0.0001$). Therefore, uPAR(I) levels were used in the multivariate analyses with other risk factors in ovarian cancer included. The results obtained by replacing the covariates uPAR(I) and CA125 by their actual values on the log scale are shown in Table 5, model 1. The number of patients in this analysis was 78 with 38 deaths, mainly due missing CA125 values. Removing CA125 from the multivariate analysis shows that age is now included as well as residual tumor and uPAR(I) (Table 5, model 2, 48 deaths). The number of events in a full multivariate model including all covariates could result in unstable estimates of these; however, the final models have a sufficient number of events. A multivariate model including preoperatively available covariates CA125 and uPAR(I) showed that CA125 is nonsignificant (HR, 1.18; 95% CI, 0.97-1.43; $P = 0.10$) as well as age (HR, 2.04; 95% CI, 0.97-4.31; $P = 0.06$), whereas uPAR(I) is significant (HR, 1.84; 95% CI, 1.15-2.95; $P = 0.011$).

Discussion

The aim of the study was to investigate whether concentrations of the individual suPAR forms in peripheral blood plasma from women with adnexal lesions can be used for diagnosing ovarian cancer or for predicting postoperative prognosis in patients with ovarian cancer. We identified the product of suPAR(I-III) + suPAR(II-III) and CA125 as a diagnostic marker for malignant and possibly malignant (borderline) ovarian tumors with higher accuracy than each of these variables separately. We also identified high plasma levels of uPAR(I) as an independent preoperative prognostic marker for poor overall survival in multivariate analyses.

Plasma levels of all separately analyzed suPAR variants were increased in patients with borderline and invasive tumors compared with those with benign tumors. The levels of suPAR(I-III) + suPAR(II-III) and suPAR(II-III) were also higher in invasive tumors than in borderline tumors. On the other hand, among invasive tumors, none of the suPAR forms varied with histologic differentiation or clinical stage. In a previous study of a much smaller number of ovarian tumor patients, we measured suPAR (all forms) with an ELISA in serum prepared from both peripheral blood and tumor blood and found increased levels of suPAR in invasive but not in borderline tumors (22). Apparently, the TR-FIAs, which are used in this article, allow us to distinguish benign from borderline tumors, which is very important in a diagnostic context. The present observations suggest that cleavage of uPAR as well as shedding of uPAR from the cell surface is increased already in borderline tumors but is most pronounced in the invasive tumors. Because plasma suPAR was independent of clinical stage, it appears not to be dependent on tumor burden. Although stage does not alone determine tumor burden, it reflects tumor extension with involvement of peritoneal surfaces, formation of ascitic fluid, etc.

The level of suPAR in peripheral blood from patients with ovarian cancer has been assayed previously using ELISA, which measure the total amount of all suPAR forms (22, 29, 36-38). In contrast to our findings, two of these studies found a correlation between the concentration of suPAR and the clinical stage. Sier et al., analyzing serum samples from 87 patients with ovarian cancer, found the highest levels in stage II (111 ± 20 pmol/L) with decreasing levels in stage III (98 ± 10 pmol/L) and stage IV (72 ± 7 pmol/L), and this was compared with healthy controls (49 ± 3 pmol/L; ref. 38). Riisbro et al., who studied citrate plasma from 53 ovarian cancer patients, reported that the level of suPAR increased gradually from clinical stage I (36 pmol/L) to stage IV (52 pmol/L) and that elevated level of suPAR was associated with poor postoperative prognosis (29).

We have shown previously that uPAR mRNA in the tumor tissue increase gradually when histology progress from well-differentiated to poorly differentiated tumors (34). However, tumor tissue content of uPAR protein is actually highest in borderline and well-differentiated malignant tumors and is substantially reduced in poorly differentiated tumors (39). Because of this inverse correlation with tumor differentiation, high tumor tissue content of uPAR is actually a marker for good postoperative prognosis in these patients. We also found the same inverse correlation between histologic differentiation and suPAR concentration in cystic fluid (22). The lack of correlation

Table 3. Comparisons in peripheral blood concentrations of suPAR(I-III) + suPAR(II-III), suPAR(I-III), the calculated suPAR(II-III), uPAR(I) ($n = 335$), and CA125 ($n = 278$) in women with benign, borderline, and malignant ovarian tumors

P	Benign vs borderline	Borderline vs malignant	Benign vs malignant
suPAR(I-III) + suPAR(II-III)	<0.0001	0.03	<0.0001
suPAR(I-III)	0.0002	0.36	<0.0001
suPAR(II-III)	<0.0001	0.009	<0.0001
uPAR(I)	<0.0001	0.76	<0.0001
CA125	<0.0001	<0.0001	<0.0001

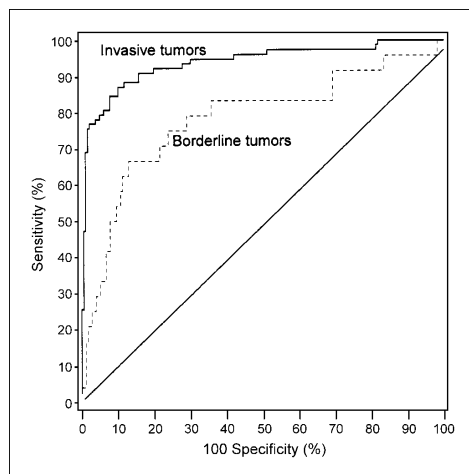


Fig. 2. ROC curves of the combination of suPAR (I-III) + suPAR (II-III) and CA125 estimated by logistic regression value to discriminate between malignant tumors, borderline tumors, and benign lesions. The diagonal line is also shown.

between the levels of uPAR mRNA and uPAR protein in tumor tissue and cystic fluid could be due to increased shedding of uPAR from poorly differentiated tumor cells to blood and body fluids (other than cystic fluid), because ovarian cancer cells shed uPAR (40). Alternatively, this may result from increased degradation of uPAR(I-III) during internalization with the uPA/plasminogen activator inhibitor-1 complex (41), but this would not hold for uPAR(II-III) because it cannot be internalized by this mechanism (19). A third possibility is that only a fraction of the uPAR mRNA is translated.

Ovarian cancer has a high mortality rate due to few symptoms in the early stage often resulting in diagnosis in late stages and subsequent poor prognosis. In addition, long-term outcome for these patients with advanced disease has not improved significantly despite introduction of more radical surgery and improved chemotherapy. The only measure that could radically change the prognostic situation in ovarian cancer would be diagnosis of the tumors in early

stages. This can be achieved provided a biomarker with high enough sensitivity and specificity can be found. Because the composition of ovarian cystic fluid largely reflects the content of the tumor tissue, we previously measured the collective amounts of suPAR forms in cystic fluids from 68 patients admitted for surgery of ovarian tumors (22). The concentrations were generally high (651-8,468 pmol/L) and separated clearly benign and malignant cysts with both sensitivity and specificity above 90%. Furthermore, concentrations in borderline cysts were as high as in malignant cysts. However, cystic fluid cannot be aspirated without leakage in the abdomen and up-staging the patient, not even when fine-needle technique is used.

Thus, we conclude that any marker, which is intended to for screening purpose, should be found in the peripheral blood. The previously well-studied marker CA125 has not met the requirements mainly because of too low sensitivity in patients with early-stage ovarian cancer. Any potential marker needs to prove sufficient sensitivity in early-stage and borderline tumors, which is the ultimate target group for detection because it has excellent survival data. Analysis of ROC curves showed that suPAR(I-III) + suPAR(II-III) and CA125 clearly discriminated between invasive and benign tumors as well as between borderline and benign. Similar results is found when restricting the analysis to early-stage invasive tumors; however, the result should be interpreted with caution as the number of patients in the invasive group is small. This means that surgery has to be done in less than two women to find an invasive ovarian cancer in women with adnexal lesion and high levels of the linear combination of suPAR(I-III) + suPAR(II-III) and CA125. Thus, the combination of these two markers detects early-stage tumors more accurately than each marker separately. Because comparisons between early stages + borderline tumors and benign tumors are not readily available in the literature, we compared AUC between all stages malignant tumors and benign tumors. In fact, AUC 0.94 is higher than most other proposed plasma markers as well as combinations of transvaginal ultrasonography and plasma marker algorithms (42). The linear combination of suPAR(I-III) + suPAR(II-III) and CA125 may in patients with serious comorbidity be a way of monitoring the patient with adnexal lesion and eventually avoid a stressful laparotomy or laparoscopy. This variable may also, in conjunction with transvaginal and abdominal ultrasonography, be a way to select those patients with ovarian cysts, who should be sent to centers with oncologist expertise to have optimal primary surgery.

Table 4. ROC analysis: sensitivities and specificities in discriminating borderline from benign and invasive ovarian cancer from benign cases

	Specificity at 85% sensitivity	Specificity at 90% sensitivity	Specificity at 95% sensitivity
Borderline vs benign	23.9%	19.9%	11.9%
Invasive vs benign	87.0%,* 8.7% †	86.5%,* 5.4% †	87.1%,* 4.5% †
	89.2%	82.4%	52.3%
	22.4%,* 7.1% †	30.7%,* 5.2% †	53.2%,* 4.2% †

*False-positive rate.
† False-negative rate.

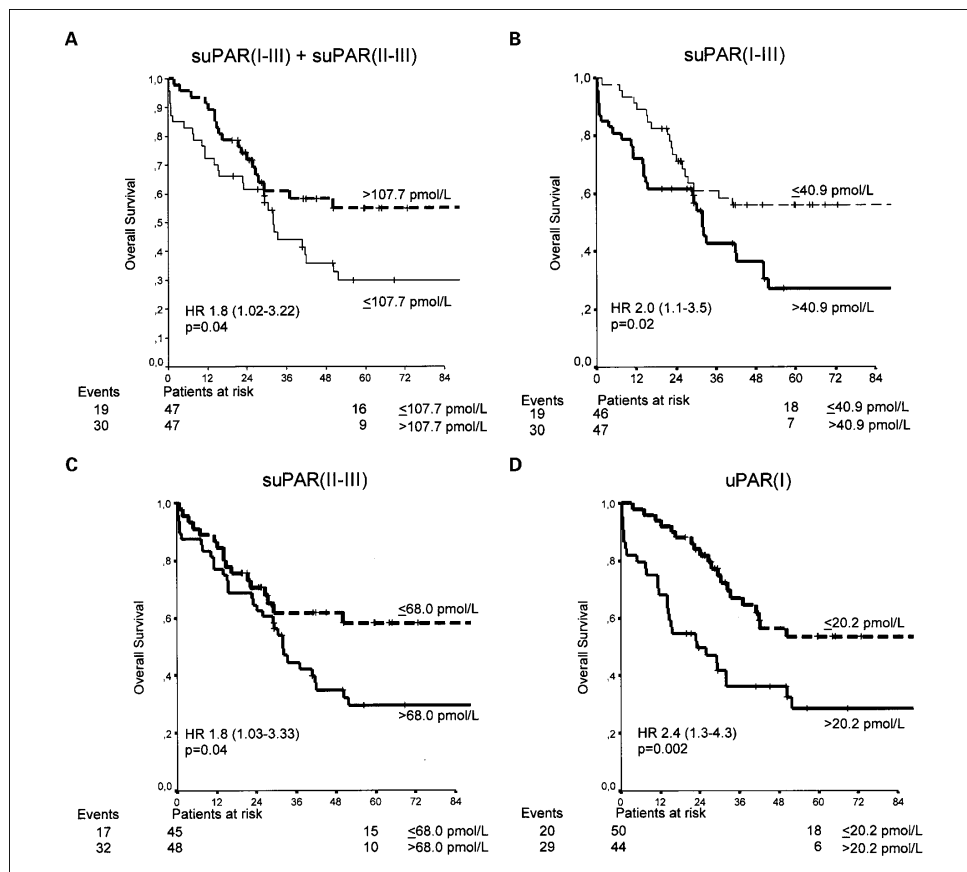


Fig. 3. Kaplan-Meier estimates of survival probabilities using peripheral blood concentrations dichotomized by the median of suPAR(I-III) + suPAR(II-III) (A), suPAR(I-III) (B), suPAR(II-III) (C), and uPAR(I) (D) dichotomized by the detection limit. P value is the log-rank statistic with HR (95% CI) calculated using the Cox proportional hazards model. The number of patients at risk in each stratum at time 0 and 60 mo after surgery are shown below the axis with the number of deaths (events) to the left.

We found that high levels of uPAR(I) in the plasma samples correlated with poor survival of the patients. In fact, uPAR(I) was an independent marker of poor prognosis in multivariate analyses. The level of uPAR(I) reflects the activity of uPA, because uPA has been shown to cleave uPAR with high efficiency on the cell surface both *in vitro* and *in vivo* (17-19). Interestingly, high uPA levels in tumor tissue extracts reportedly associate with poor histologic differentiation (39) and with short progression-free and overall survival in patients with primary ovarian cancer all stages (n = 82; ref. 43). In contrast, the plasma level of the other cleavage product suPAR(I-III) is dependent both on uPA-mediated cleavage of uPAR(I-III) at the cell surface and on subsequent shedding of uPAR(II-III) from the cell surface.

The long-term follow-up time and the consistent treatment regimes in this study are advantages, which increase reliability. Overall survival was chosen as the only endpoint, because progression-free survival is dependent on variables such as follow-up intervals and other variables chosen to indicate progression (increased CA125, CT scan findings, positive cytology or histopathology, or use of follow-up symptom questionnaires). Furthermore, death among patients diagnosed with ovarian cancer is to a large extent related to progression of the malignant disease. The Swedish Population Register, which includes all citizens, made a complete follow-up of all the patients. However, the results of the multivariate analysis should be interpreted with caution, because the power of the study is limited with 49 events in the analyses. Future studies

Table 5. Multivariate Cox regression analysis models of overall survival estimating HR for included variables

Covariate	Model 1		Model 2	
	HR (95% CI)	P	HR (95% CI)	P
suPAR(I)	1.58 (1.01-2.48)	0.046	2.02 (1.33-3.07)	0.0009
CA125		0.84*	Not included	
Age >70 vs <70		0.06*	2.66 (1.37-5.16)	0.004
Grade		0.21*		0.07*
Stage (>I vs I)		0.65*		0.69*
Residual tumor	4.64 (2.37-9.11)	<0.0001	3.94 (2.16-7.20)	<0.0001

*P value to include in model.

should confirm the results and may also suggest clinically relevant cutoff levels.

Patients with stage II to IV ovarian cancer almost exclusively undergo primary surgery, and postoperative morbidity depends to a great extent on how radical the surgery can be done. Several studies have indicated that amount of residual

tumor is the most critical factor for postoperative prognosis (44, 45). This of course calls for maximal effort during the primary operation; consequently, surgery has become more radical during recent years. We found that patients with ovarian cancer and high preoperative levels of plasma uPAR(I) had very poor prognosis, 85% were dead within 5 years. Because uPAR(I) is a prognostic variable, which is available already preoperatively, it can be used to guide the effort of surgery. The subgroup of patients with high uPAR(I), and thus poor prognosis, may in fact benefit from even more radical surgery, as well as more extensive postoperative chemotherapy including additional or new drugs and/or i.p. treatment. Alternatively, elderly patients in late stages with high uPAR(I), which suggests both advanced disease and aggressive tumor, may benefit more from neoadjuvant chemotherapy and interval debulking surgery or palliative therapy to minimize morbidity.

Disclosure of Potential Conflicts of Interest

No potential conflicts of interest were disclosed.

Acknowledgments

We thank Ruth Petersson for excellent technical assistance.

References

- Socialstyrelsen, Causes of death 2004, in Statistik, Hälsa och sjukdomar, 2007:1, p. 67.
- Heintz AP, Odicino F, Maisonneuve P, Beller U, Benedet JL. Carcinoma of the ovary. J Epidemiol Biostat 2001;6:107-38.
- Hakama M, Stenman UH, Knekt P, et al. CA 125 as a screening test for ovarian cancer. J Med Screen 1996; 3:40-2.
- Jacobs IJ, Skates S, Davies AP, et al. Risk of diagnosis of ovarian cancer after raised serum CA 125 concentration: a prospective cohort study. BMJ 1996; 313:1355-8.
- Rosenthal AN, Jacobs IJ. The role of CA 125 in screening for ovarian cancer. Int J Biol Markers 1998; 13:216-20.
- Taylor KJ, Schwartz PE. Screening for early ovarian cancer. Radiology 1994;192:1-10.
- Tingulstad S, Hagen B, Skjeldstad FE, et al. Evaluation of a risk of malignancy index based on serum CA125, ultrasound findings and menopausal status in the pre-operative diagnosis of pelvic masses. Br J Obstet Gynaecol 1996;103:826-31.
- Woolas RP, Xu FJ, Jacobs IJ, et al. Elevation of multiple serum markers in patients with stage I ovarian cancer. J Natl Cancer Inst 1993;85: 1748-51.
- Dano K, Behrendt N, Hoyer-Hansen G, et al. Plasminogen activation and cancer. Thromb Haemost 2005; 93:676-81.
- Huai Q, Mazar AP, Kuo A, et al. Structure of human urokinase plasminogen activator in complex with its receptor. Science 2006;311:656-9.
- Linás P, Le Du MH, Gårdsvoll H, et al. Crystal structure of the human urokinase plasminogen activator receptor bound to an antagonist peptide. EMBO J 2005;24:1655-63.
- Behrendt NE, Ronne, Dano K. Domain interplay in the urokinase receptor. Requirement for the third domain in high affinity ligand binding and demonstration of ligand contact sites in distinct receptor domains. J Biol Chem 1996;271:22885-94.
- Hoyer-Hansen G, Behrendt N, Ploug M, Dano K, Preissner KT. The intact urokinase receptor is required for efficient vitronectin binding: receptor cleavage prevents ligand interaction. FEBS Lett 1997;420:79-85.
- Sidenius N, Blasi F. Domain 1 of the urokinase receptor (uPAR) is required for uPAR-mediated cell binding to vitronectin. FEBS Lett 2000;470: 40-6.
- Hoyer-Hansen G, Ploug M, Behrendt N, Ronne E, Dano K. Cell-surface acceleration of urokinase-catalyzed receptor cleavage. Eur J Biochem 1997;243: 21-6.
- Hoyer-Hansen G, Ronne E, Solberg H, et al. Urokinase plasminogen activator cleaves its cell surface receptor releasing the ligand-binding domain. J Biol Chem 1992;267:18224-9.
- Bolon I, Zhou HM, Charron Y, Wohlwend A, Vassalli JD. Plasminogen mediates the pathological effects of urokinase-type plasminogen activator overexpression. Am J Pathol 2004;164:2299-304.
- Zhou HM, Nichols A, Meda P, Vassalli JD. Urokinase-type plasminogen activator and its receptor synergize to promote pathogenic proteolysis. EMBO J 2000;19:4817-26.
- Hoyer-Hansen G, Lund IK. Urokinase receptor variants in tissue and body fluids. Adv Clin Chem 2007; 44:65-102.
- Mustjoki S, Sidenius N, Sier CF, et al. Soluble urokinase receptor levels correlate with number of circulating tumor cells in acute myeloid leukemia and decrease rapidly during chemotherapy. Cancer Res 2000;60:7126-32.
- Piironen T, Laursen B, Pass J, et al. Specific immunoassays for detection of intact and cleaved forms of the urokinase receptor. Clin Chem 2004;50: 2059-68.
- Wahlberg K, Hoyer-Hansen G, Casslen B. Soluble receptor for urokinase plasminogen activator in both full-length and a cleaved form is present in high concentration in cystic fluid from ovarian cancer. Cancer Res 1998;58:3294-8.
- Wilhelm OG, Wilhelm S, Escott GM, et al. Cellular glycosylphosphatidylinositol-specific phospholipase D regulates urokinase receptor shedding and cell surface expression. J Cell Physiol 1999; 180:225-35.
- Hoyer-Hansen G, Pessara U, Holm A, et al. Urokinase-catalysed cleavage of the urokinase receptor requires an intact glycolipid anchor. Biochem J 2001; 358:673-9.
- Kruger A, Soelll R, Lutz V, et al. Reduction of breast carcinoma tumor growth and lung colonization by overexpression of the soluble urokinase-type plasminogen activator receptor (CD87). Cancer Gene Ther 2000;7:292-9.
- Lutz V, Reuning U, Krüger A, et al. High level synthesis of recombinant soluble urokinase receptor (CD87) by ovarian cancer cells reduces intraperitoneal tumor growth and spread in nude mice. Biol Chem 2001; 382:789-98.
- Resnati M, Guttinger M, Valcamonica S, Sidenius N, Blasi F, Fazioli F. Proteolytic cleavage of the urokinase receptor substitutes for the agonist-induced chemotactic effect. EMBO J 1996;15:1572-82.
- Selleri C, Montuori N, Ricci P, et al. Involvement of the urokinase-type plasminogen activator receptor in hematopoietic stem cell mobilization. Blood 2005; 105:2198-205.
- Riisbro R, Stephens RW, Brünner N, et al. Soluble urokinase plasminogen activator receptor in preoperatively obtained plasma from patients with gynecological cancer or benign gynecological diseases. Gynecol Oncol 2001;82:523-31.
- Pappot H, Hoyer-Hansen G, Ronne E, et al. Elevated plasma levels of urokinase plasminogen activator receptor in non-small cell lung cancer patients. Eur J Cancer 1997;33:867-72.
- Stephens RW, Pedersen AN, Nielsen HJ, et al. ELISA determination of soluble urokinase receptor in blood from healthy donors and cancer patients. Clin Chem 1997;43:1868-76.
- Riisbro R, Christensen LJ, Piironen T, et al. Prognostic significance of soluble urokinase plasminogen activator receptor in serum and cytosol of tumor tissue from patients with primary breast cancer. Clin Cancer Res 2002;8:1132-41.
- Stephens RW, Nielsen HJ, Christensen LJ, et al.

- Plasma urokinase receptor levels in patients with colorectal cancer: relationship to prognosis. *J Natl Cancer Inst* 1999;91:869–74.
34. Borgfeldt C, Hansson SR, Gustavsson B, Måsbäck A, Casslén B. Dedifferentiation of serous ovarian cancer from cystic to solid tumors is associated with increased expression of mRNA for urokinase plasminogen activator (uPA), its receptor (uPAR) and its inhibitor (PAI-1). *Int J Cancer* 2001;92:497–502.
35. Casslén B, Bossmar T, Lecander I, Åstedt B. Plasminogen activators and plasminogen activator inhibitors in blood and tumour fluids of patients with ovarian cancer. *Eur J Cancer* 1994;30A:1302–9.
36. Pedersen N, Schmitt M, Rønne E, et al. A ligand-free, soluble urokinase receptor is present in the ascitic fluid from patients with ovarian cancer. *J Clin Invest* 1993;92:2160–7.
37. Sier CF, Nicoletti I, Santovito ML, et al. Metabolism of tumour-derived urokinase receptor and receptor fragments in cancer patients and xenografted mice. *Thromb Haemost* 2004;91:403–11.
38. Sier CF, Stephens R, Bizik J, et al. The level of urokinase-type plasminogen activator receptor is increased in serum of ovarian cancer patients. *Cancer Res* 1998;58:1843–9.
39. Borgfeldt C, Bendahl PO, Gustavsson B, et al. High tumor tissue concentration of urokinase plasminogen activator receptor is associated with good prognosis in patients with ovarian cancer. *Int J Cancer* 2003;107:658–65.
40. Henic E, Sixt M, Hansson S, Høyer-Hansen G, Casslén B. EGF-stimulated migration in ovarian cancer cells is associated with decreased internalization, increased surface expression, and increased shedding of the urokinase plasminogen activator receptor. *Gynecol Oncol* 2006;101:28–39.
41. Olson D, Pollänen J, Høyer-Hansen G, et al. Internalization of the urokinase-plasminogen activator inhibitor type-1 complex is mediated by the urokinase receptor. *J Biol Chem* 1992;267:9129–33.
42. Mol BW, Boll D, De Kanter M, et al. Distinguishing the benign and malignant adnexal mass: an external validation of prognostic models. *Gynecol Oncol* 2001;80:162–7.
43. Konecny G, Untch M, Pihan A, et al. Association of urokinase-type plasminogen activator and its inhibitor with disease progression and prognosis in ovarian cancer. *Clin Cancer Res* 2001;7:1743–9.
44. Bristow RE, Tomacruz RS, Armstrong DK, Trimble EL, Montz FJ. Survival effect of maximal cytoreductive surgery for advanced ovarian carcinoma during the platinum era: a meta-analysis. *J Clin Oncol* 2002;20:1248–59.
45. Tingulstad S, Skjeldestad FE, Halvorsen TB, Hagen B. Survival and prognostic factors in patients with ovarian cancer. *Obstet Gynecol* 2003;101:885–91.

